Методы и средства Цифровой Обработки Сигналов

Фильтры

Круглов Евгений Владимирович, аспирант МИФИ
Решетов Владимир Николаевич, к.ф.-м. н. доцент МИФИ.

Москва 2008

Цифра или аналог?

DIGITAL VERSUS ANALOG FILTERING

DIGITAL FILTERS	ANALOG FILTERS
High Accuracy	Less Accuracy - Component Tolerances
Linear Phase (FIR Filters)	Non-Linear Phase
No Drift Due to Component Variations	Drift Due to Component Variations
Flexible, Adaptive Filtering Possible	Adaptive Filters Difficult
Easy to Simulate and Design	Difficult to Simulate and Design
Computation Must be Completed in Sampling Period - Limits Real Time Operation	Analog Filters Required at High Frequencies and for Anti-Aliasing Filters
Requires High Performance ADC, DAC & DSP	No ADC, DAC, or DSP Required

DIGITAL FILTERING

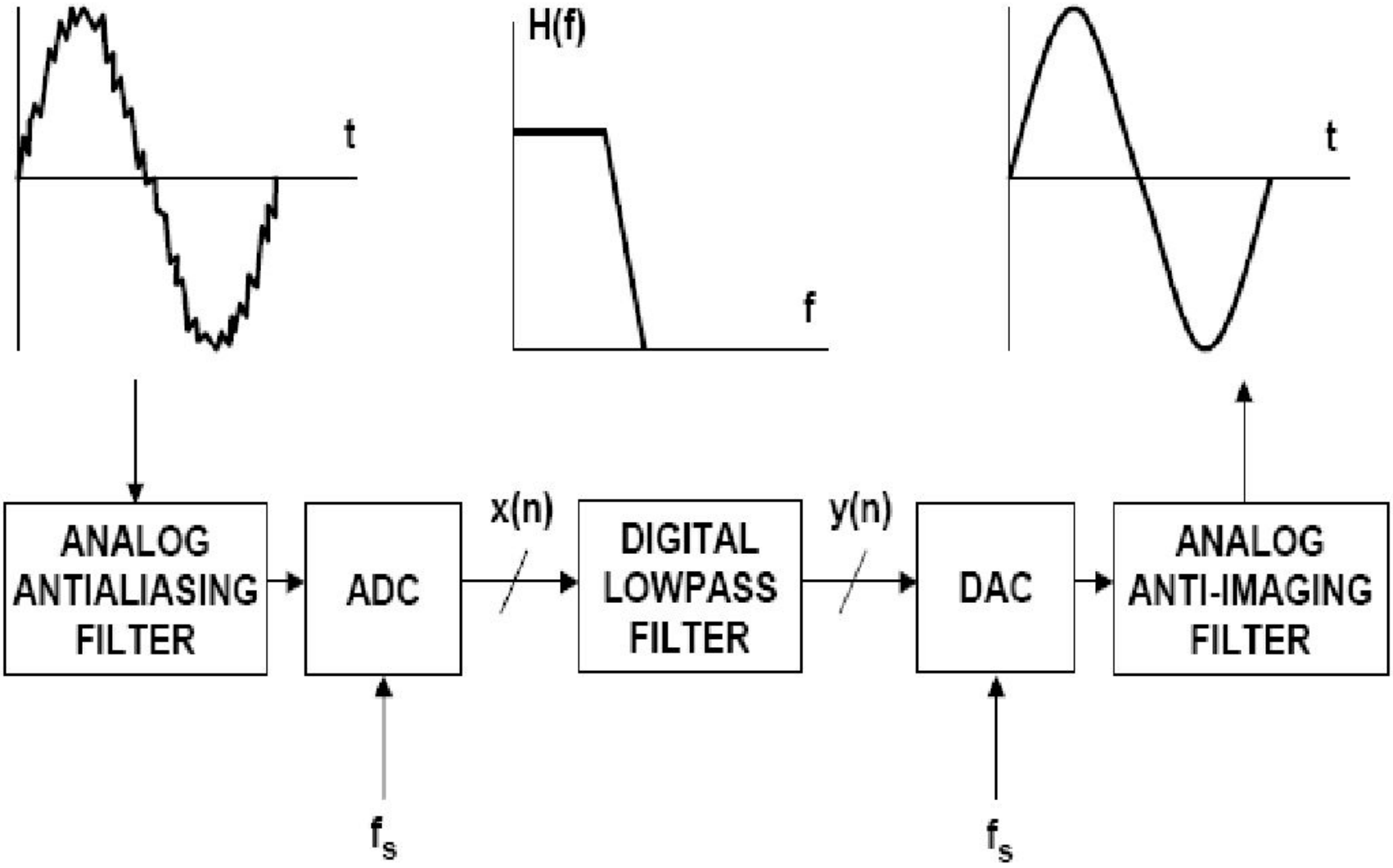

N-TAP FINITE IMPULSE RESPONSE (FIR) FILTER

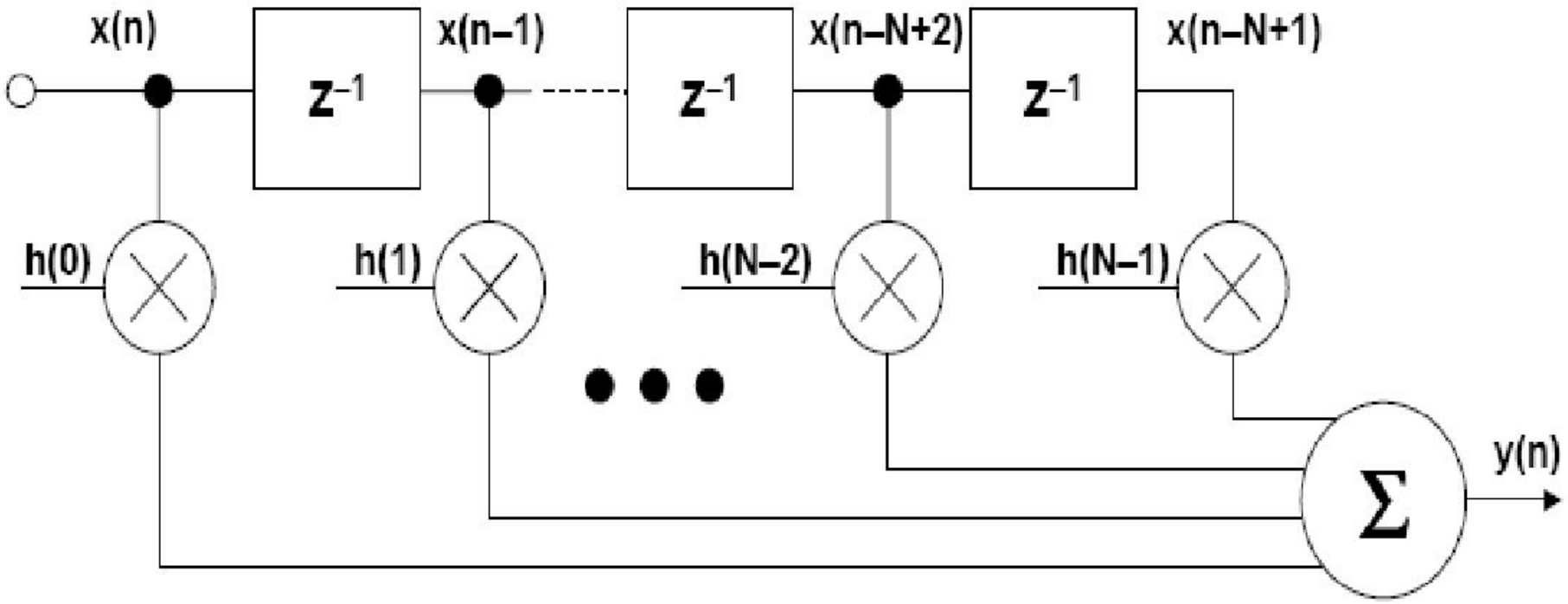

- $y(n) = h(n) * x(n) = \sum_{k=0}^{N-1} h(k)\, x(n-k)$
- $*$ = Symbol for Convolution
- Requires N multiply-accumulates for each output

SIMPLIFIED FILTER NOTATIONS

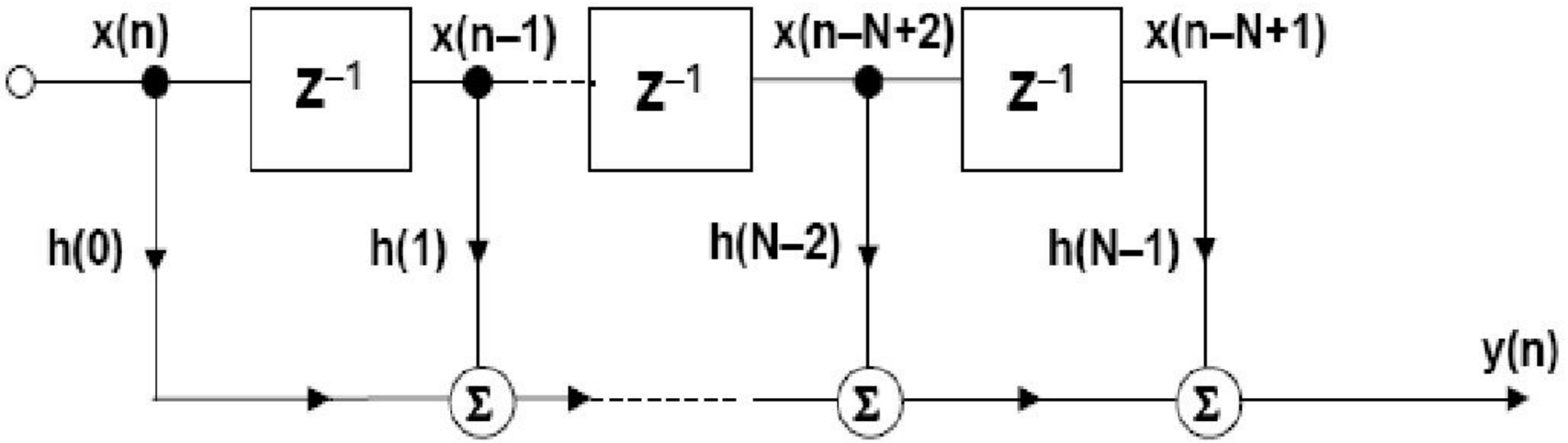

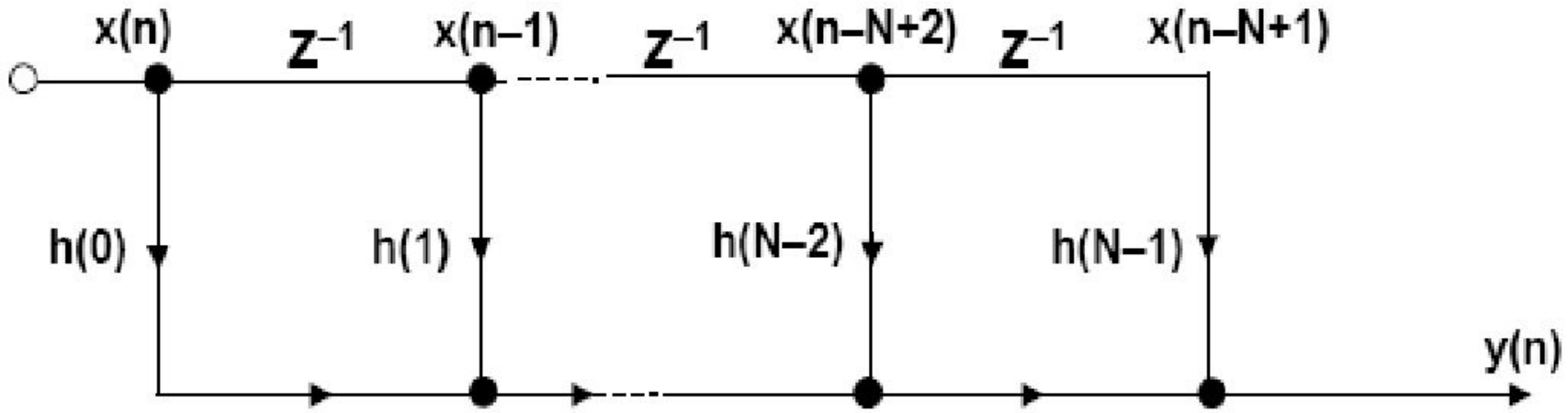

FIR FILTER IMPULSE RESPONSE DETERMINES THE FILTER COEFFICIENTS

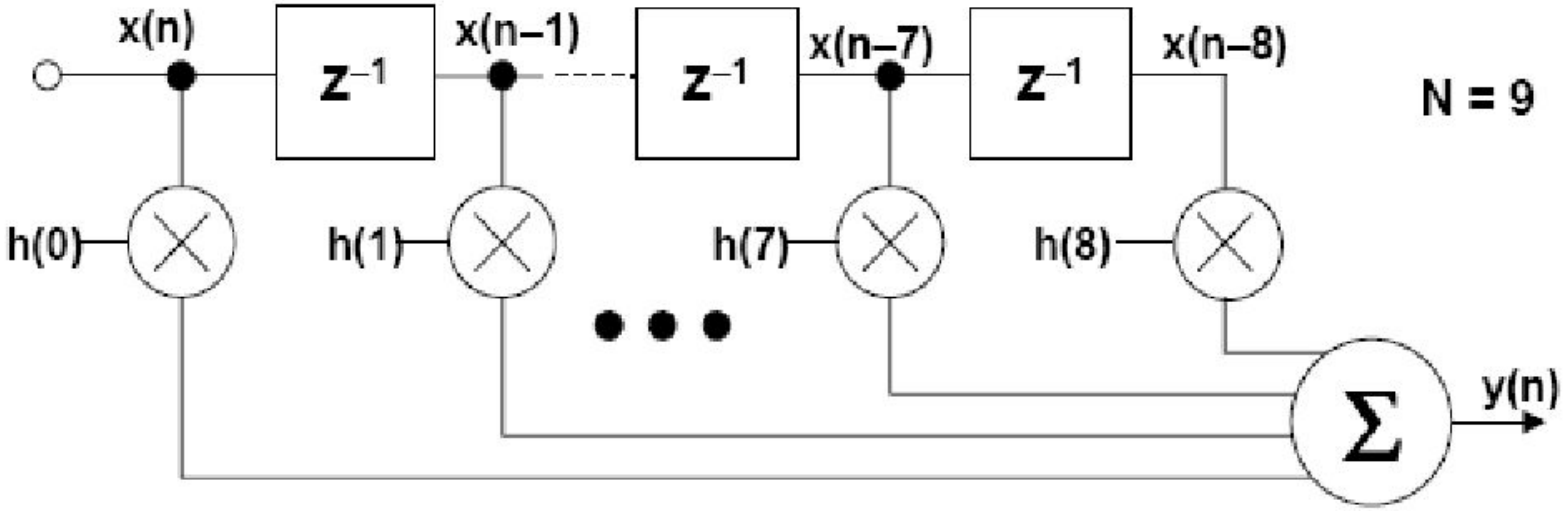

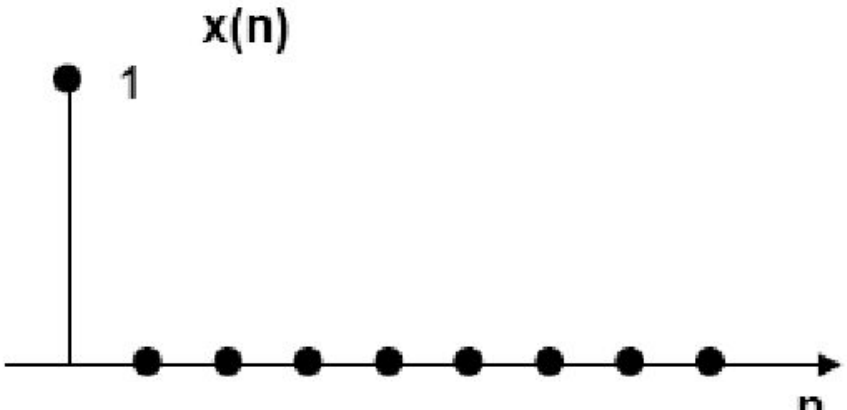

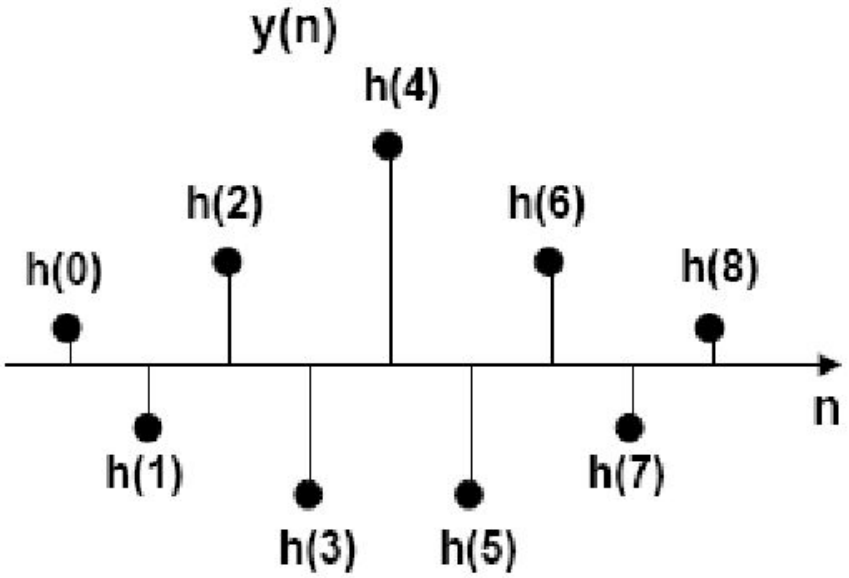

DUALITY OF TIME AND FREQUENCY

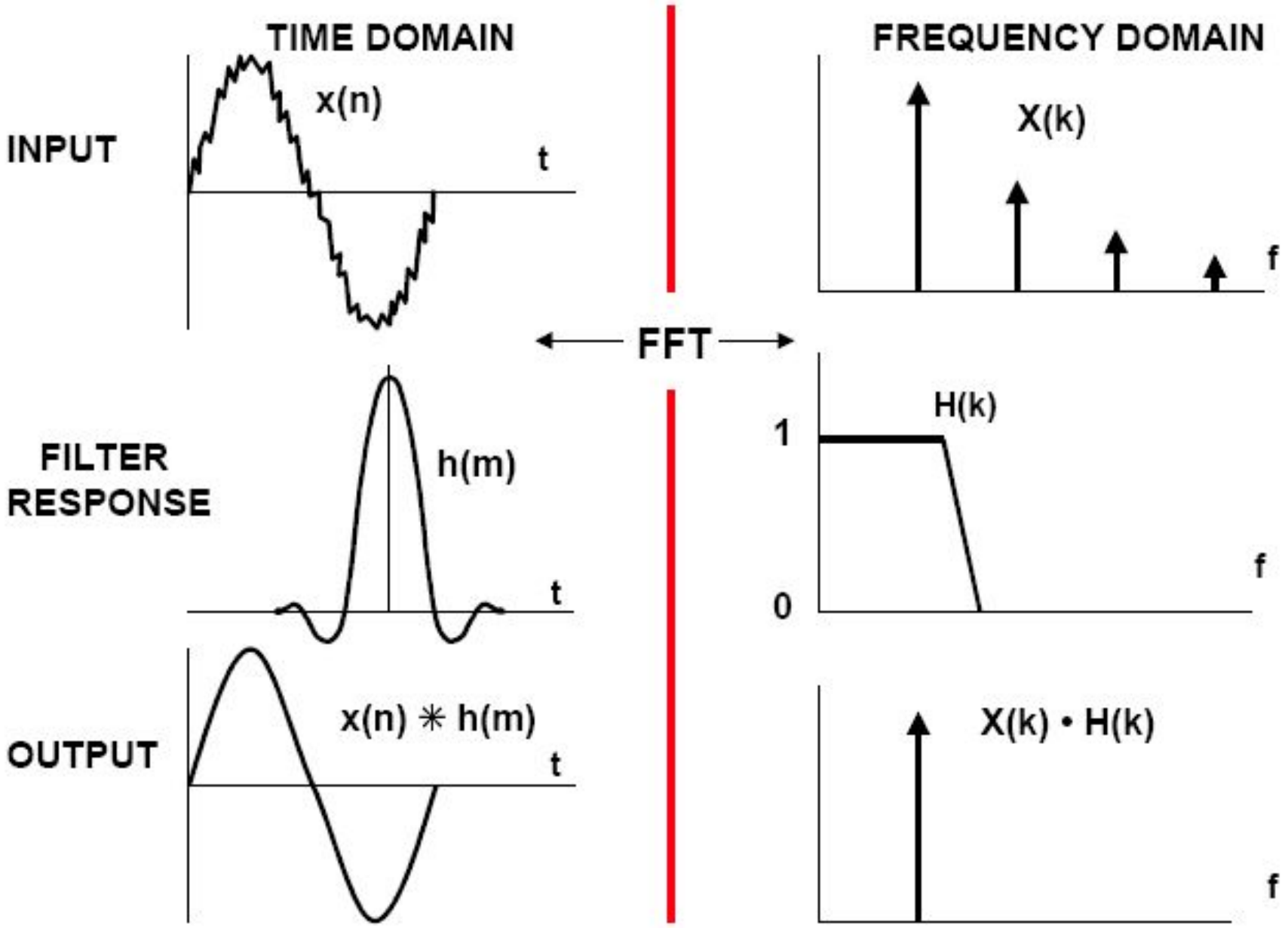

FIR FILTER DESIGN USING THE WINDOWED-SINC METHOD

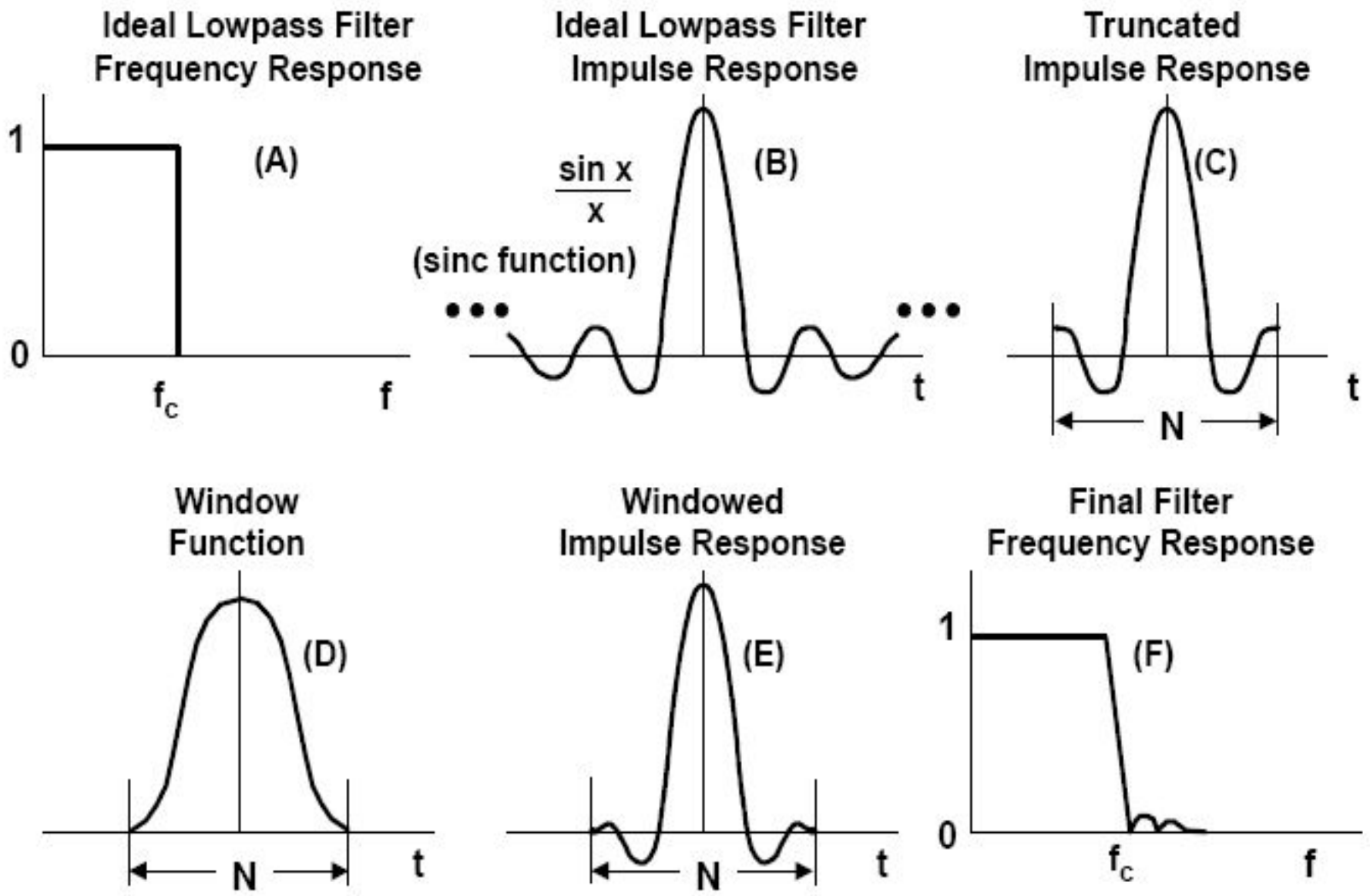

BANDPASS AND BANDSTOP FILTERS DESIGNED FROM LOWPASS AND HIGHPASS FILTERS

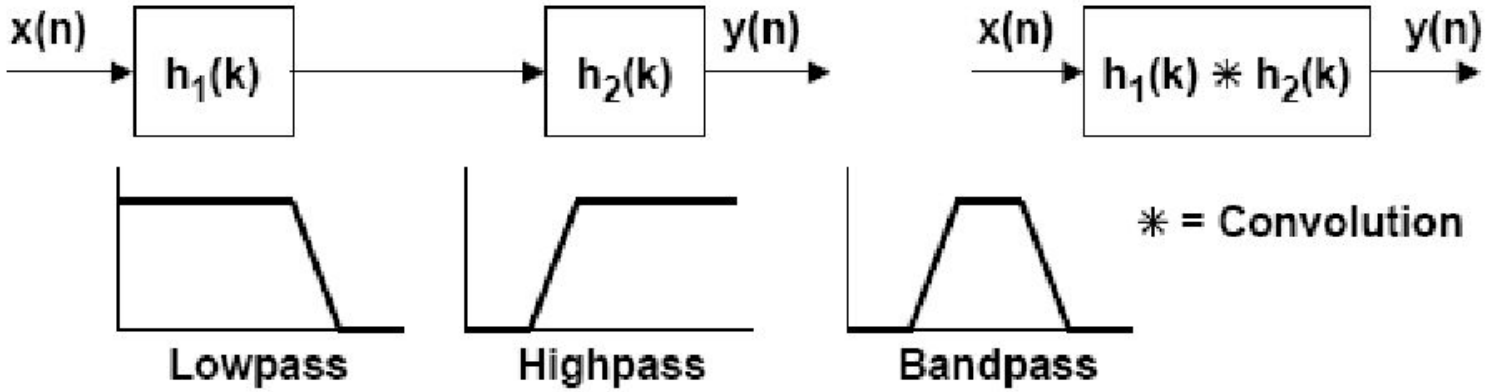

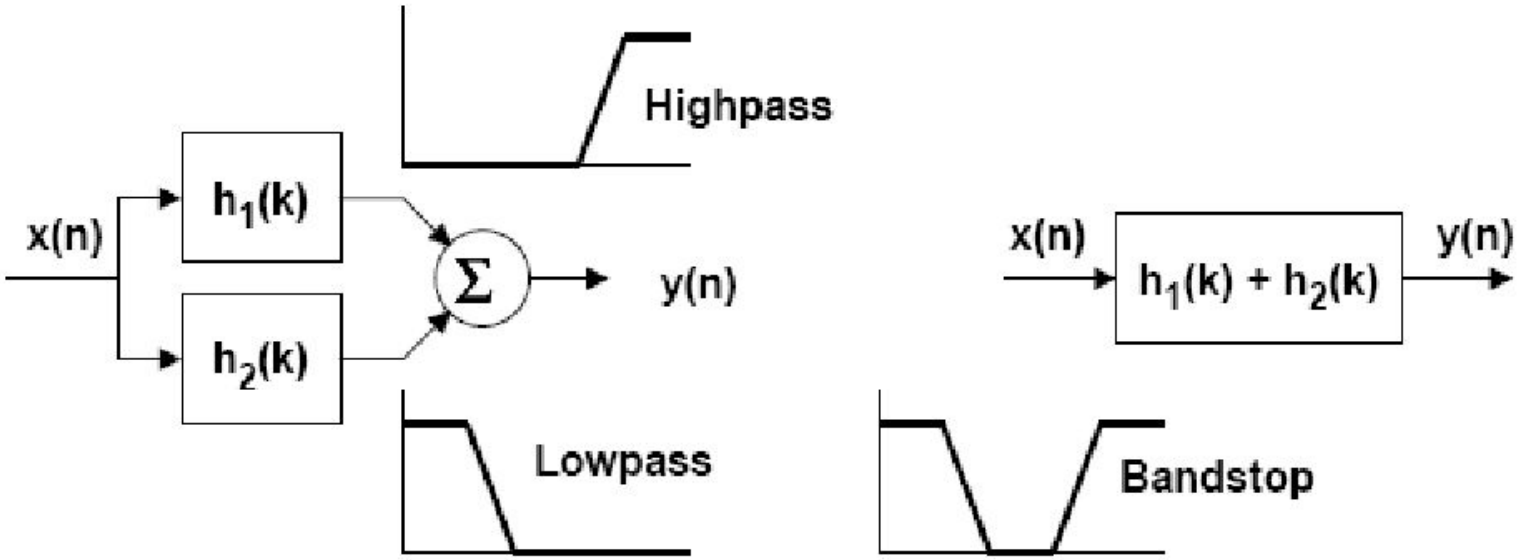

HARDWARE IMPLEMENTATION OF SECOND-ORDER IIR FILTER (BIQUAD) DIRECT FORM 1

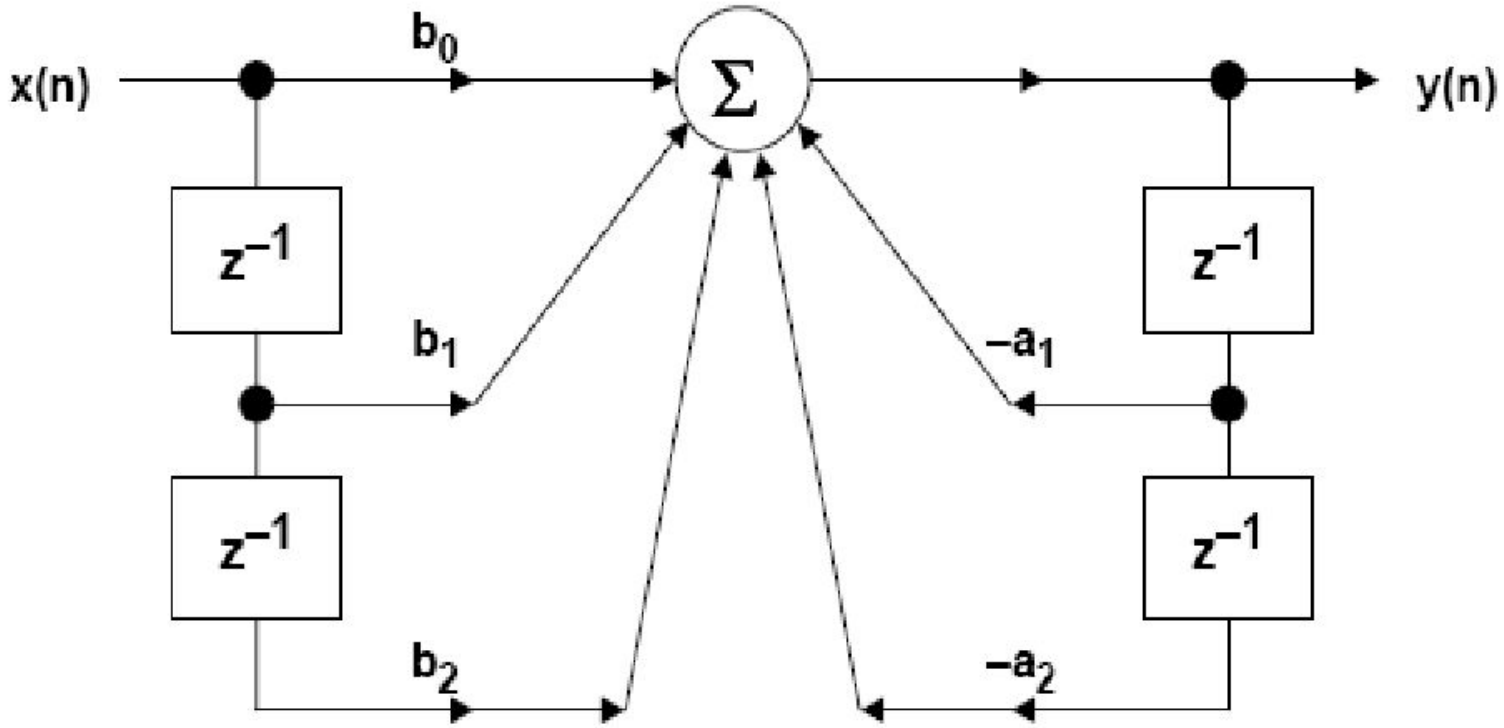

- $y(n) = b_0x(n) + b_1x(n-1) + b_2x(n-2) - a_1y(n-1) - a_2y(n-2)$

- $y(n) = \sum_{k=0}^{M} b_k x(n-k) - \sum_{k=1}^{N} a_k y(n-k)$

- $H(z) = \dfrac{\sum_{k=0}^{M} b_k z^{-k}}{1 + \sum_{k=1}^{N} a_k z^{-k}}$ (Zeros) / (Poles)

IIR BIQUAD FILTER DIRECT FORM 2

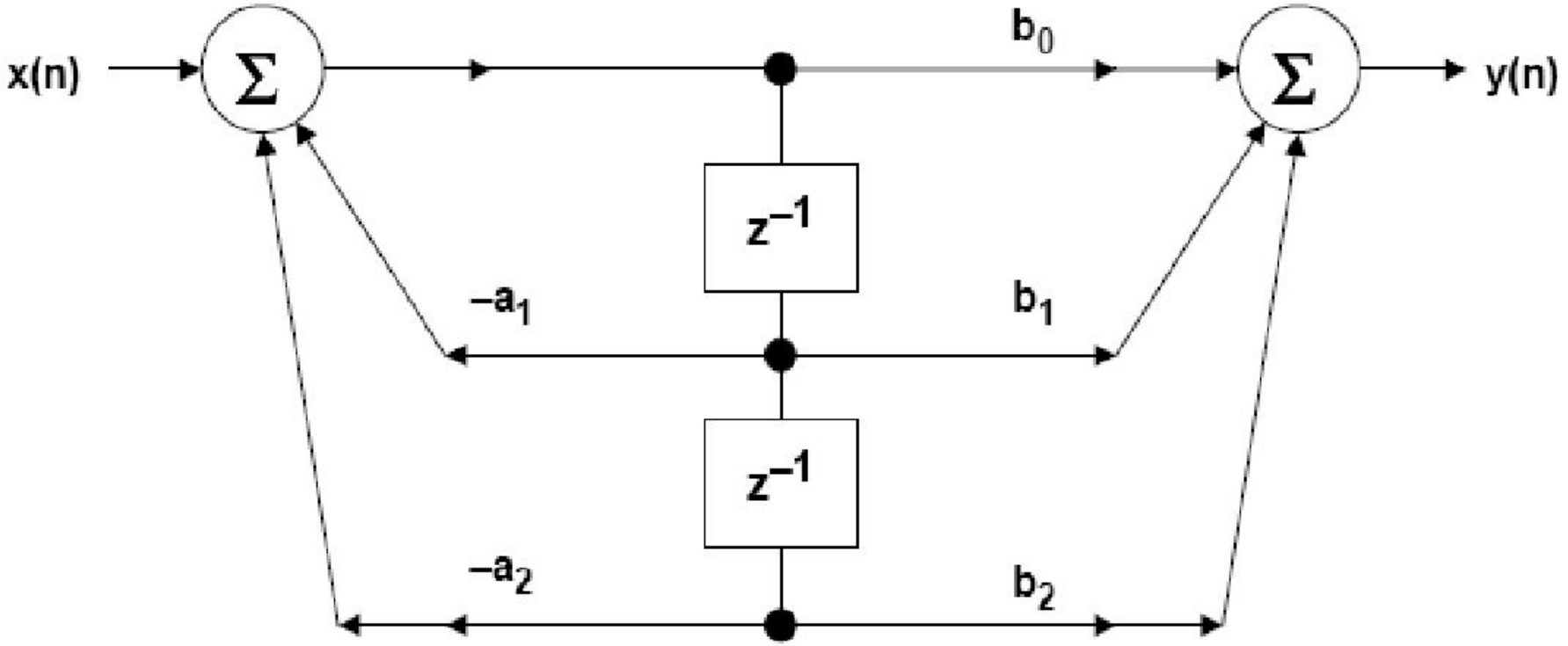

- Reduces to the same equation as Direct Form 1:
- $y(n) = b_0x(n) + b_1x(n–1) + b_2x(n–2) – a_1y(n–1) – a_2y(n–2)$
- Requires Only 2 Delay Elements (Registers)

IIR BIQUAD FILTER SIMPLIFIED NOTATIONS

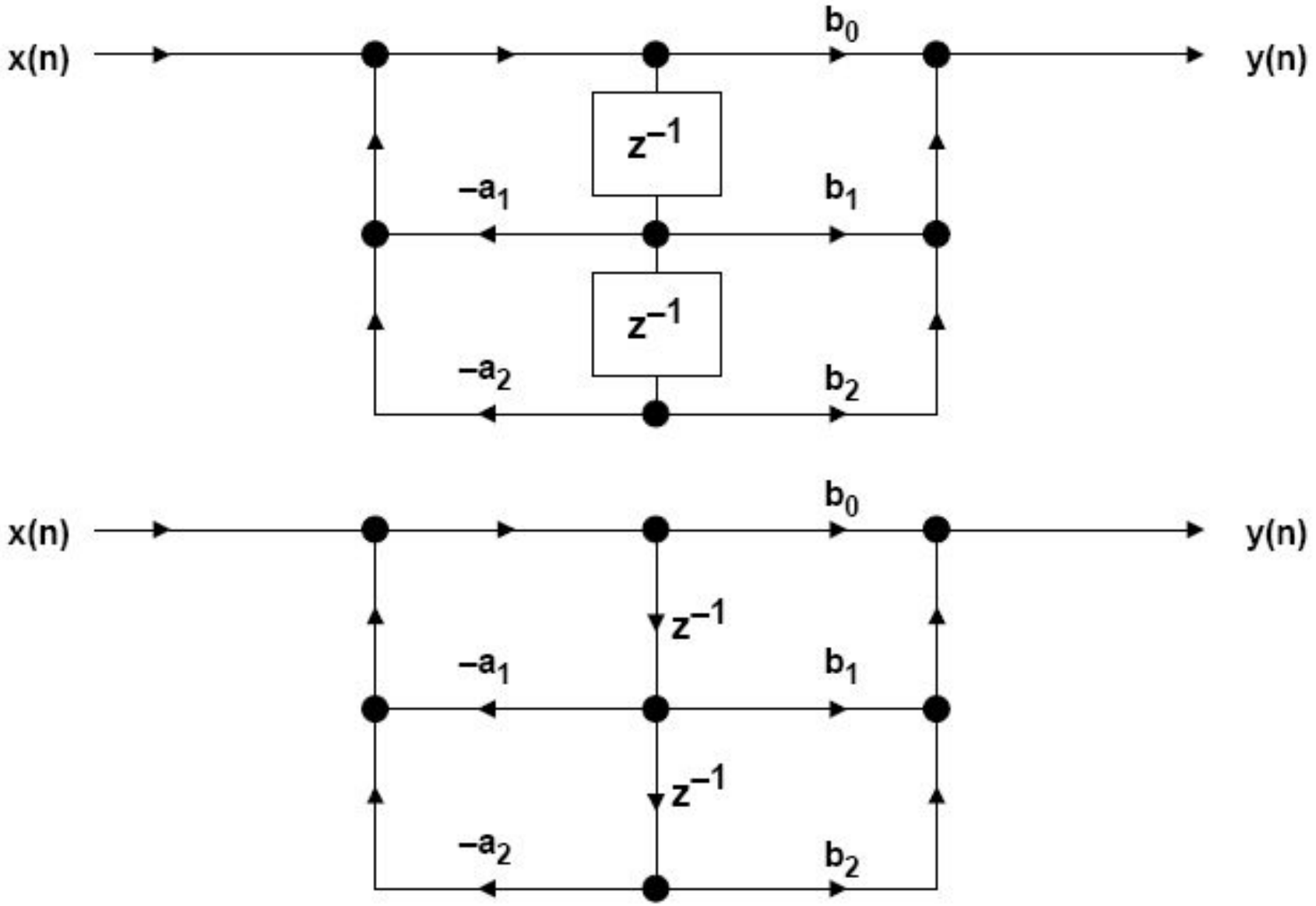

Простейшие фильтры

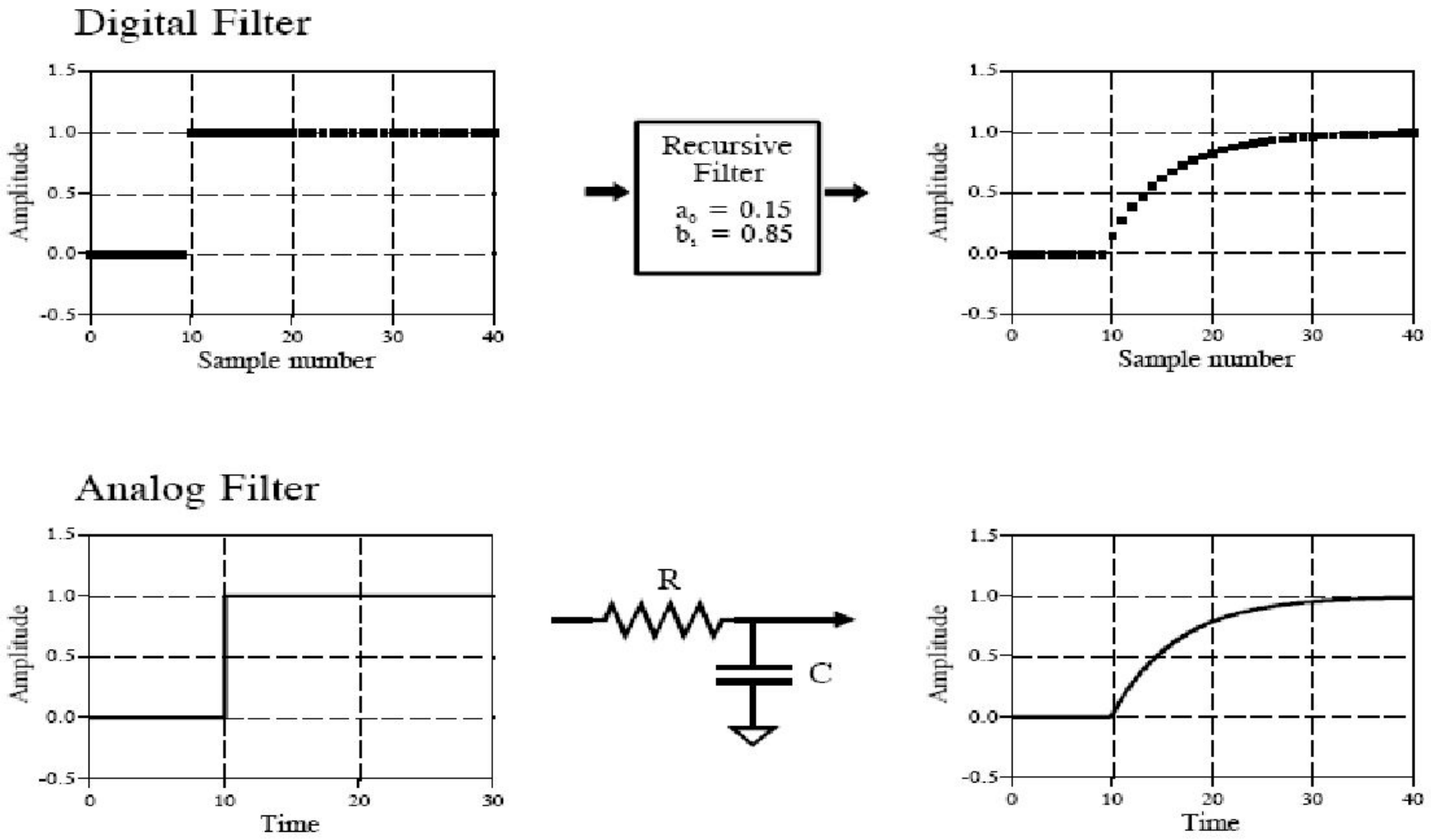

FIGURE 19-2
Single pole low-pass filter. Digital recursive filters can mimic analog filters composed of resistors and capacitors. As shown in this example, a single pole low-pass recursive filter smoothes the edge of a step input, just as an electronic RC filter.

Простейшие фильтры

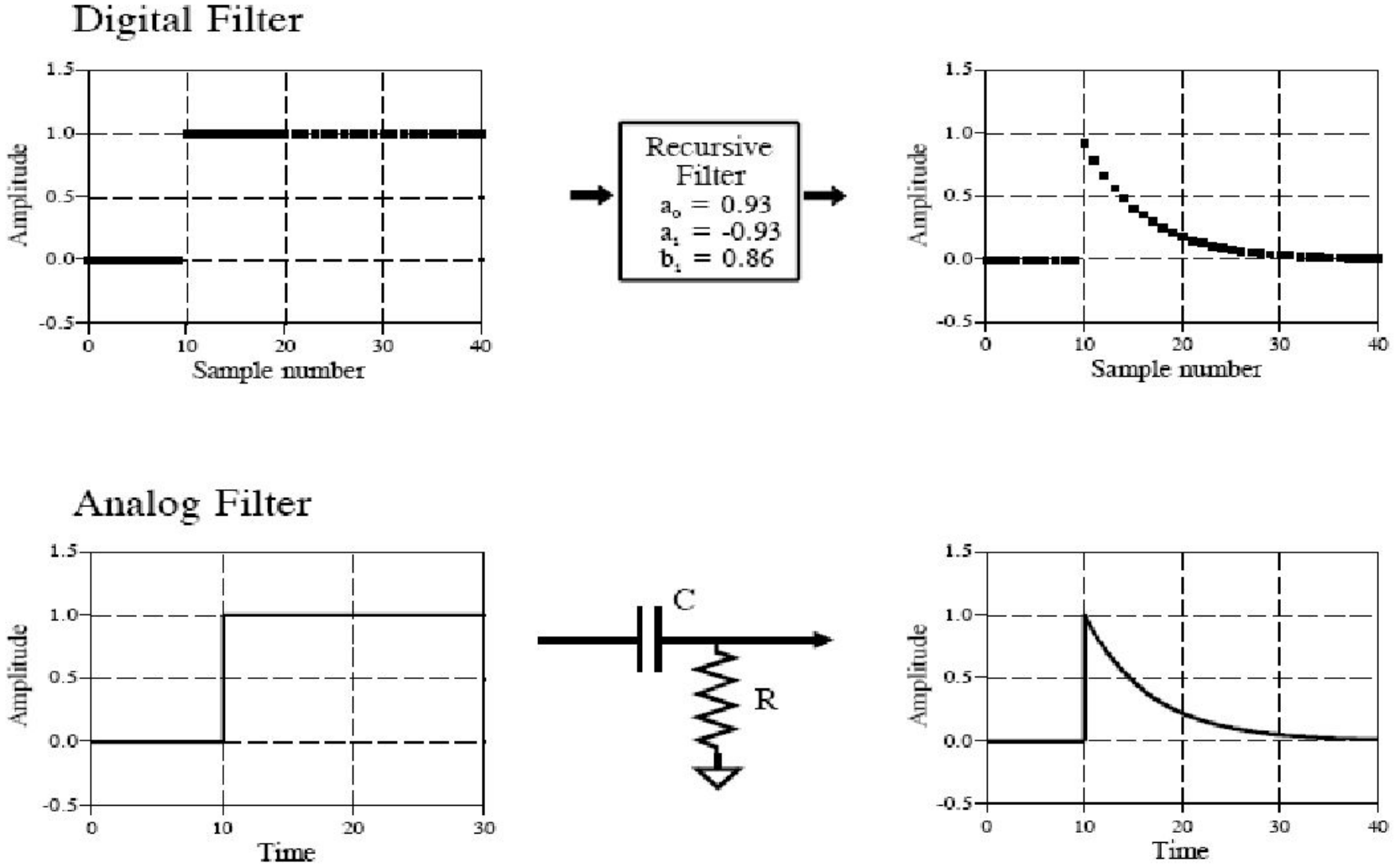

FIGURE 19-3
Single pole high-pass filter. Proper coefficient selection can also make the recursive filter mimic an electronic RC high-pass filter. These single pole recursive filters can be used in DSP just as you would use RC circuits in analog electronics.

Иллюстрация фильтрации

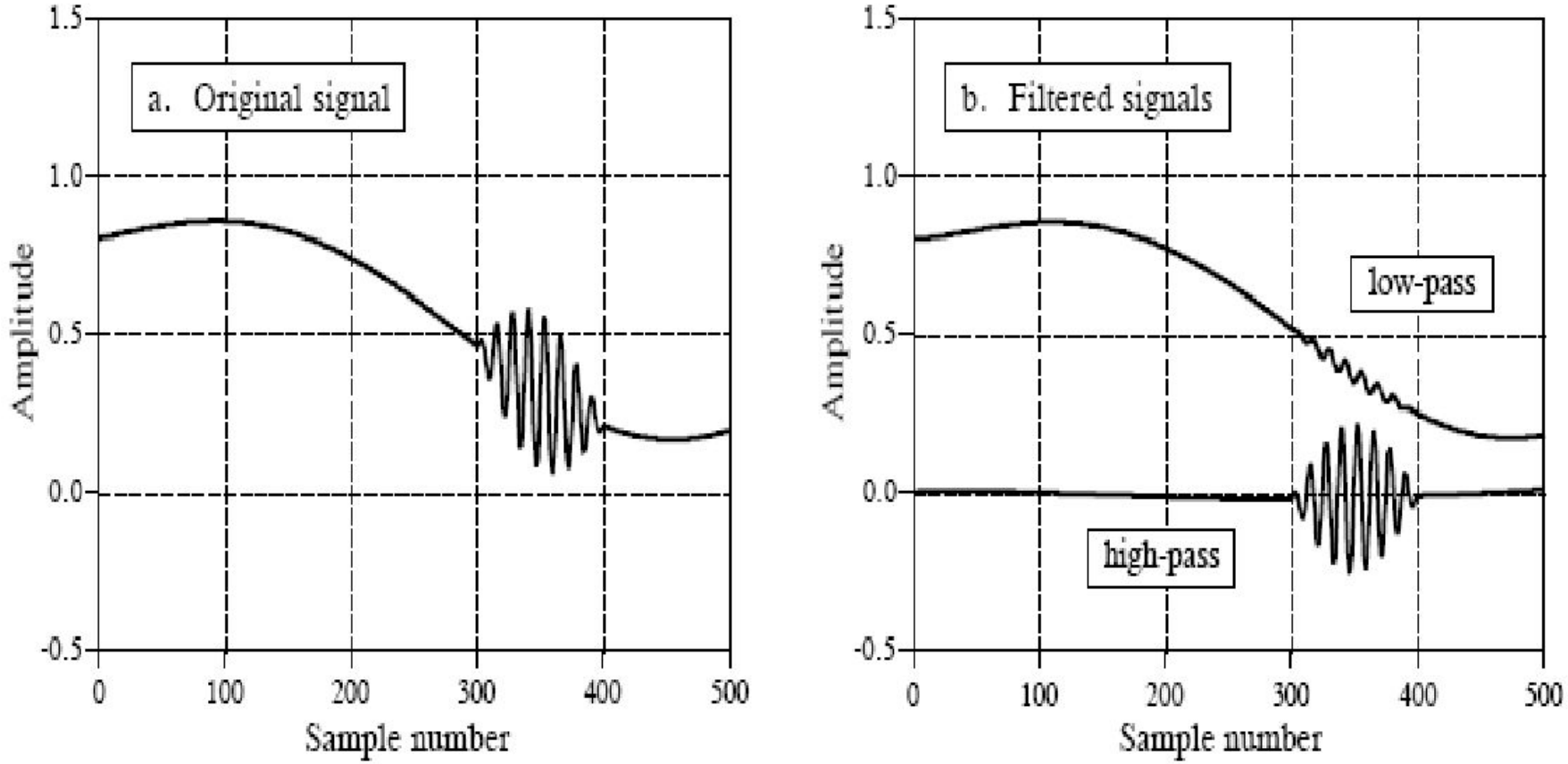

FIGURE 19-4
Example of single pole recursive filters. In (a), a high frequency burst rides on a slowly varying signal. In (b), single pole low-pass and high-pass filters are used to separate the two components. The low-pass filter uses $x = 0.95$, while the high-pass filter is for $x = 0.86$.

Переходная область

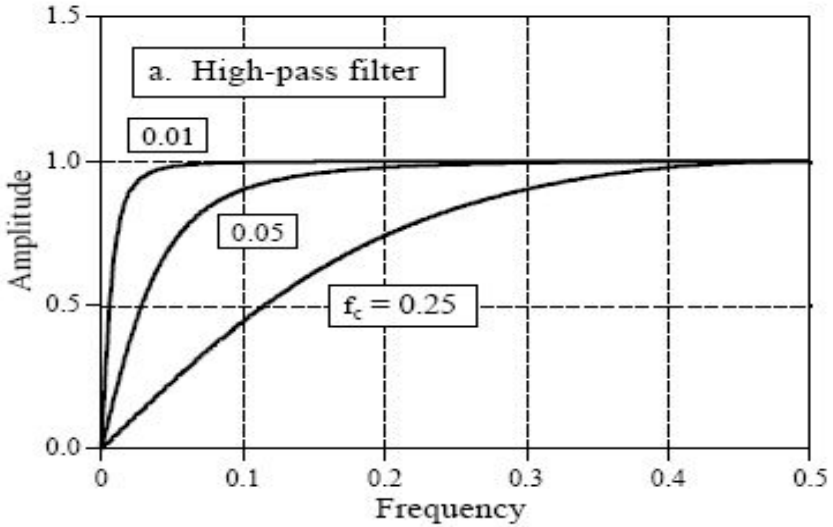

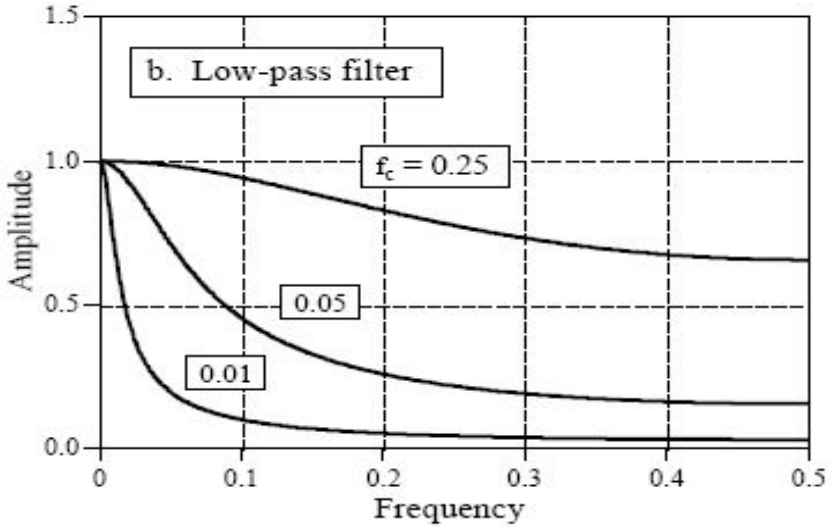

FIGURE 19-5
Single pole frequency responses. Figures (a) and (b) show the frequency responses of high-pass and low-pass single pole recursive filters, respectively. Figure (c) shows the frequency response of a cascade of four low-pass filters. The frequency response of recursive filters is not always what you expect, especially if the filter is pushed to extreme limits. For example, the f_C = 0.25 curve in (c) is quite useless. Many factors are to blame, including: aliasing, round-off noise, and the nonlinear phase response.

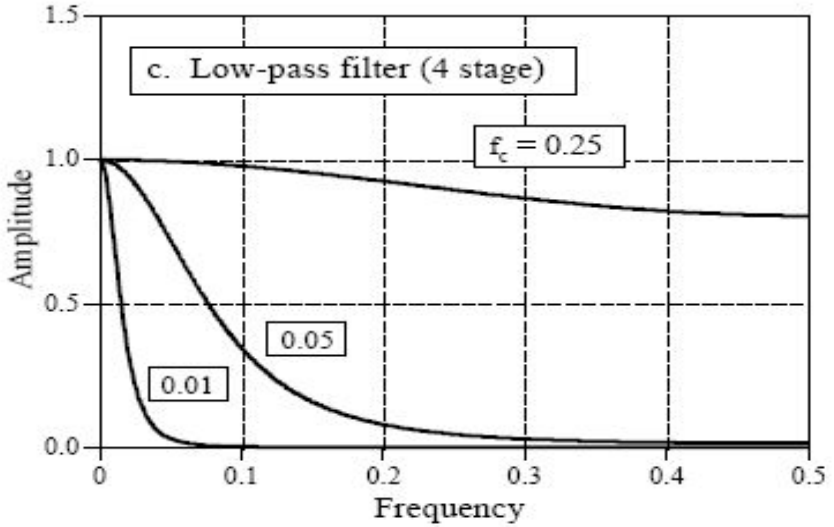

Узкополосная фильтрация

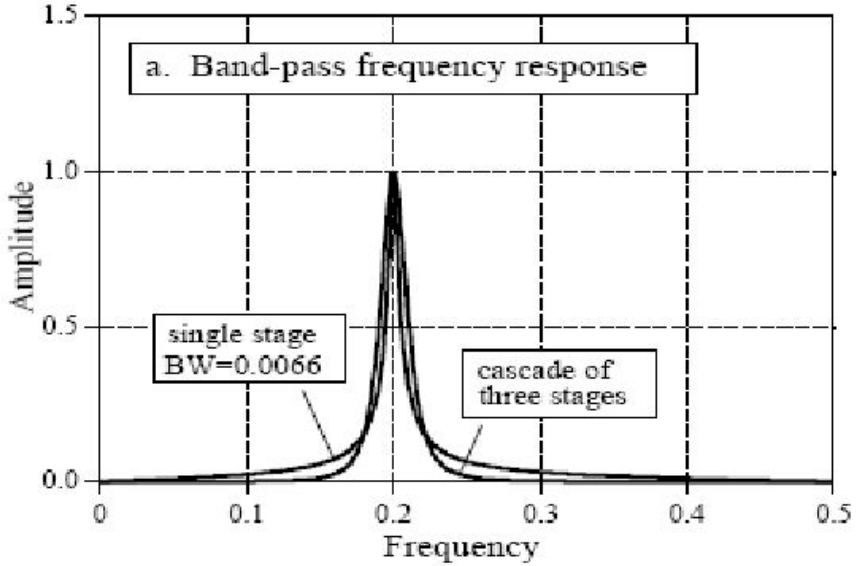

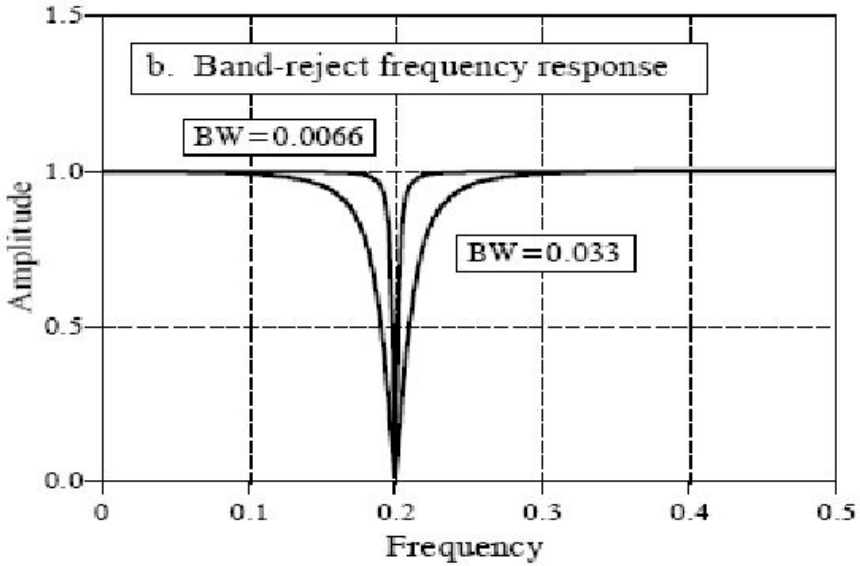

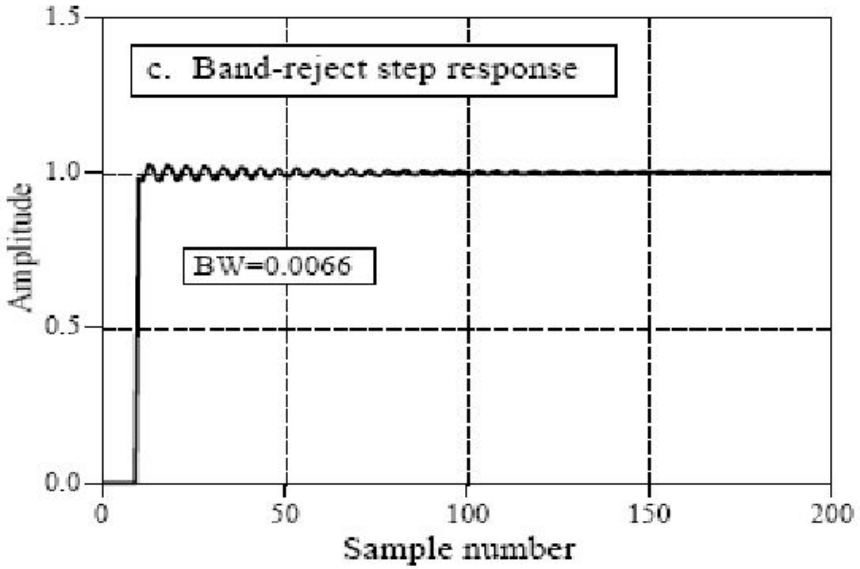

FIGURE 19-6
Characteristics of narrow-band filters. Figure (a) and (b) shows the frequency responses of various band-pass and band-reject filters. The step response of the band-reject filter is shown in (c). The band-reject (notch) filter is useful for removing 60 Hz and similar interference from time domain encoded waveforms.

Фильтры

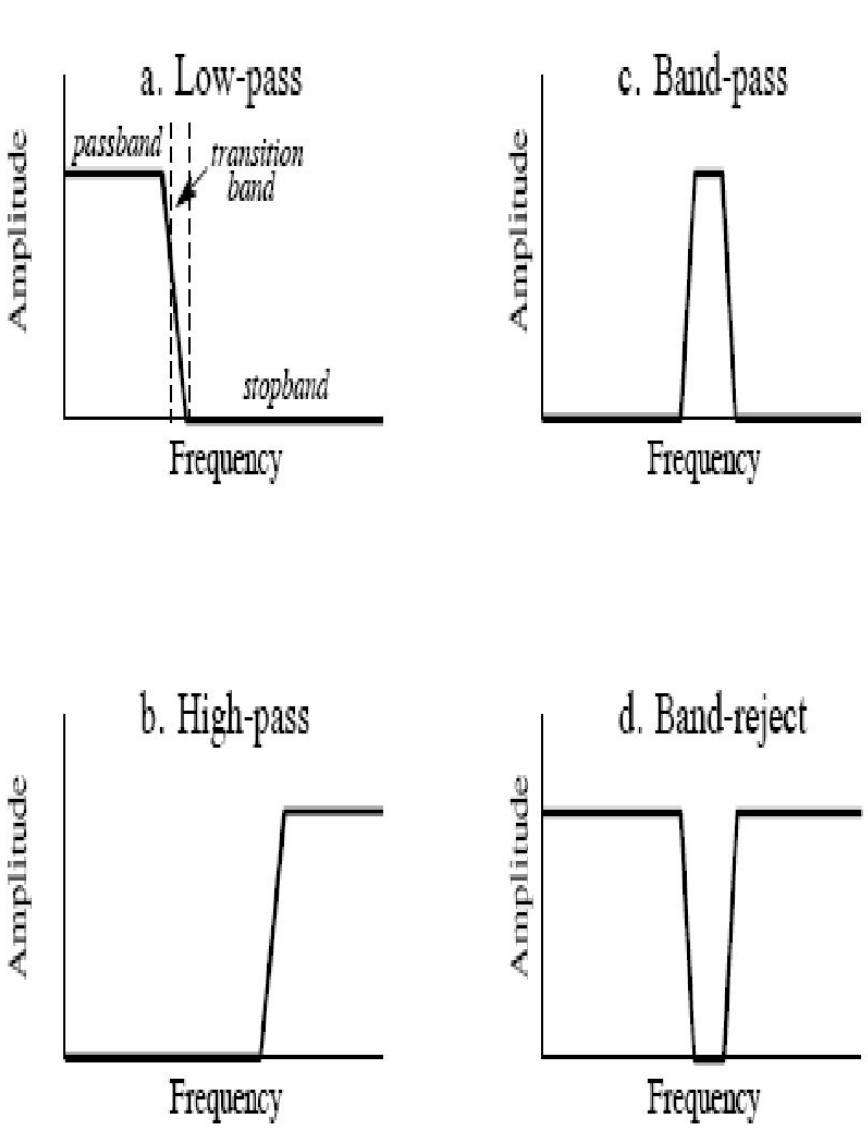

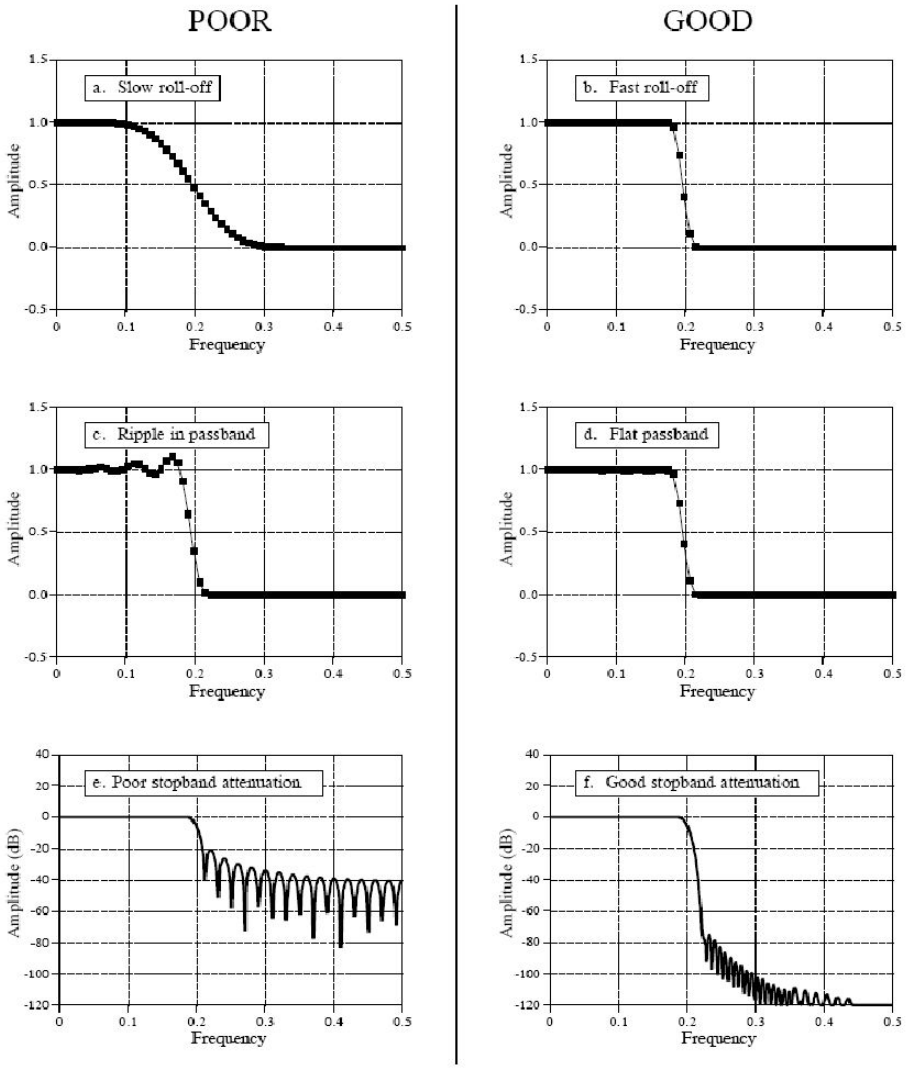

FIGURE 14-4
Parameters for evaluating *frequency domain* performance. The frequency responses shown are for low-pass filters. Three parameters are important: (1) roll-off sharpness, shown in (a) and (b), (2) passband ripple, shown in (c) and (d), and (3) stopband attenuation, shown in (e) and (f).

Варианты сборки

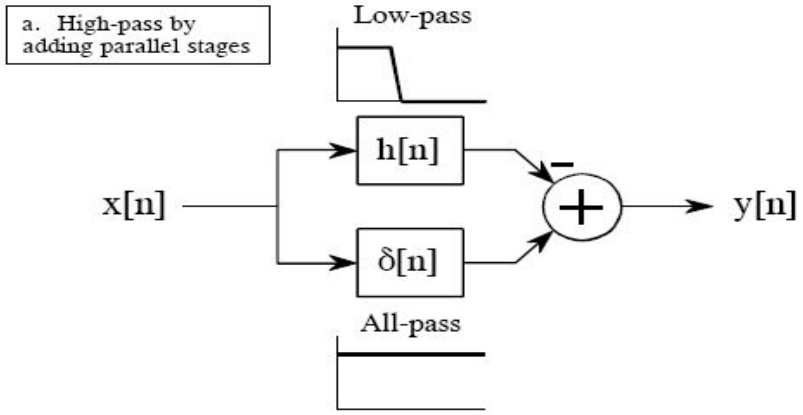

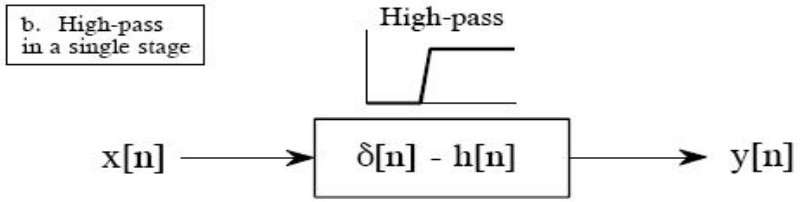

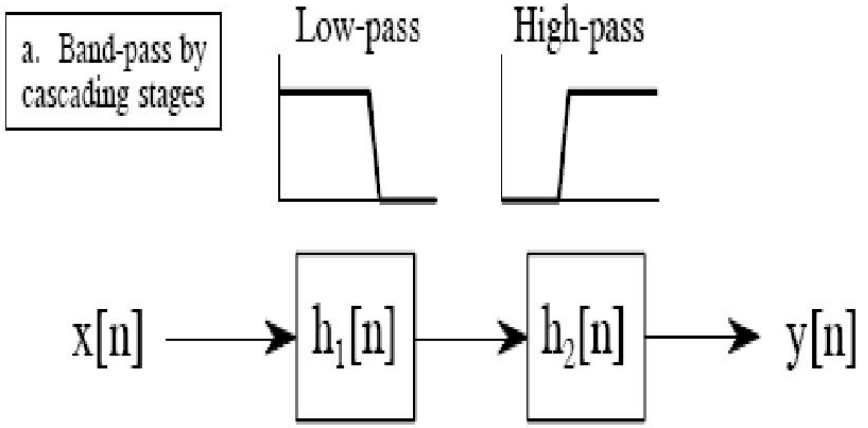

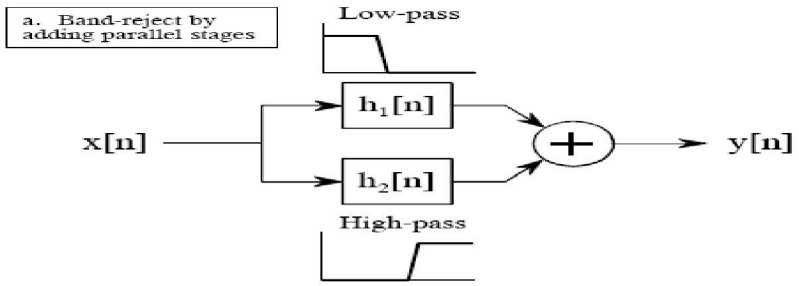

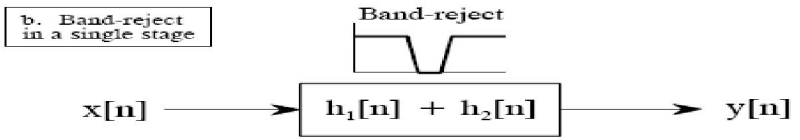

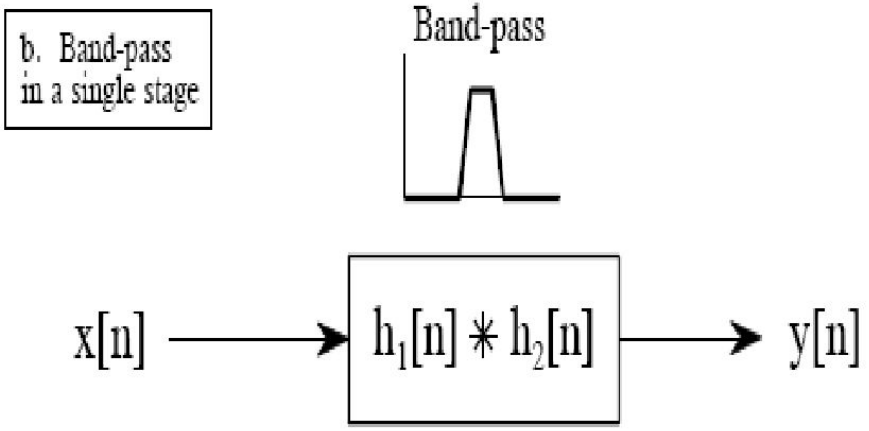

Параметры фильтров

	Voltage gain at DC	Step Response			Frequency Response		
		Overshoot	Time to settle to 1%	Time to settle to 0.1%	Ripple in passband	Frequency for x100 attenuation	Frequency for x1000 attenuation
Bessel							
2 pole	1.27	0.4%	0.60	1.12	0%	12.74	40.4
4 pole	1.91	0.9%	0.66	1.20	0%	4.74	8.45
6 pole	2.87	0.7%	0.74	1.18	0%	3.65	5.43
8 pole	4.32	0.4%	0.80	1.16	0%	3.35	4.53
Butterworth							
2 pole	1.59	4.3%	1.06	1.66	0%	10.0	31.6
4 pole	2.58	10.9%	1.68	2.74	0%	3.17	5.62
6 pole	4.21	14.3%	2.74	3.92	0%	2.16	3.17
8 pole	6.84	16.4%	3.50	5.12	0%	1.78	2.38
Chebyshev							
2 pole	1.84	10.8%	1.10	1.62	6%	12.33	38.9
4 pole	4.21	18.2%	3.04	5.42	6%	2.59	4.47
6 pole	10.71	21.3%	5.86	10.4	6%	1.63	2.26
8 pole	28.58	23.0%	8.34	16.4	6%	1.34	1.66

TABLE 3-2
Characteristics of the three classic filters. The Bessel filter provides the best step response, making it the choice for time domain encoded signals. The Chebyshev and Butterworth filters are used to eliminate frequencies in the stopband, making them ideal for frequency domain encoded signals. Values in this table are in the units of *seconds* and *hertz*, for a one hertz cutoff frequency.

Прохождение ступеньки

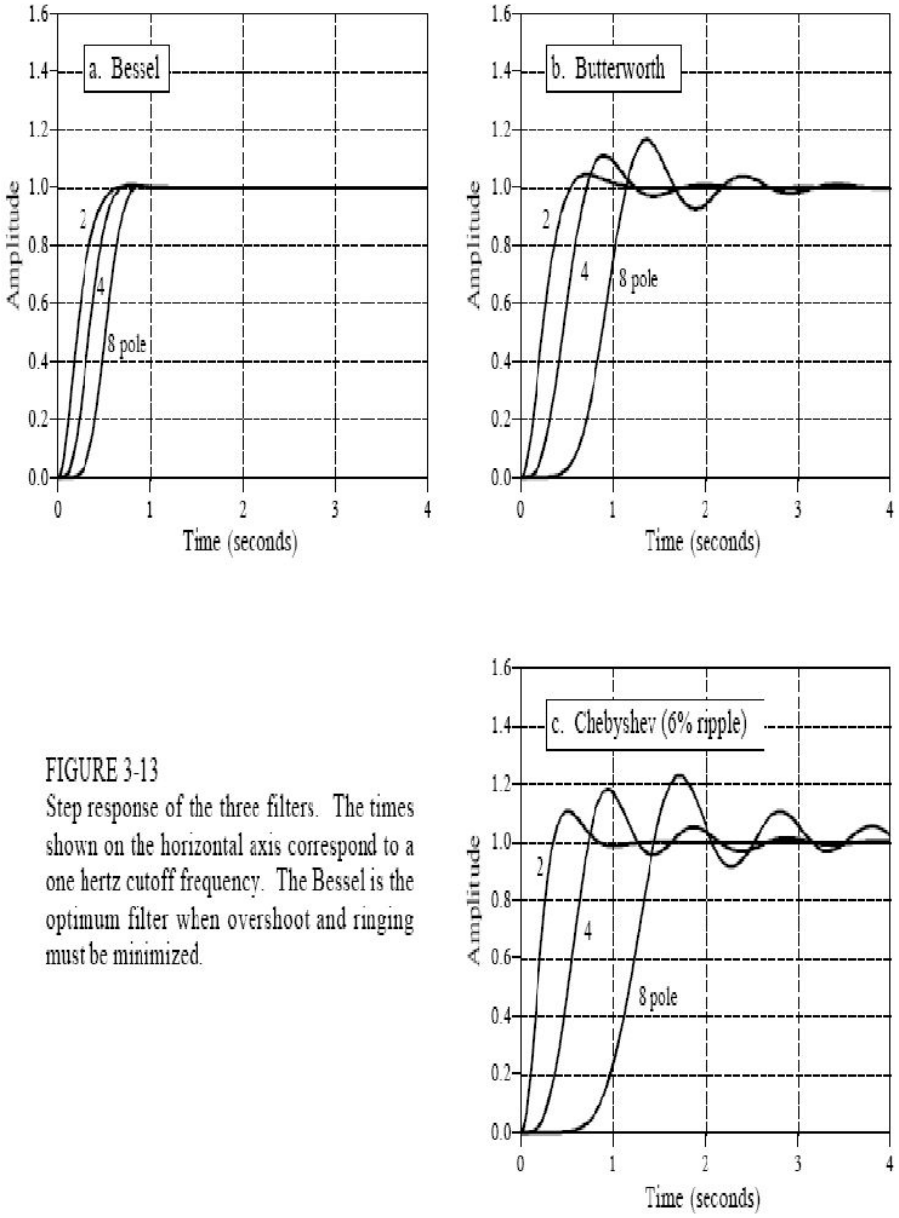

FIGURE 3-13
Step response of the three filters. The times shown on the horizontal axis correspond to a one hertz cutoff frequency. The Bessel is the optimum filter when overshoot and ringing must be minimized.

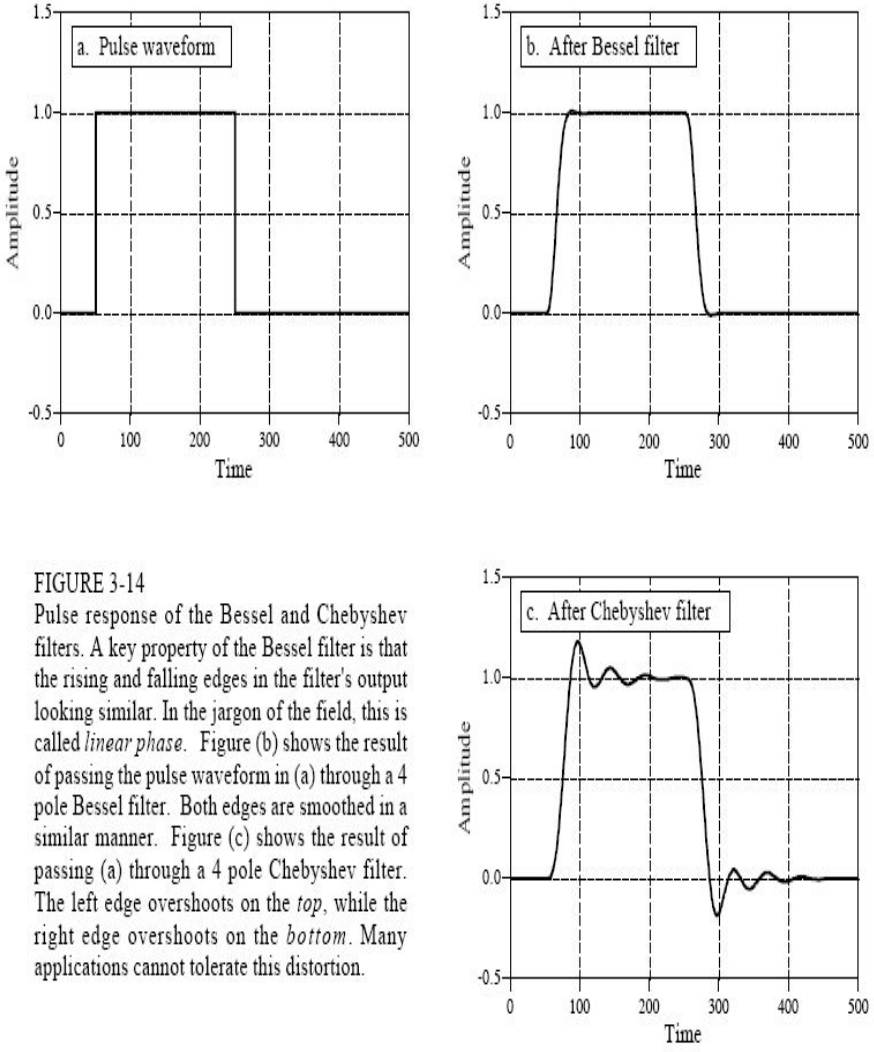

FIGURE 3-14
Pulse response of the Bessel and Chebyshev filters. A key property of the Bessel filter is that the rising and falling edges in the filter's output looking similar. In the jargon of the field, this is called *linear phase*. Figure (b) shows the result of passing the pulse waveform in (a) through a 4 pole Bessel filter. Both edges are smoothed in a similar manner. Figure (c) shows the result of passing (a) through a 4 pole Chebyshev filter. The left edge overshoots on the *top*, while the right edge overshoots on the *bottom*. Many applications cannot tolerate this distortion.

АЧХ фильтров

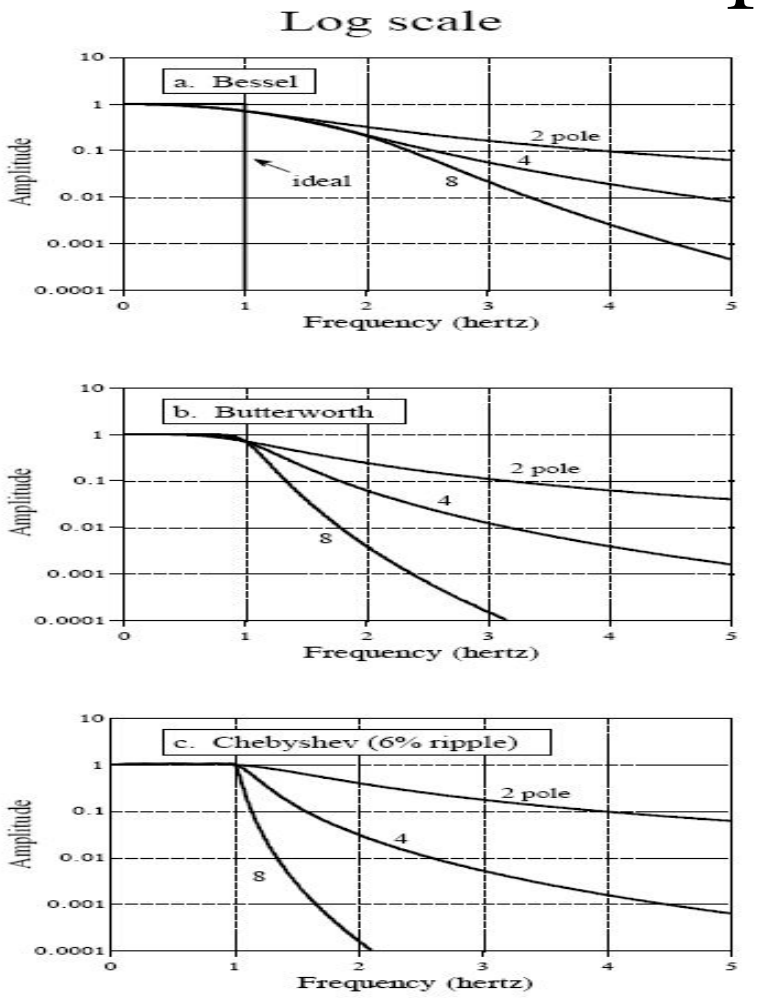

FIGURE 3-11
Frequency response of the three filters on a *logarithmic* scale. The Chebyshev filter has the sharpest roll-off.

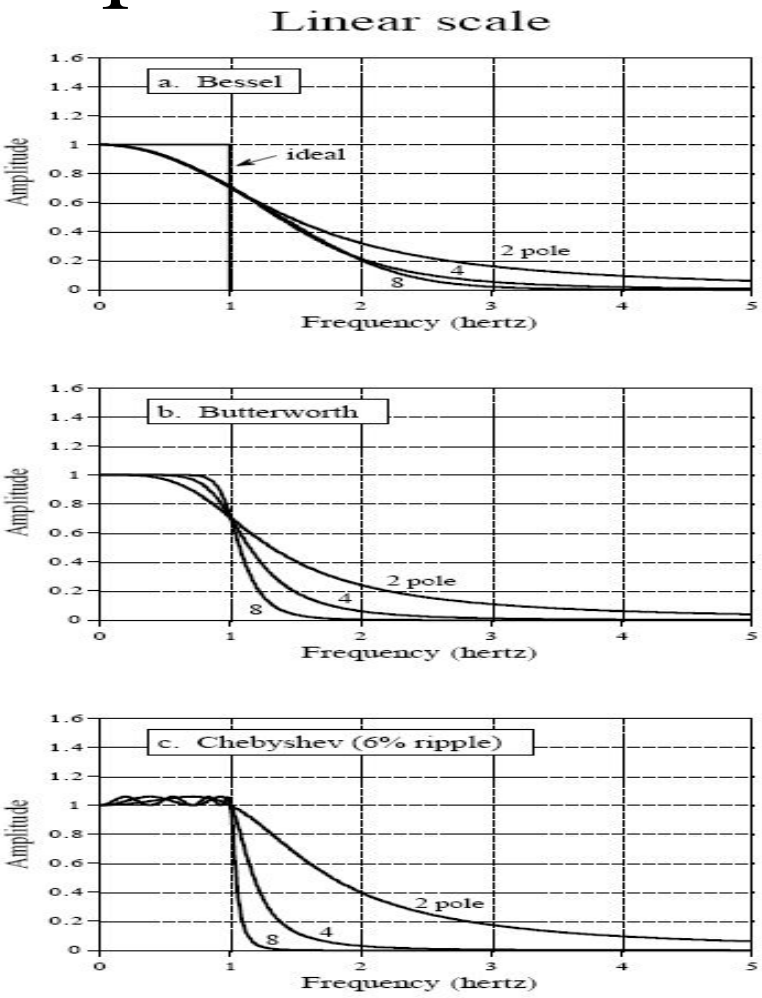

FIGURE 3-12
Frequency response of the three filters on a *linear* scale. The Butterworth filter provides the flattest passband.

in Fig. 3-12. **Passband ripple** can now be seen in the Chebyshev filter (wavy variations in the amplitude of the passed frequencies). In fact, the Chebyshev filter obtains its excellent roll-off by *allowing* this passband ripple. When more passband ripple is allowed in a filter, a faster roll-off

Влияние временного окна

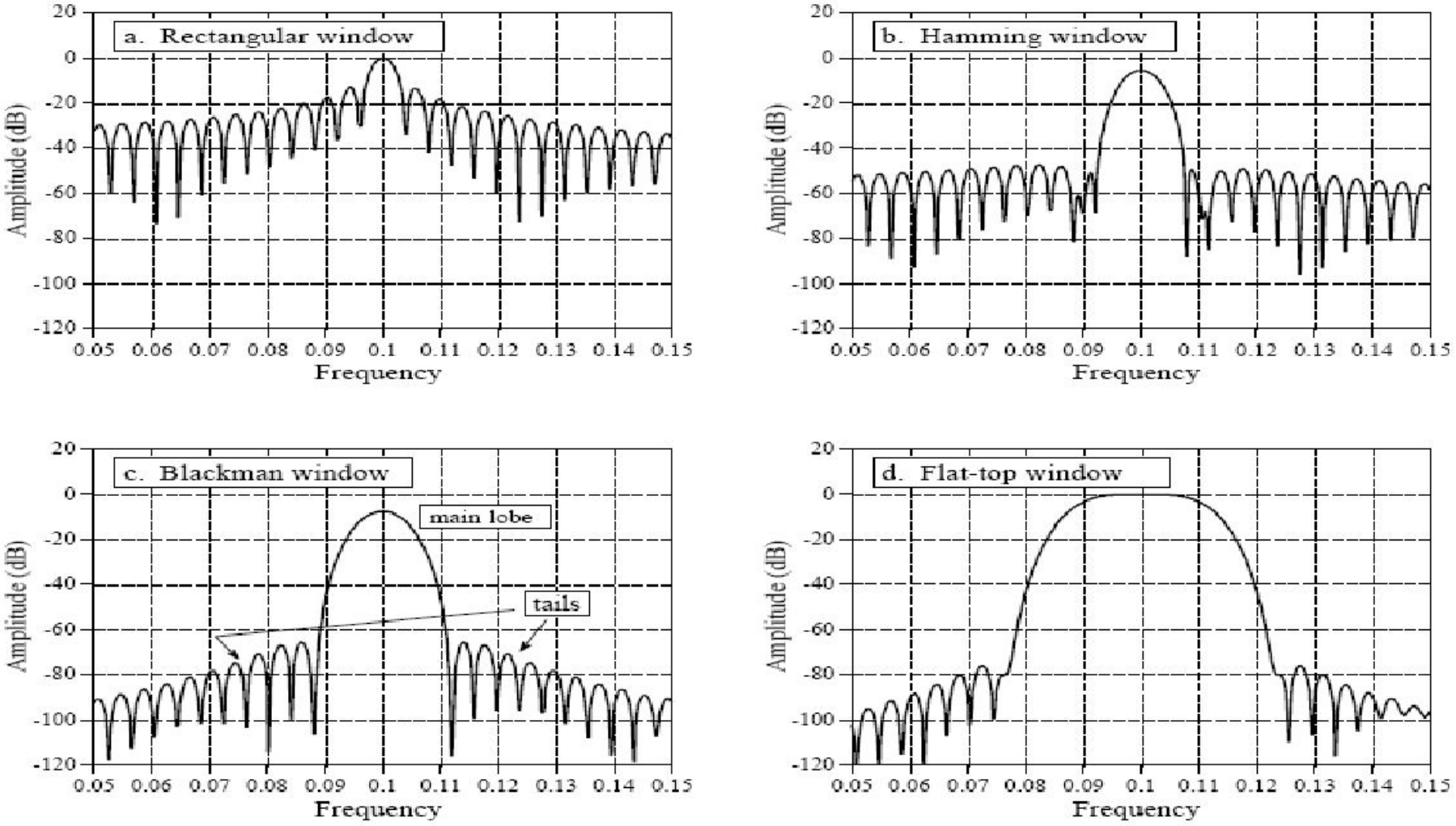

FIGURE 9-5
Detailed view of a spectral peak using various windows. Each peak in the frequency spectrum is a central lobe surrounded by tails formed from side lobes. By changing the window shape, the amplitude of the side lobes can be reduced at the expense of making the main lobe wider. The rectangular window, (a), has the narrowest main lobe but the largest amplitude side lobes. The Hamming window, (b), and the Blackman window, (c), have lower amplitude side lobes at the expense of a wider main lobe. The flat-top window, (d), is used when the amplitude of a peak must be accurately measured. These curves are for 255 point windows; longer windows produce proportionately narrower peaks.

Инверсия вида фильтра

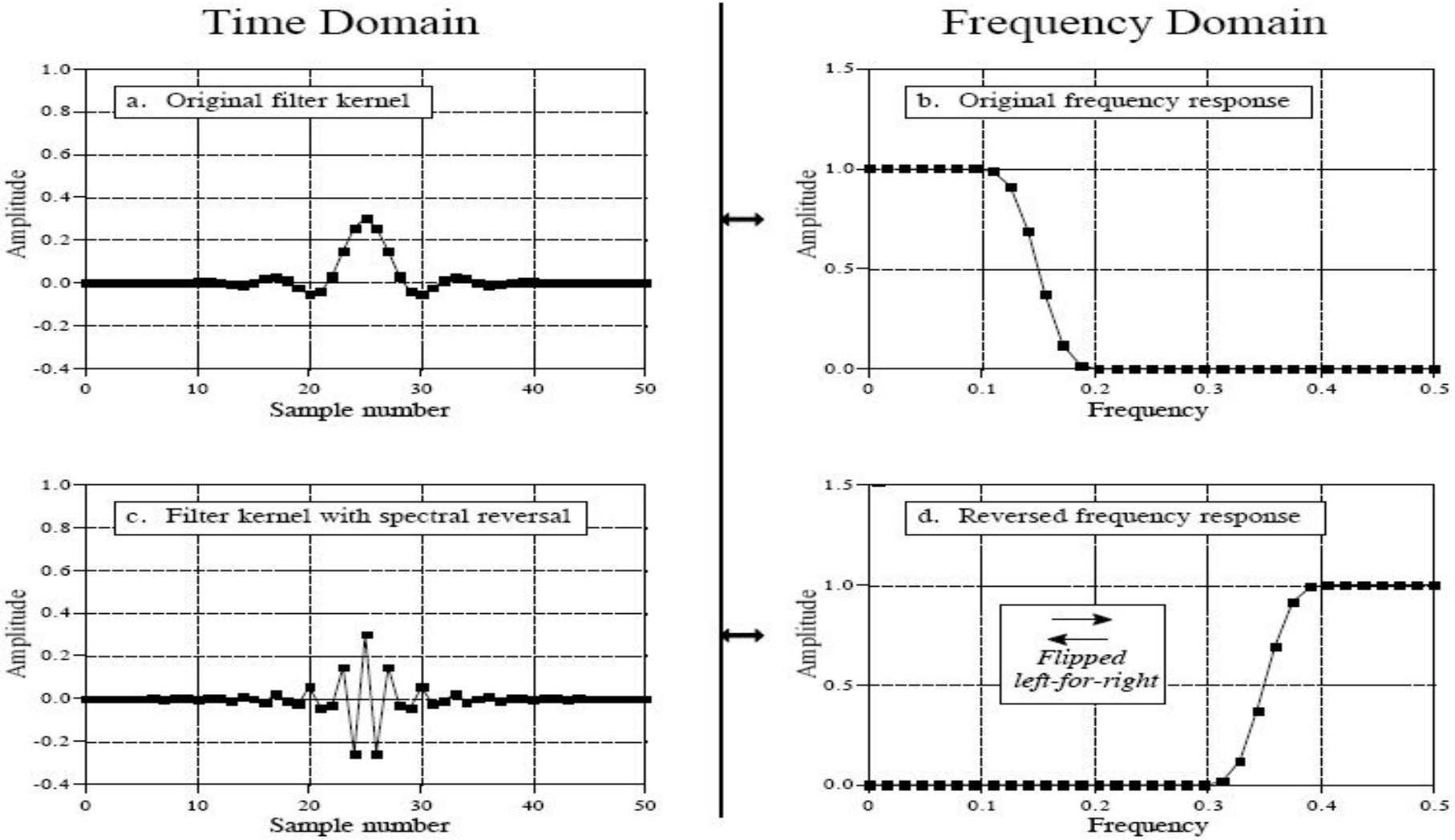

FIGURE 14-7
Example of spectral reversal. The low-pass filter kernel in (a) has the frequency response shown in (b). A high-pass filter kernel, (c), is formed by changing the sign of every other sample in (a). This action in the time domain results in the frequency domain being flipped *left-for-right*, resulting in the high-pass frequency response shown in (d).

Усредняющий фильтр

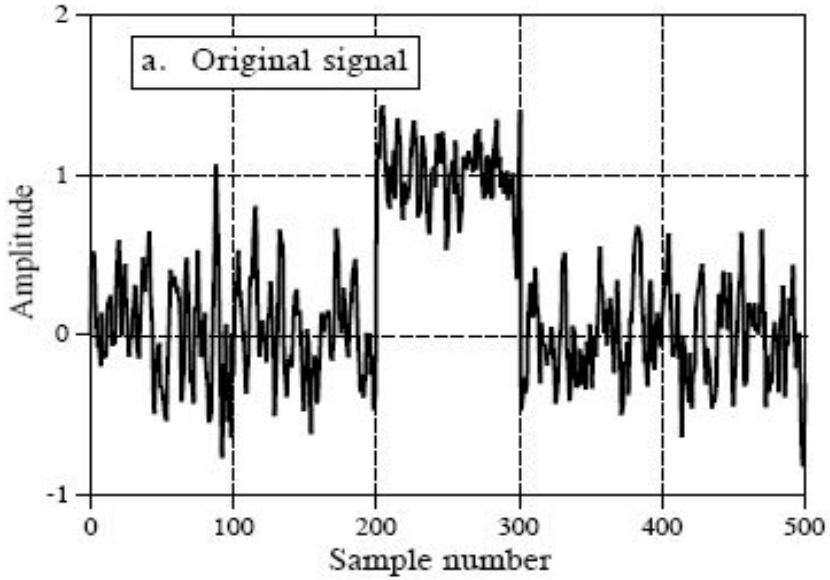

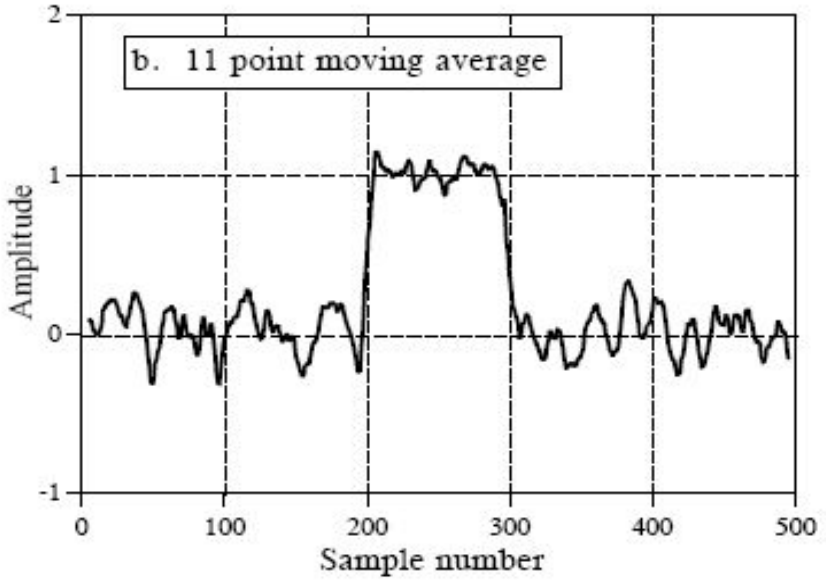

FIGURE 15-1
Example of a moving average filter. In (a), a rectangular pulse is buried in random noise. In (b) and (c), this signal is filtered with 11 and 51 point moving average filters, respectively. As the number of points in the filter increases, the

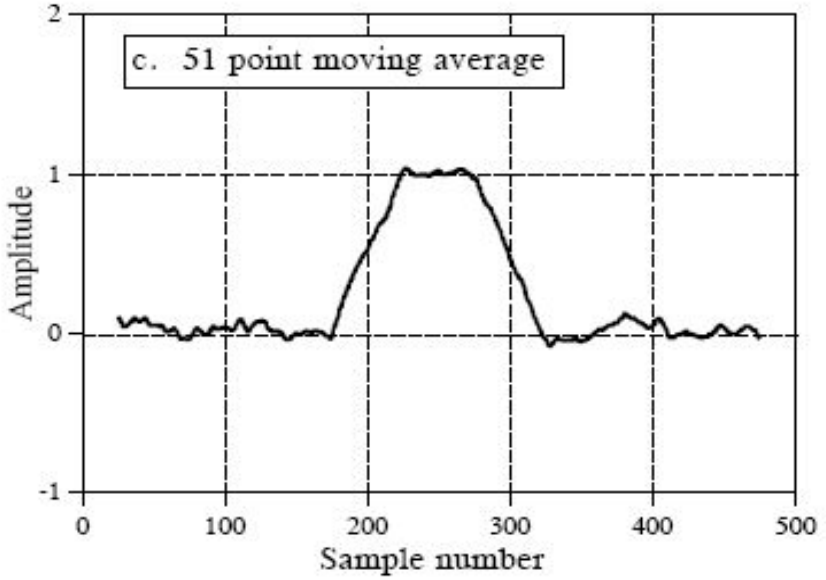

$$y[i] = \frac{1}{M} \sum_{j=0}^{M-1} x[i+j]$$

Чем больше точек тем лучше фильтрация

MOVING AVERAGE FILTER FREQUENCY RESPONSE

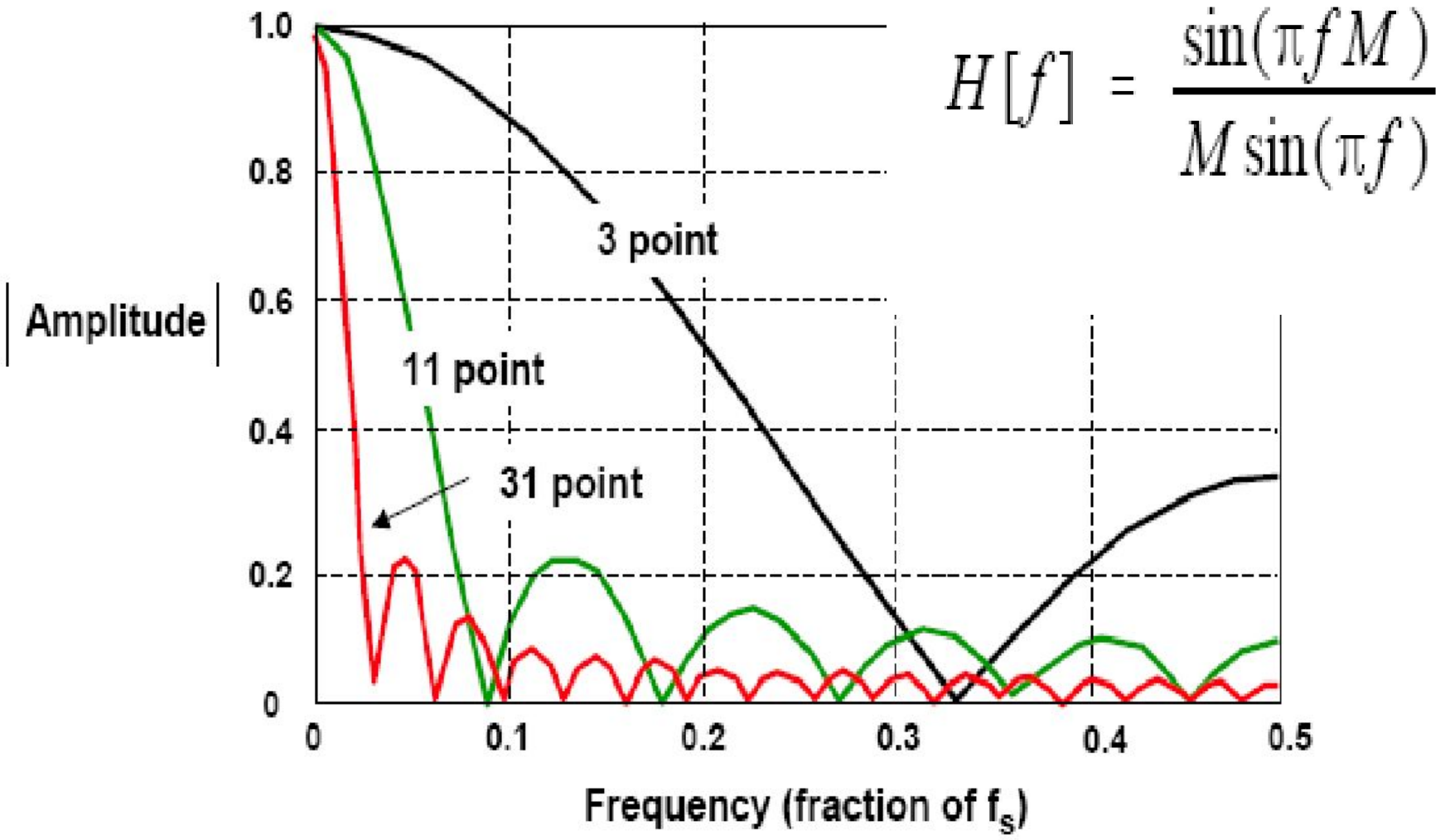

4-POINT MOVING AVERAGE FILTER

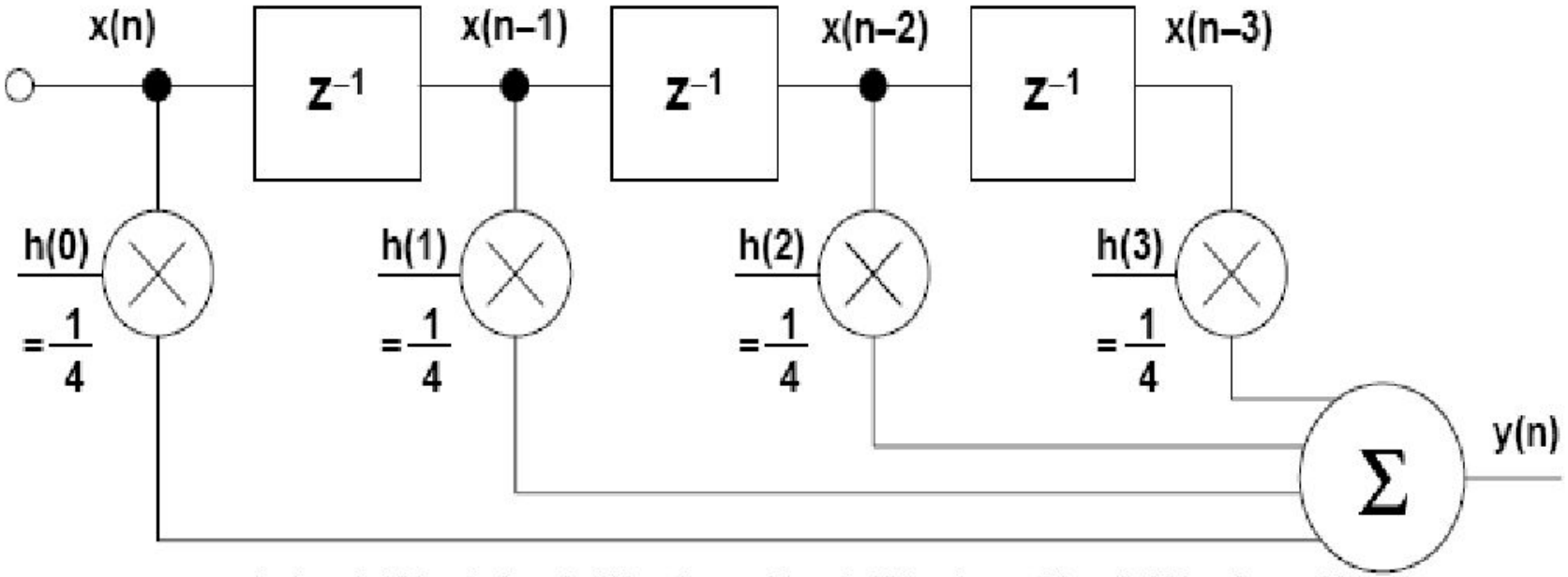

$$y(n) = h(0)\,x(n) + h(1)\,x(n-1) + h(2)\,x(n-2) + h(3)\,x(n-3)$$

$$= \frac{1}{4}\,x(n) + \frac{1}{4}\,x(n-1) + \frac{1}{4}\,x(n-2) + \frac{1}{4}\,x(n-3)$$

$$= \frac{1}{4}\left[x(n) + x(n-1) + x(n-2) + x(n-3)\right]$$

For N-Point Moving Average Filter:

$$y(n) = \frac{1}{N}\sum_{k=0}^{N-1} x(n-k)$$

CALCULATING OUTPUT OF 4-POINT MOVING AVERAGE FILTER

$$y(3) = 0.25\,[\,x(3) + x(2) + x(1) + x(0)\,]$$

$$y(4) = 0.25\,[\,x(4) + x(3) + x(2) + x(1)\,]$$

$$y(5) = 0.25\,[\,x(5) + x(4) + x(3) + x(2)\,]$$

$$y(6) = 0.25\,[\,x(6) + x(5) + x(4) + x(3)\,]$$

$$y(7) = 0.25\,[\,x(7) + x(6) + x(5) + x(4)\,]$$

- Each Output Requires:
  1 multiplication, 1 addition, 1 subtraction

4-TAP MOVING AVERAGE FILTER STEP RESPONSE

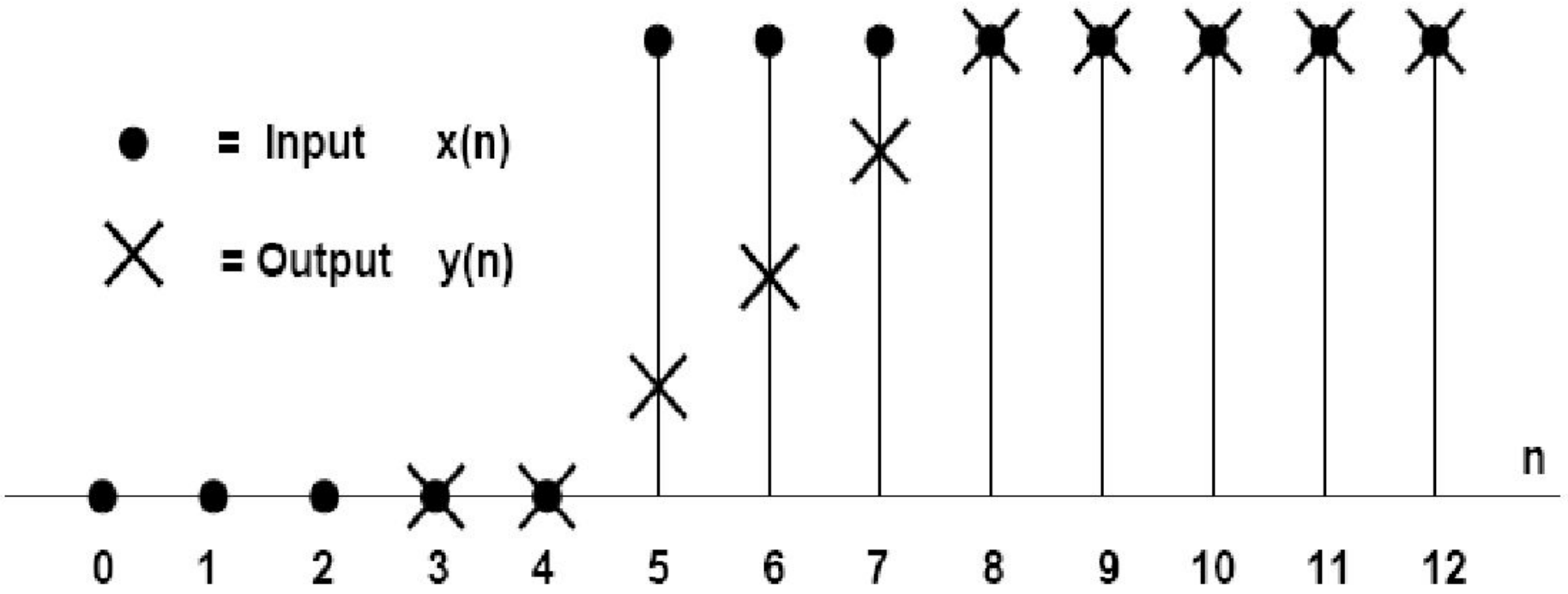

- General: $y(n) = \frac{1}{N} \sum_{k=0}^{N-1} x(n-k)$

- For N = 4: $y(n) = \frac{1}{4} \sum_{k=0}^{3} x(n-k)$

MOVING AVERAGE FILTER RESPONSE TO NOISE SUPERIMPOSED ON STEP INPUT

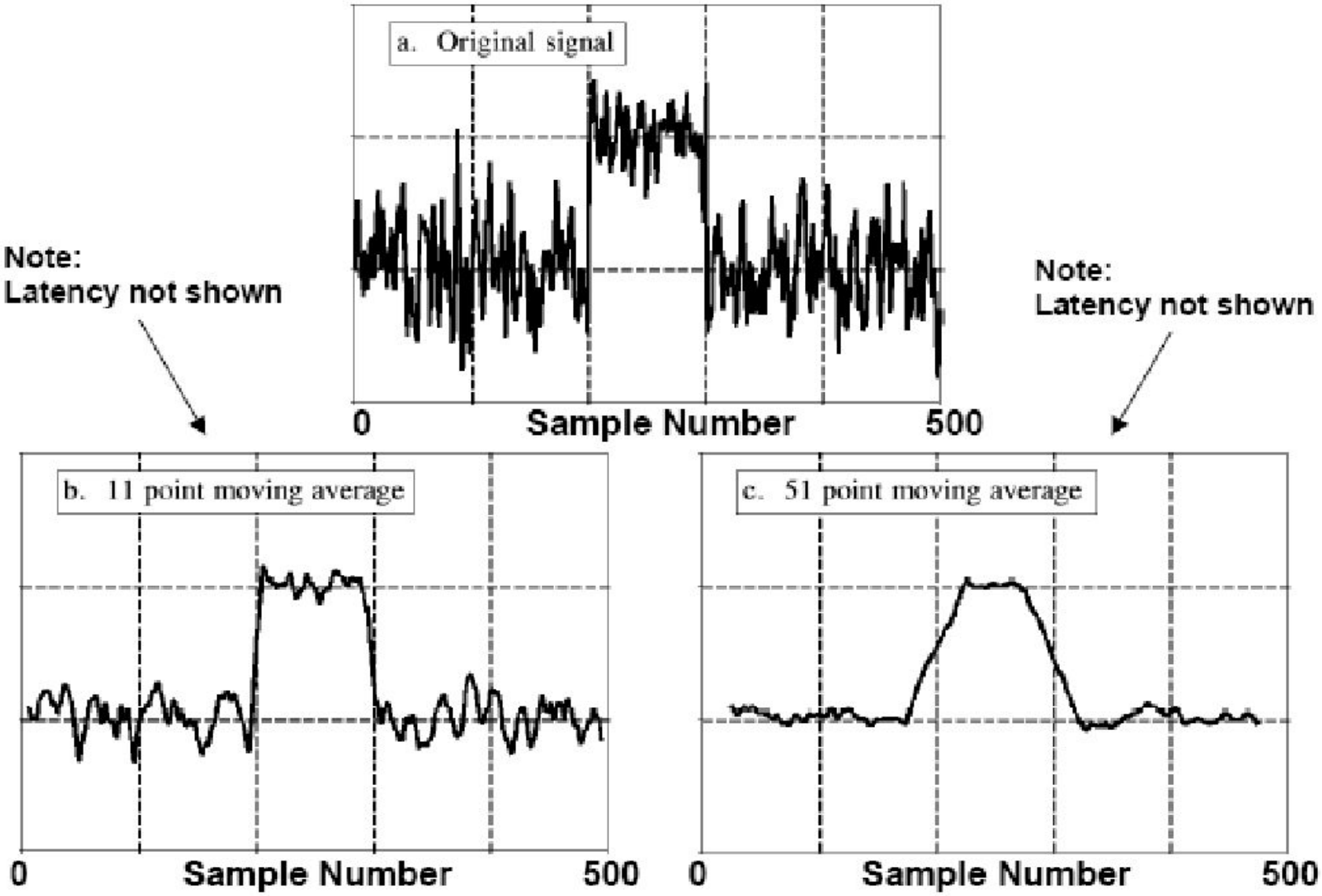

Виды осреднений

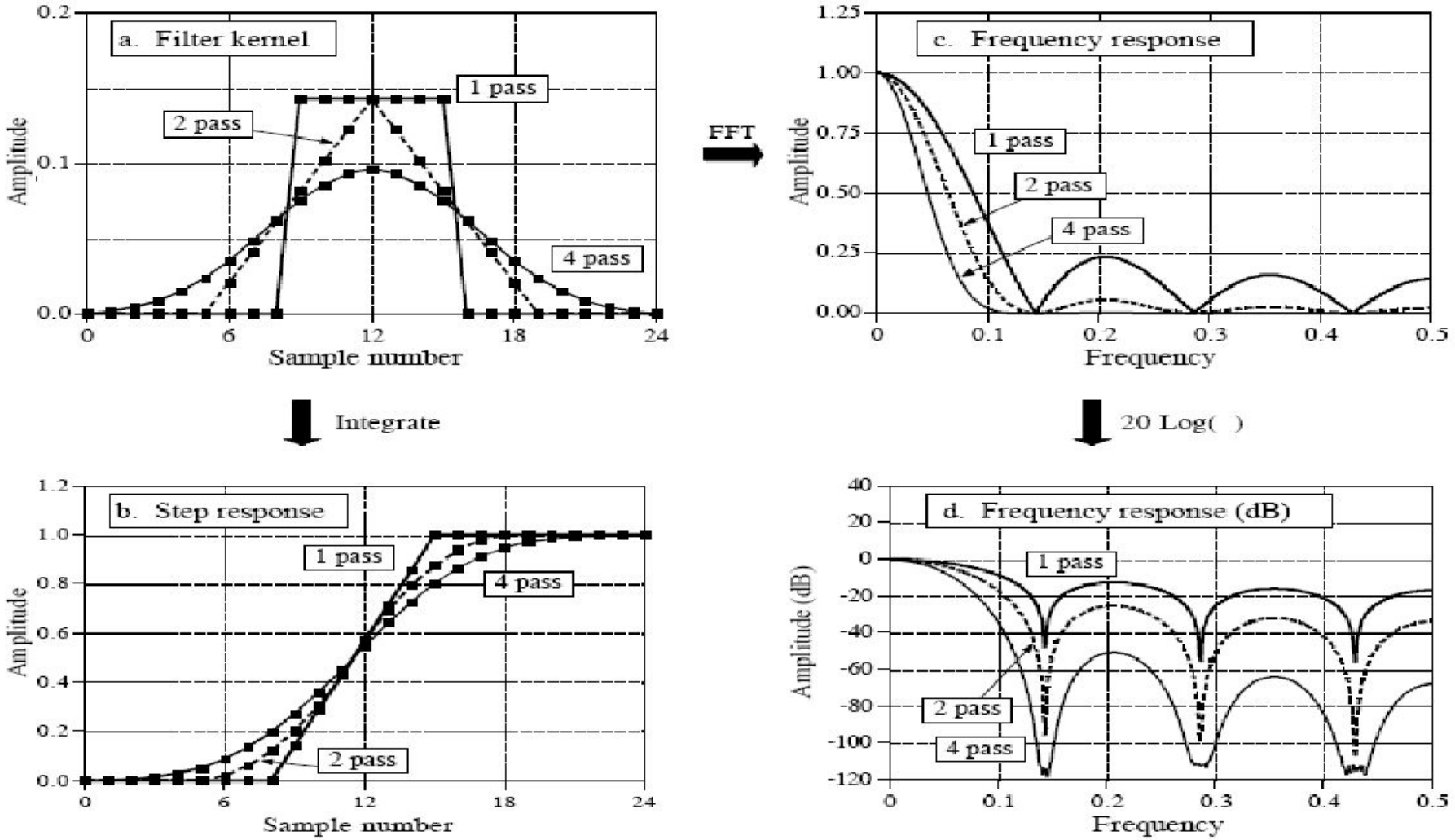

FIGURE 15-3
Characteristics of multiple-pass moving average filters. Figure (a) shows the filter kernels resulting from passing a seven point moving average filter over the data once, twice and four times. Figure (b) shows the corresponding step responses, while (c) and (d) show the corresponding frequency responses.

Характеристики фильтров

FIGURE 15-4
Frequency response of the Blackman window and Gaussian filter kernels. Both these filters provide better stopband attenuation than the moving average filter. This has no advantage in removing random noise from time domain encoded signals, but it can be useful in mixed domain problems. The disadvantage of these filters is that they must use *convolution*, a terribly slow algorithm.

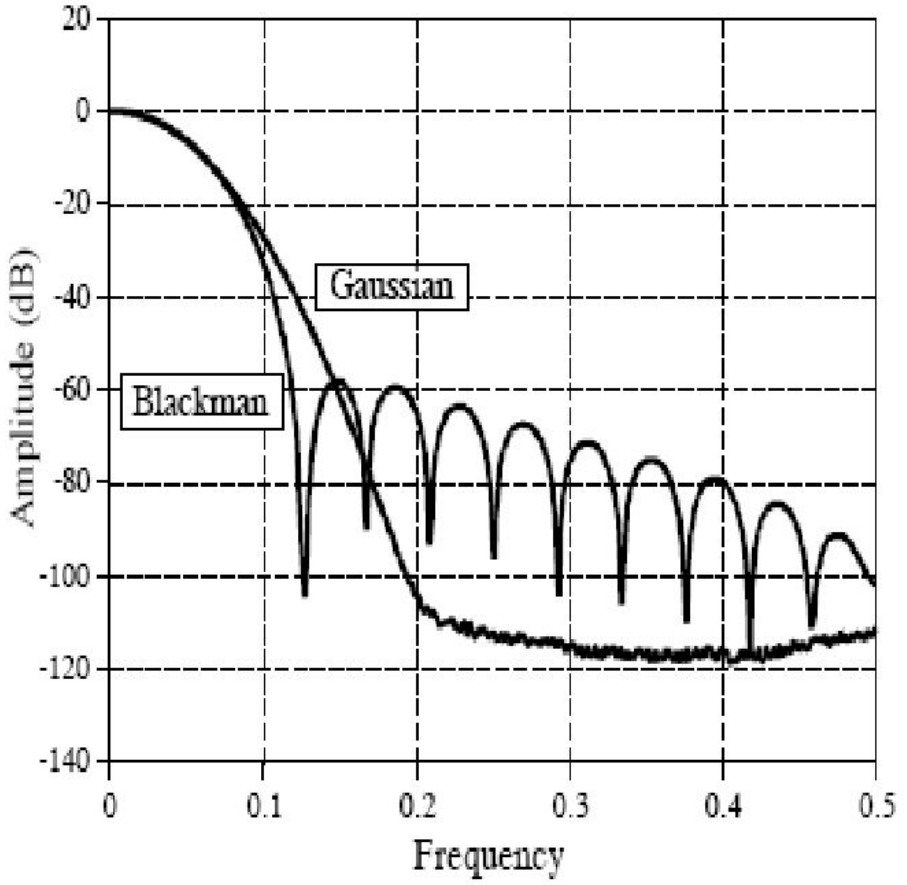

Влияние ошибок вычисления

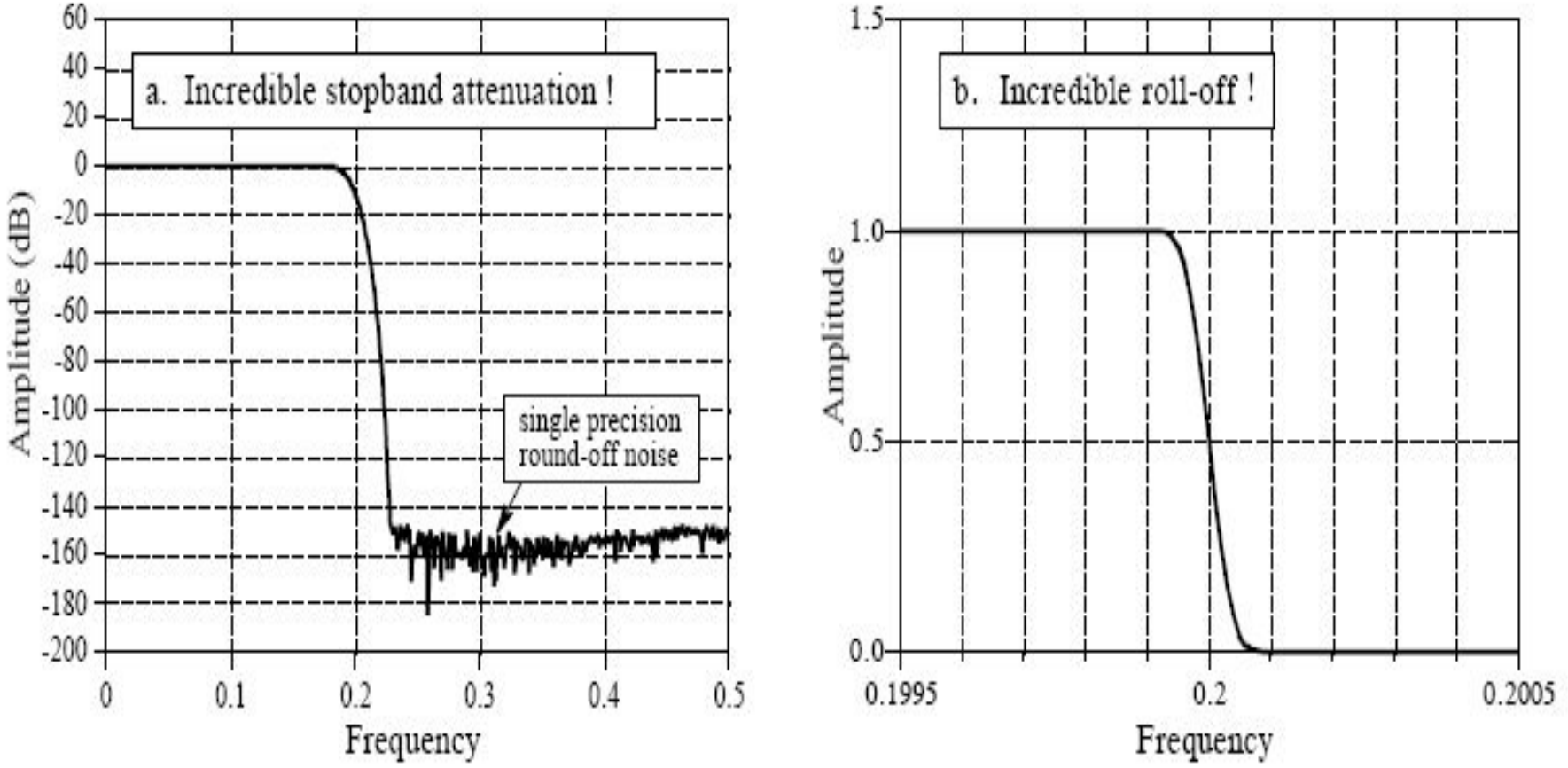

FIGURE 16-7
The incredible performance of the windowed-sinc filter. Figure (a) shows the frequency response of a windowed-sinc filter with increased stopband attenuation. This is achieved by convolving a windowed-sinc filter kernel with itself. Figure (b) shows the very rapid roll-off a 32,001 point windowed-sinc filter.

Оптимальная фильтрация

EQUATION 17-1
The Wiener filter. The frequency response, represented by $H[f]$, is determined by the frequency spectra of the noise, $N[f]$, and the signal, $S[f]$. Only the magnitudes are important; all of the phases are zero.

$$H[f] = \frac{S[f]^2}{S[f]^2 + N[f]^2}$$

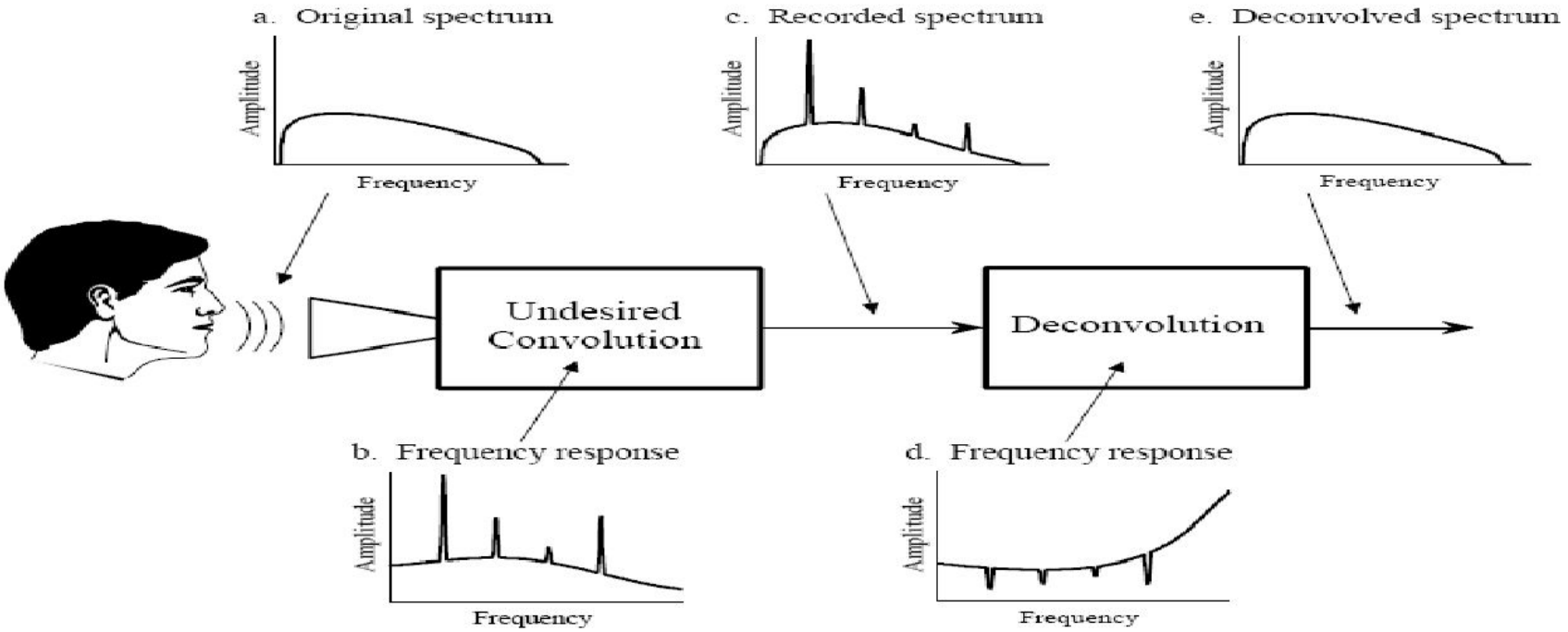

FIGURE 17-6
Deconvolution of old phonograph recordings. The frequency spectrum produced by the original singer is illustrated in (a). Resonance peaks in the primitive equipment, (b), produce distortion in the recorded frequency spectrum, (c). The frequency response of the deconvolution filter, (d), is designed to counteracts the undesired convolution, restoring the original spectrum, (e). These graphs are for illustrative purposes only; they are not actual signals.

Пример оптимальной фильтрации

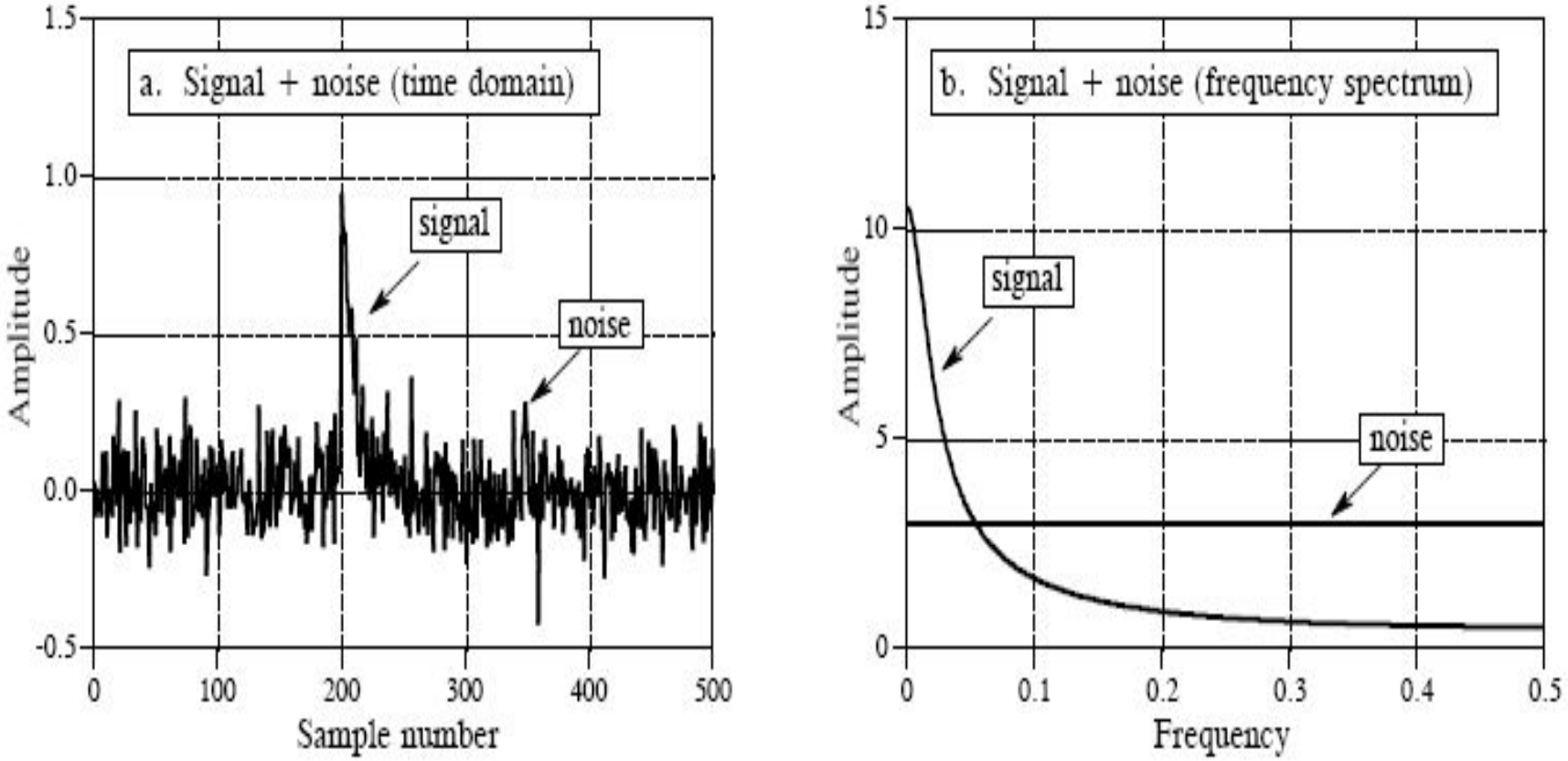

FIGURE 17-7
Example of optimal filtering. In (a), an exponential pulse buried in random noise. The frequency spectra of the pulse and noise are shown in (b). Since the signal and noise overlap in both the time and frequency domains, the best way to separate them isn't obvious.

Варианты фильтров

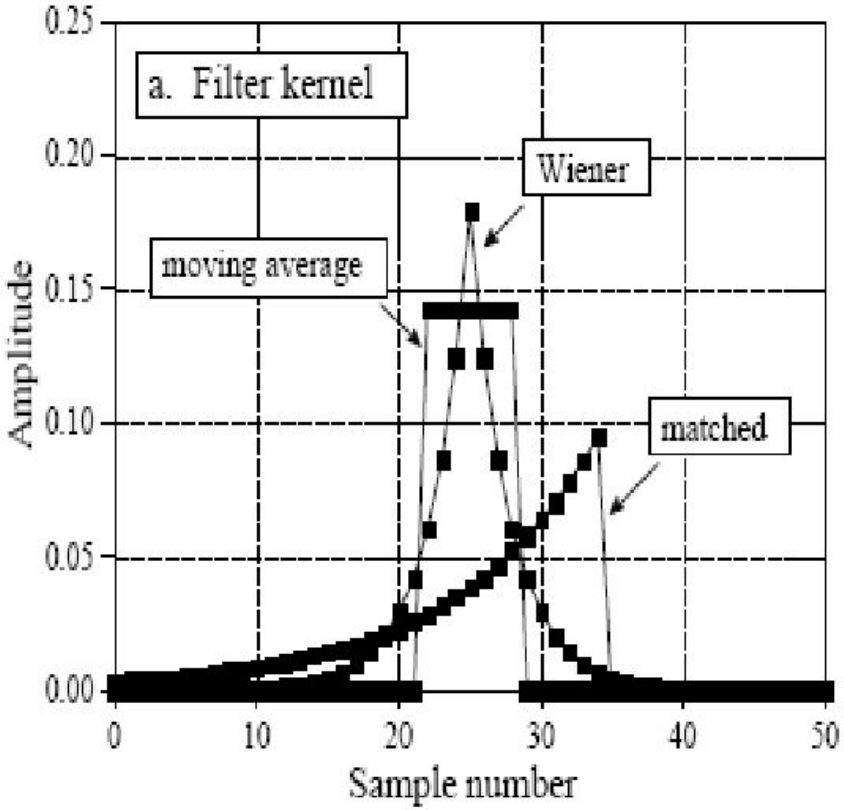

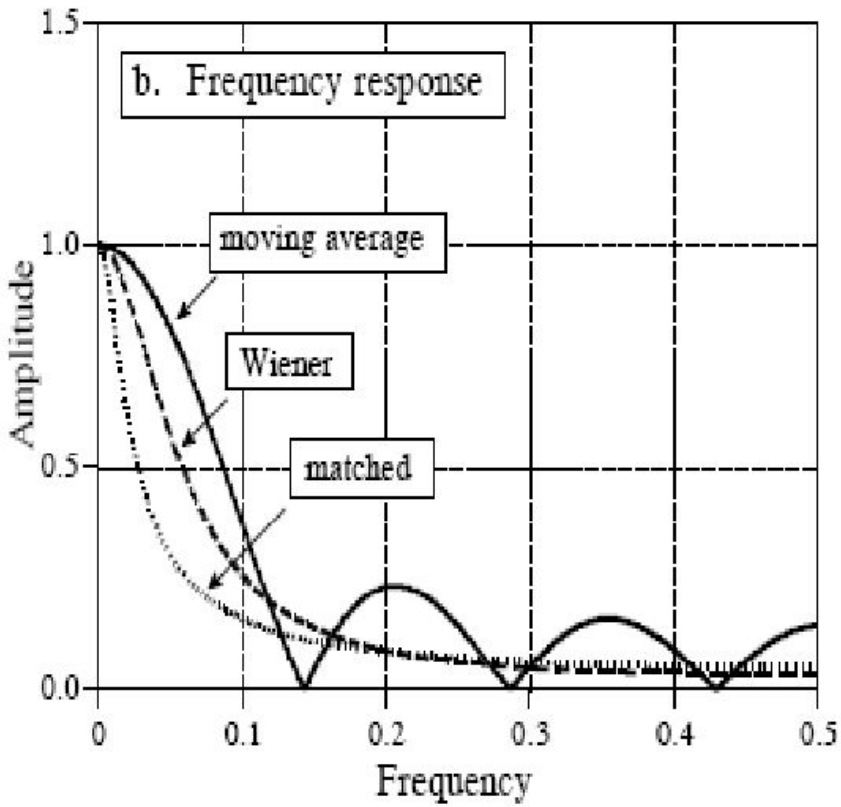

FIGURE 17-8
Example of optimal filters. In (a), three filter kernels are shown, each of which is optimal in some sense. The corresponding frequency responses are shown in (b). The moving average filter is designed to have a rectangular pulse for a filter kernel. In comparison, the filter kernel of the matched filter looks like the signal being detected. The Wiener filter is designed in the frequency domain, based on the relative amounts of signal and noise present at each frequency.

Пример оптимальной фильтрации

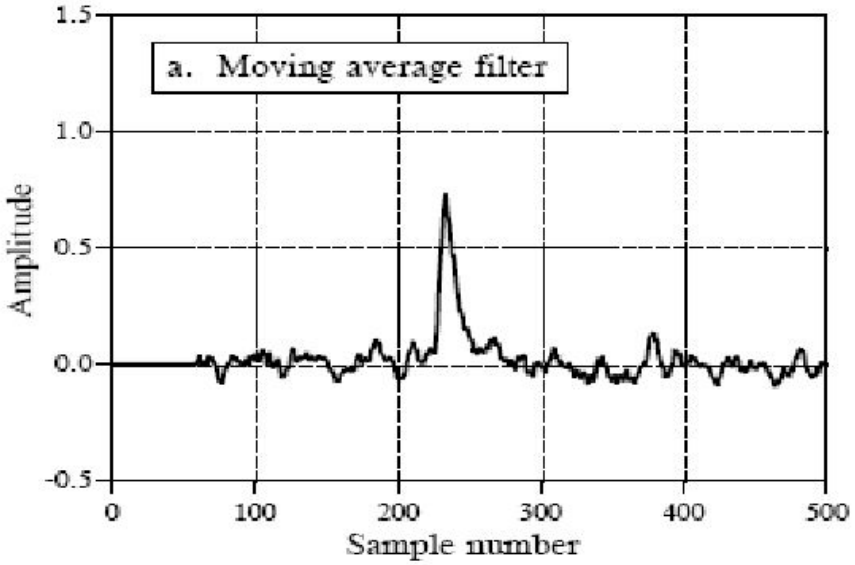

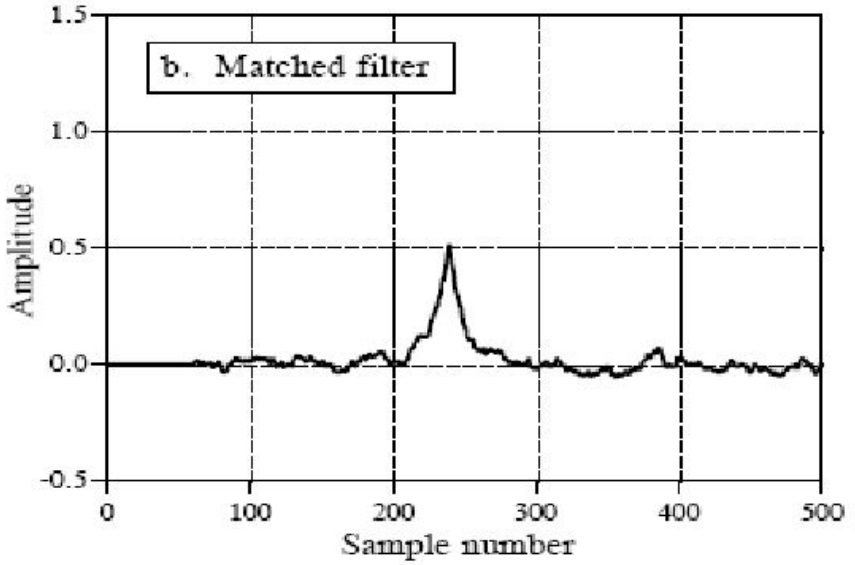

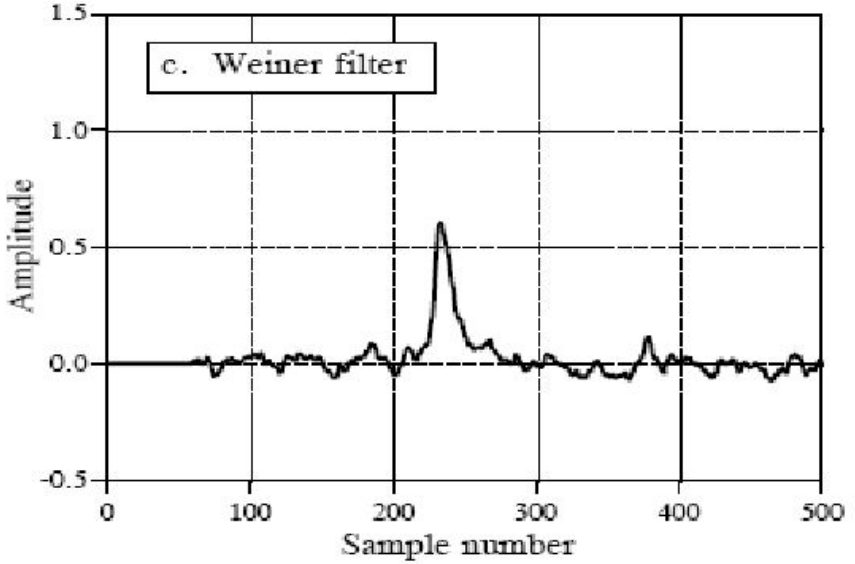

FIGURE 17-9
Example of using three optimal filters. These signals result from filtering the waveform in Fig. 17-7 with the filters in Fig. 17-8. Each of these three filters is optimal *in some sense*. In (a), the moving average filter results in the sharpest edge response for a given level of random noise reduction. In (b), the matched filter produces a peak that is farther above the residue noise than provided by any other filter. In (c), the Wiener filter optimizes the signal-to-noise ratio.

Регистрация гамма лучей

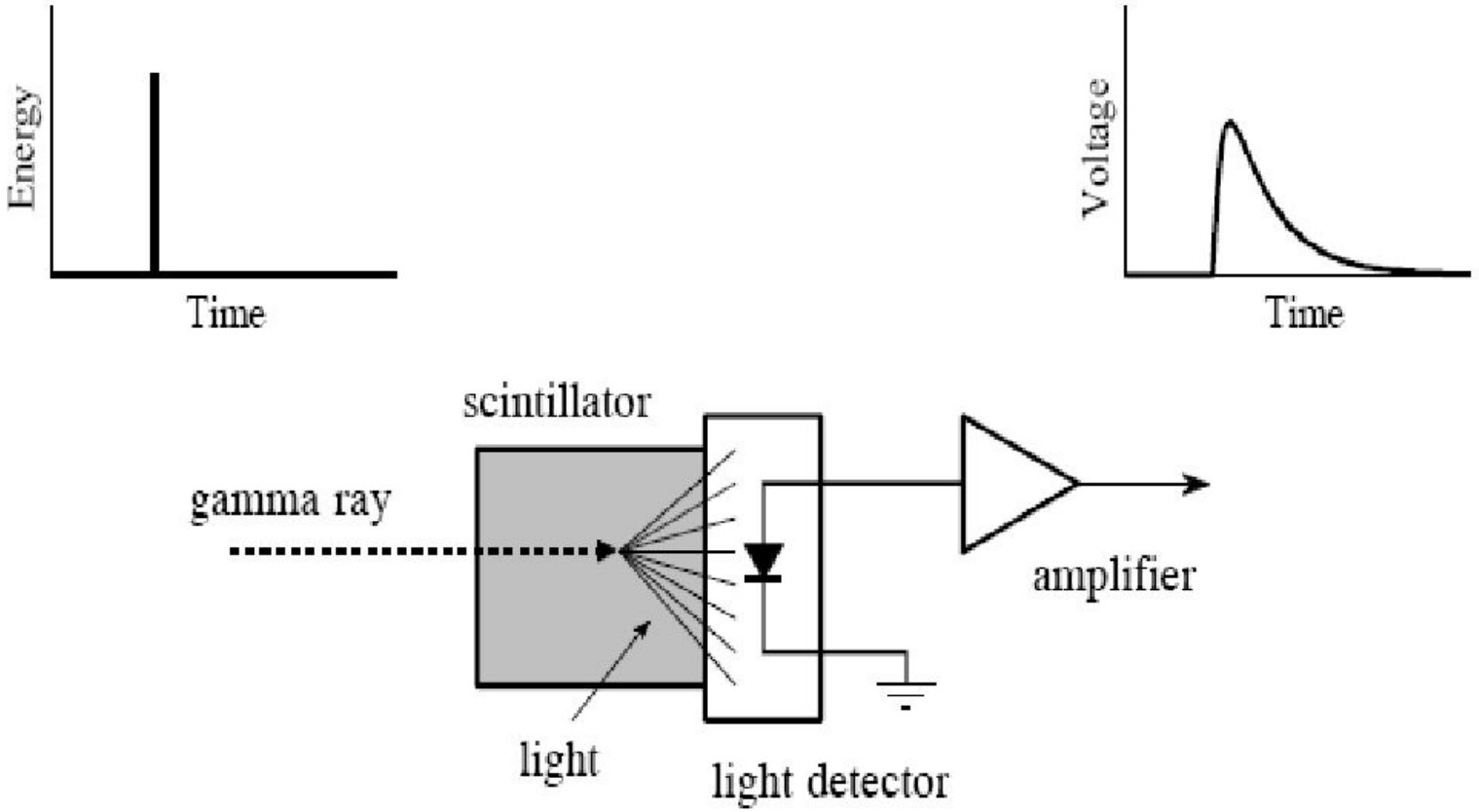

FIGURE 17-3
Example of an unavoidable convolution. A gamma ray detector can be formed by mounting a *scintillator* on a *light detector*. When a gamma ray strikes the scintillator, its energy is converted into a pulse of light. This pulse of light is then converted into an electronic signal by the light detector. The gamma ray is an *impulse*, while the output of the detector (i.e., the *impulse response*) resembles a one-sided exponential.

Обработка сигнала фотодетектора

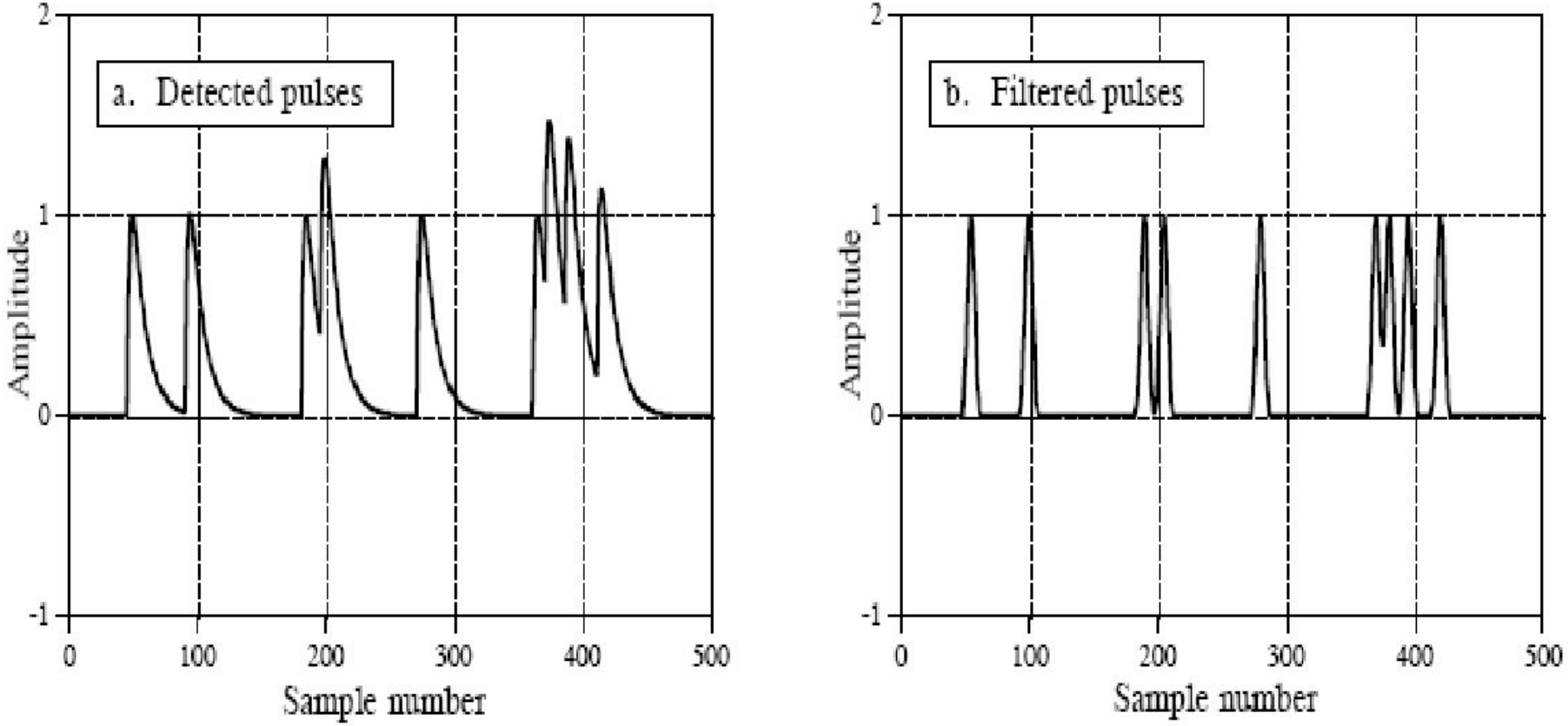

FIGURE 17-4
Example of deconvolution. Figure (a) shows the output signal from a gamma ray detector in response to a series of randomly arriving gamma rays. The deconvolution filter is designed to convert (a) into (b), by reducing the width of the pulses. This minimizes the amplitude shift when pulses land on top of each other.

Осцилляции и крутизна

FIGURE 20-1
The Chebyshev response. Chebyshev filters achieve a faster roll-off by allowing ripple in the passband. When the ripple is set to 0%, it is called a *maximally flat* or *Butterworth* filter. Consider using a ripple of 0.5% in your designs; this passband unflatness is so small that it cannot be seen in this graph, but the roll-off is much faster than the Butterworth.

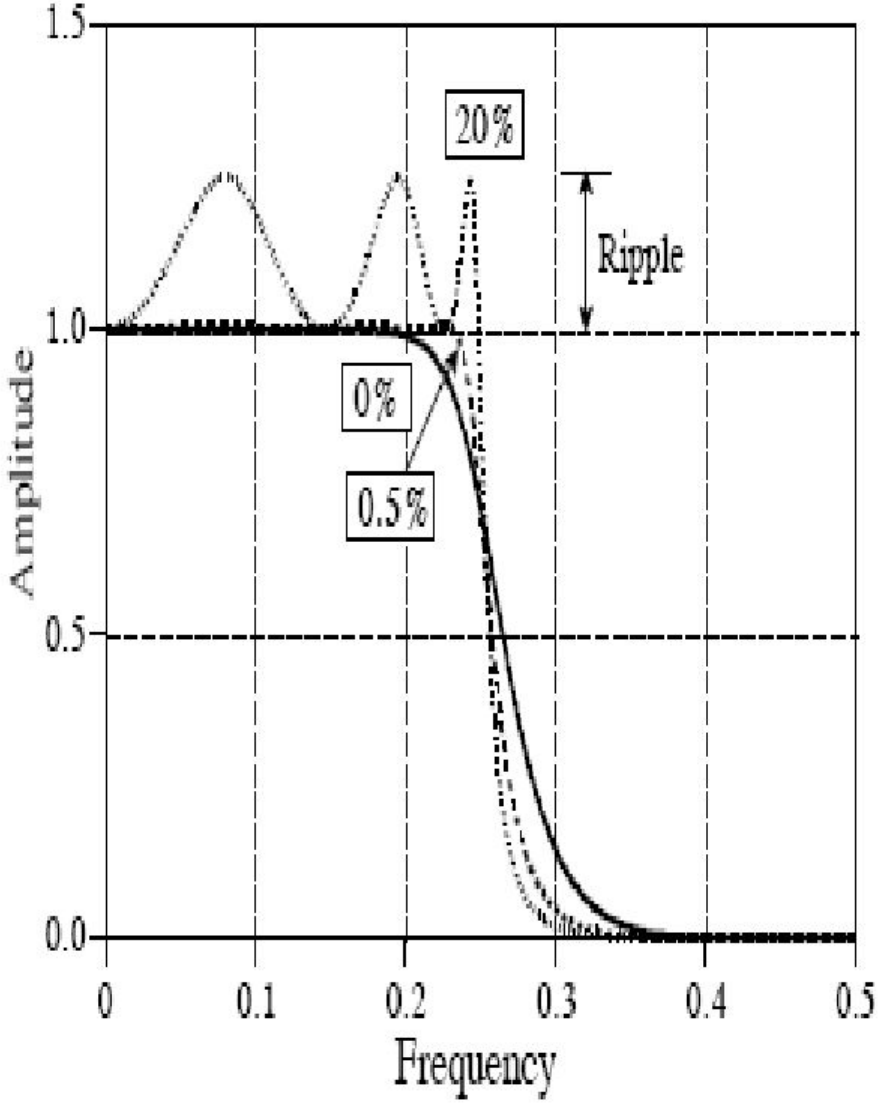

Аналоговая и цифровая фильтрация

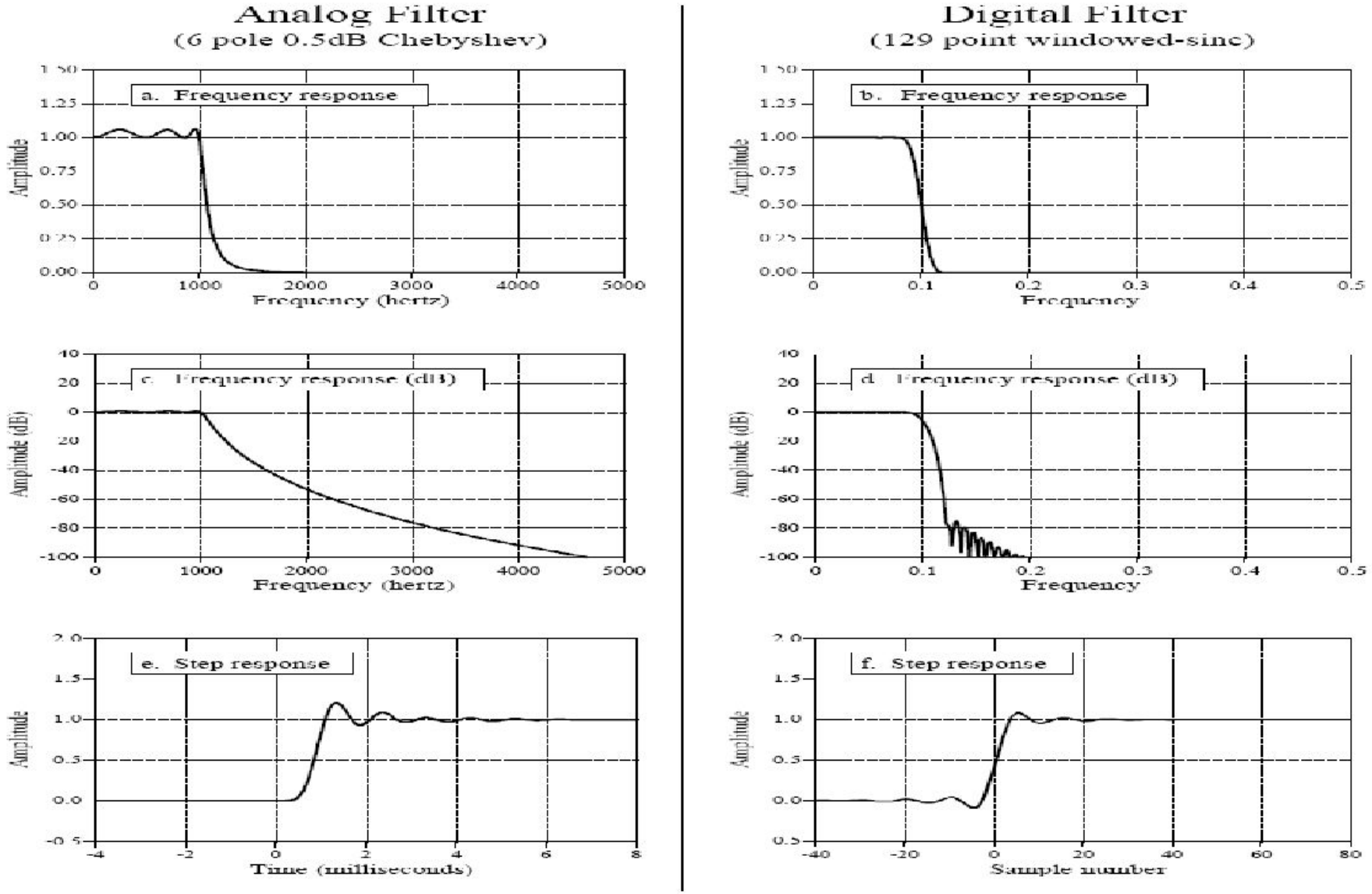

FIGURE 21-1
Comparison of analog and digital filters. Digital filters have better performance in many areas, such as: passband ripple, (a) vs. (b), roll-off and stopband attenuation, (c) vs. (d), and step response symmetry, (e) vs. (f). The digital filter in this example has a cutoff frequency of 0.1 of the 10 kHz sampling rate. This provides a fair comparison to the 1 kHz cutoff frequency of the analog filter.

Примеры аппроксимаций

(i) We begin with the Chebyshev squared magnitude response function

$$\left|H_a(\Omega)\right|^2 = \frac{1}{1+\varepsilon^2 T_N^2(\Omega/\Omega_c)} = P(\Omega), \qquad (9.116$$

The squared magnitude response function for the elliptic or Cauer filter[14] is

$$\left|H_a(\Omega)\right|^2 = \frac{1}{1+\varepsilon^2 R^2(\Omega)} = \frac{B(\Omega)}{A(\Omega)}, \qquad (9.127)$$

$$\left|H_a(\Omega)\right|^2 = \frac{1}{1+\varepsilon^2 R_N^{\ 2}(\Omega)},$$

Reverse the frequency axis to find $Q(\Omega) = 1 - P(\Omega^{-1})$:

$$Q(\Omega) = 1 - \frac{1}{1+\varepsilon^2 T_N^2(\Omega_c/\Omega)} = \frac{\varepsilon^2 T_N^2(\Omega_c/\Omega)}{1+\varepsilon^2 T_N^2(\Omega_c/\Omega)},$$

Характеристики фильтров

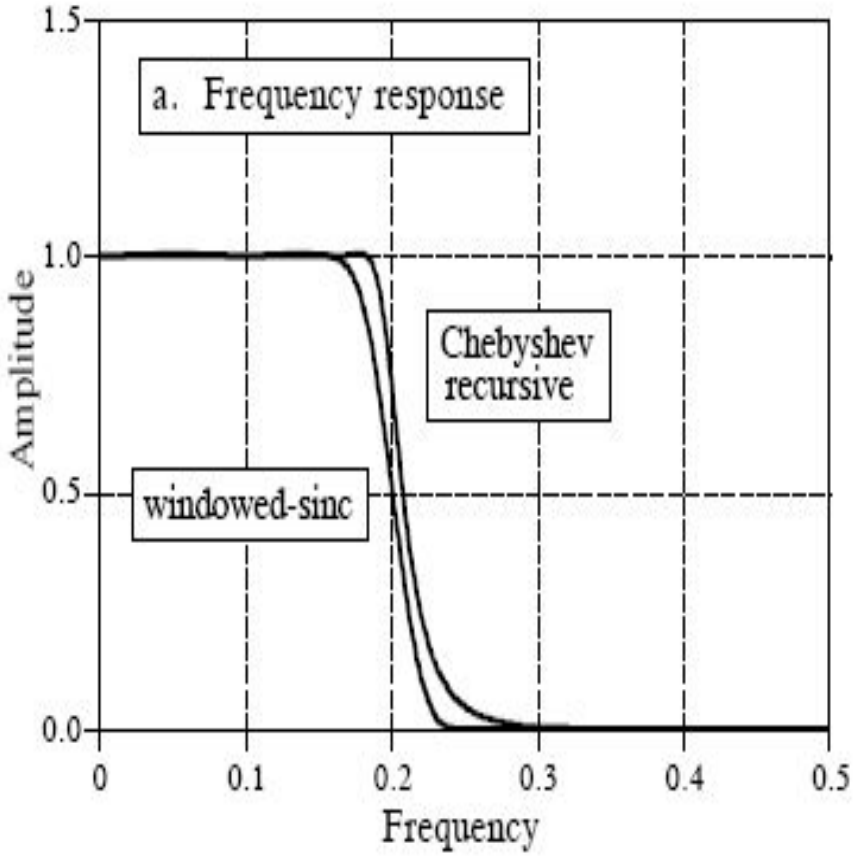

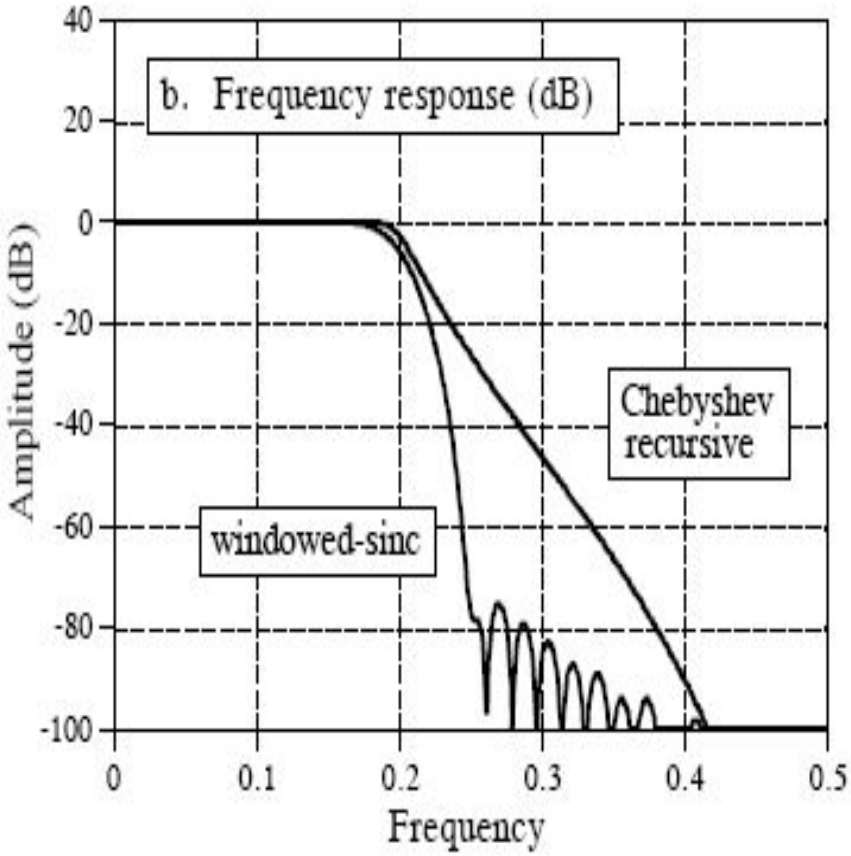

FIGURE 21-2
Windowed-sinc and Chebyshev frequency responses. Frequency responses are shown for a 51 point windowed-sinc filter and a 6 pole, 0.5% ripple Chebyshev recursive filter. The windowed-sinc has better stopband attenuation, but either will work in moderate performance applications. The cutoff frequency of both filters is 0.2, measured at an amplitude of 0.5 for the windowed-sinc, and 0.707 for the recursive.

Реакция на скачек

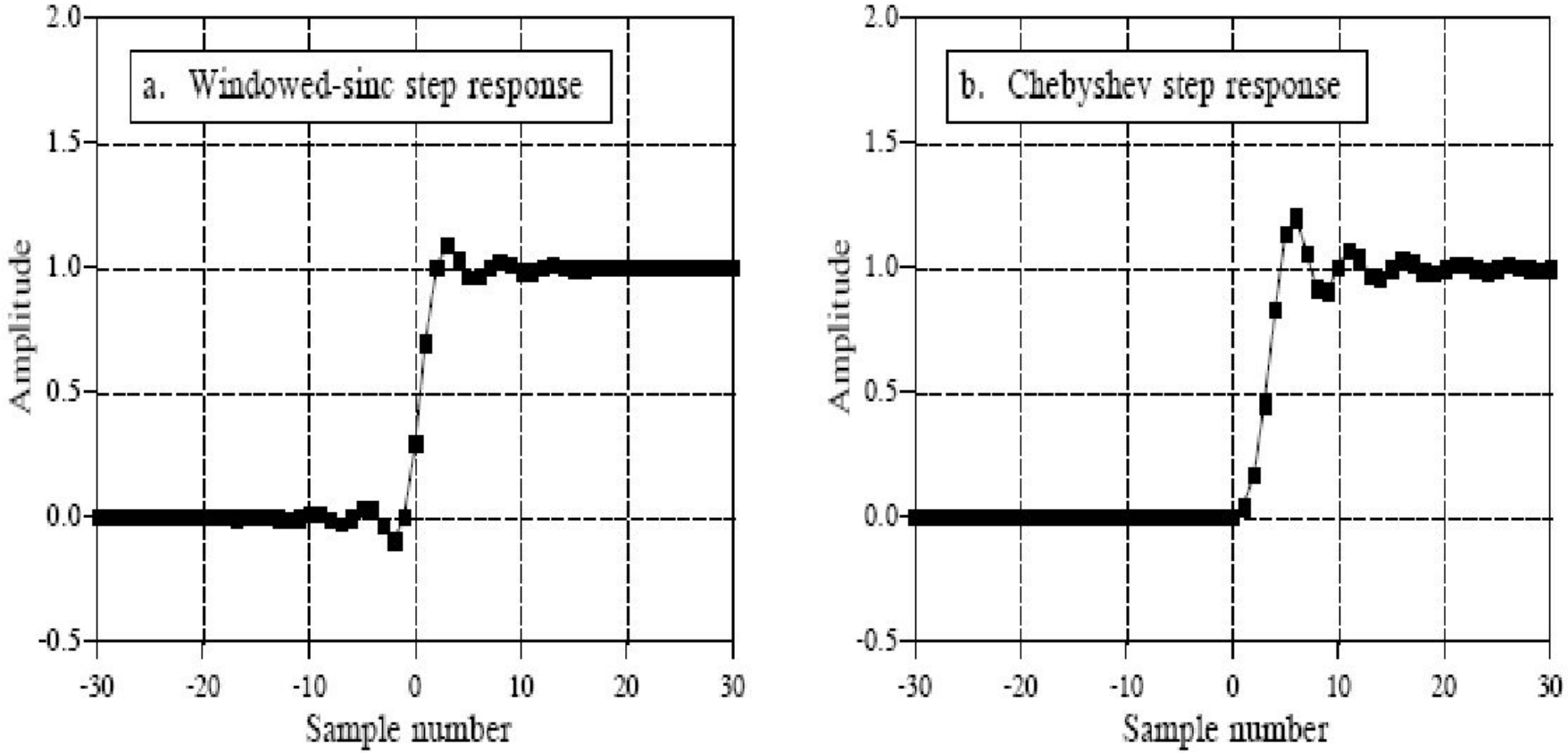

FIGURE 21-3
Windowed--sinc and Chebyshev step responses. The step responses are shown for a 51 point windowed-sinc filter and a 6 pole, 0.5% ripple Chebyshev recursive filter. Each of these filters has a cutoff frequency of 0.2. The windowed-sinc has a slightly better step response because it has less overshoot and a zero phase.

Фильтрация форма и содержание

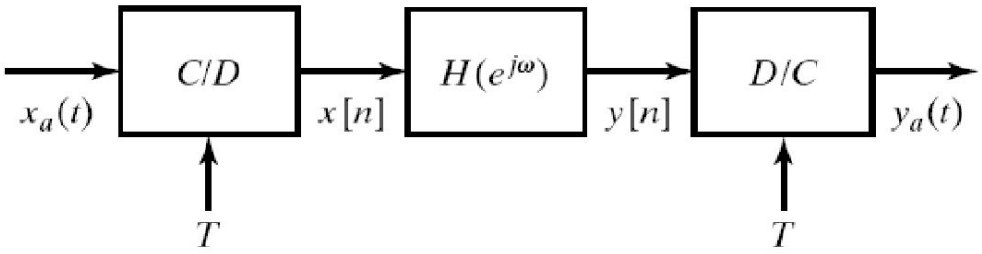

Figure 7.1 Basic system for discrete-time filtering of continuous-time signals.

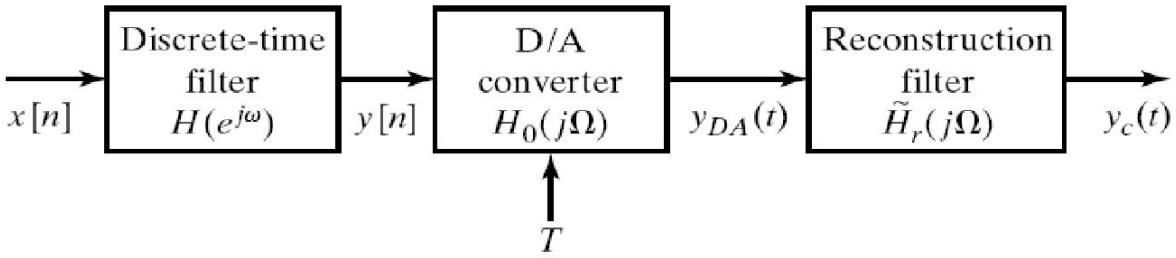

Figure 7.45 Precompensation of a discrete-time filter for the effects of a D/A converter.

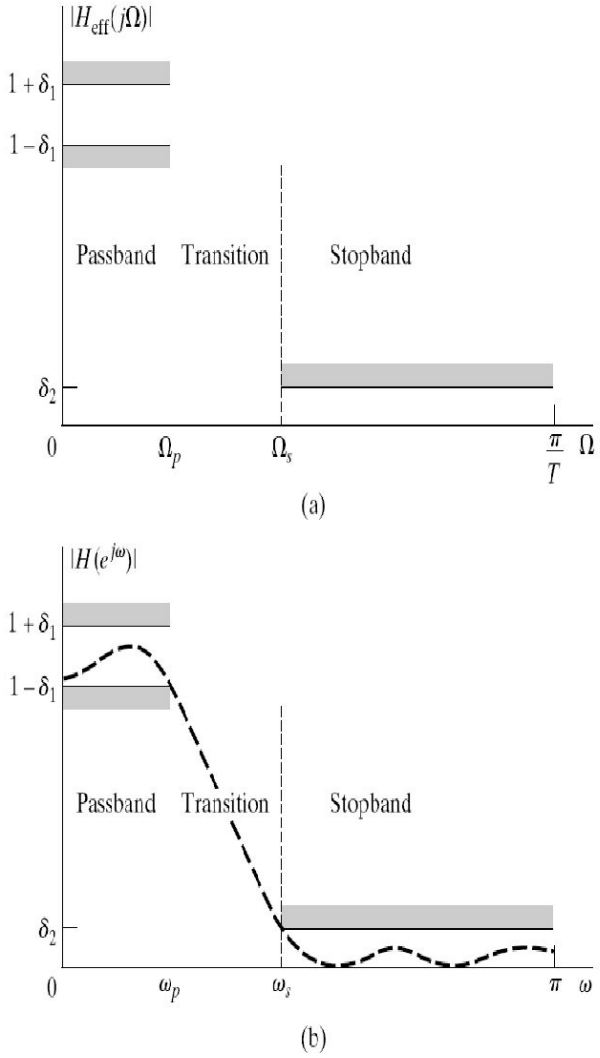

Figure 7.2 (a) Specifications for effective frequency response of overall system in Figure 7.1 for the case of a lowpass filter. (b) Corresponding specifications for the discrete-time system in Figure 7.1.

FIR CAD TECHNIQUES: PARKS McCLELLAN PROGRAM WITH REMEZ EXCHANGE ALGORITHM

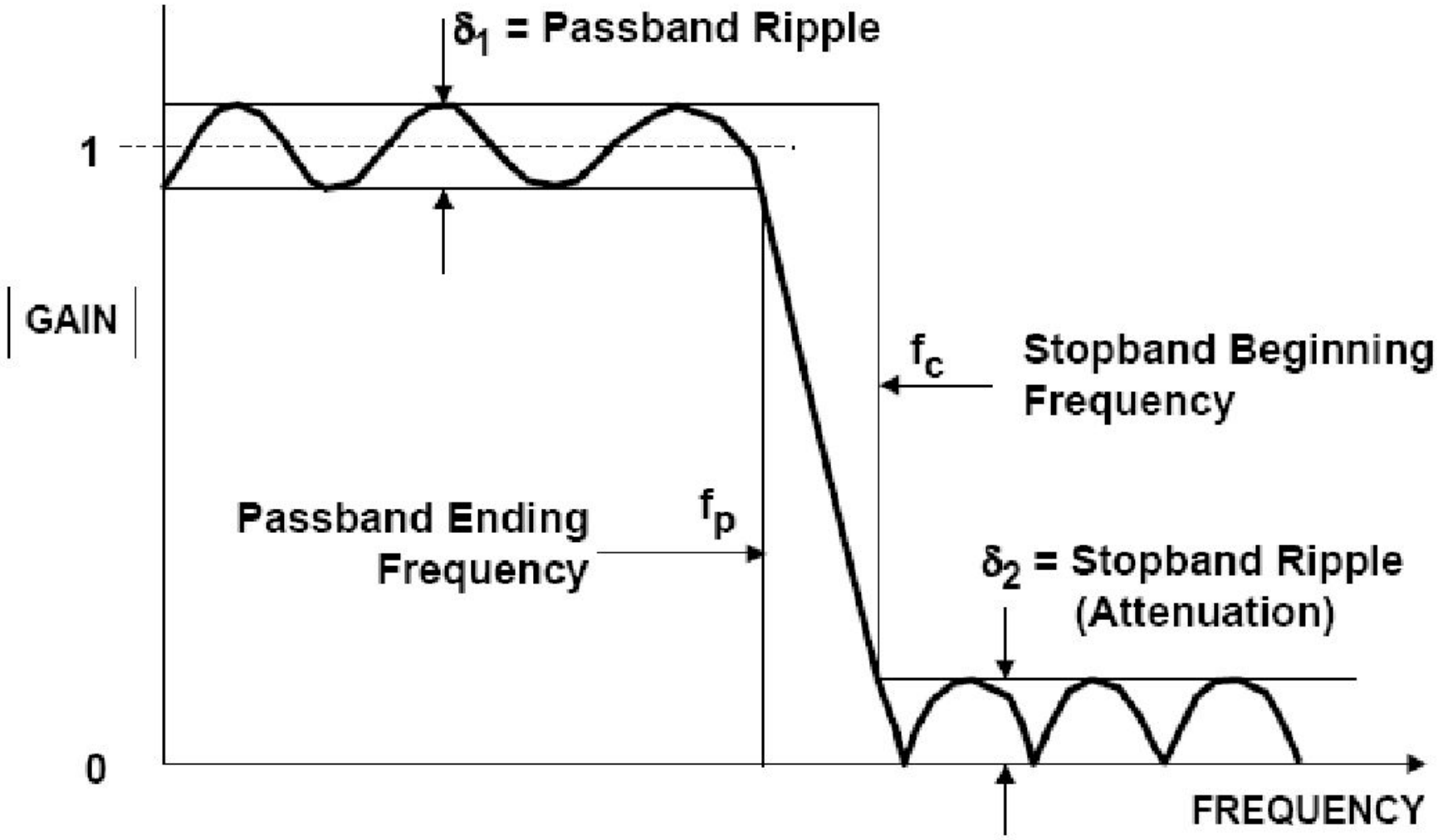

$$\text{Ripple Ratio} = \frac{\delta_2}{\delta_1}$$

Поведение амплитуды и фазы

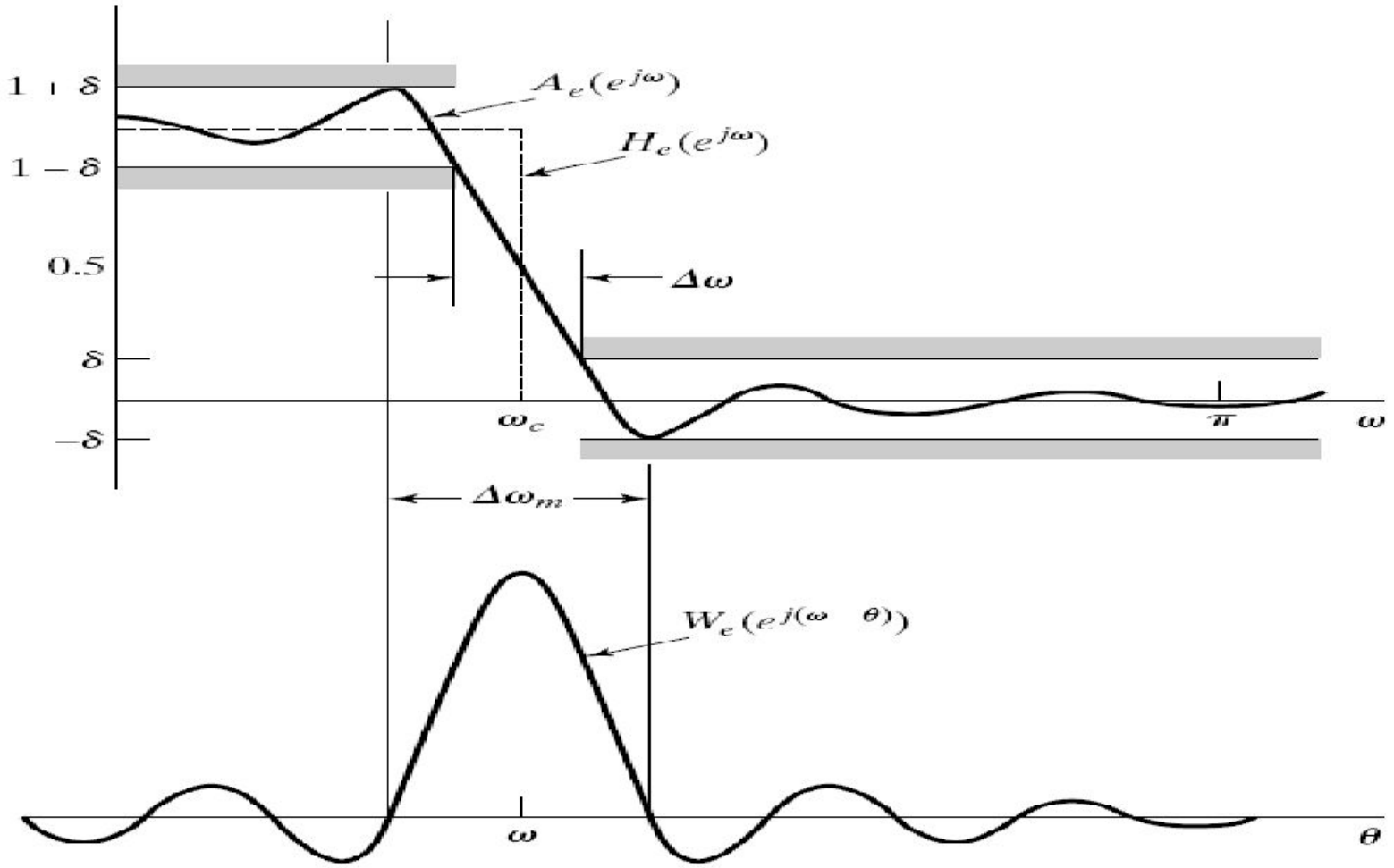

Figure 7.23 Illustration of type of approximation obtained at a discontinuity of the ideal frequency response.

Оптимизация АЧХ

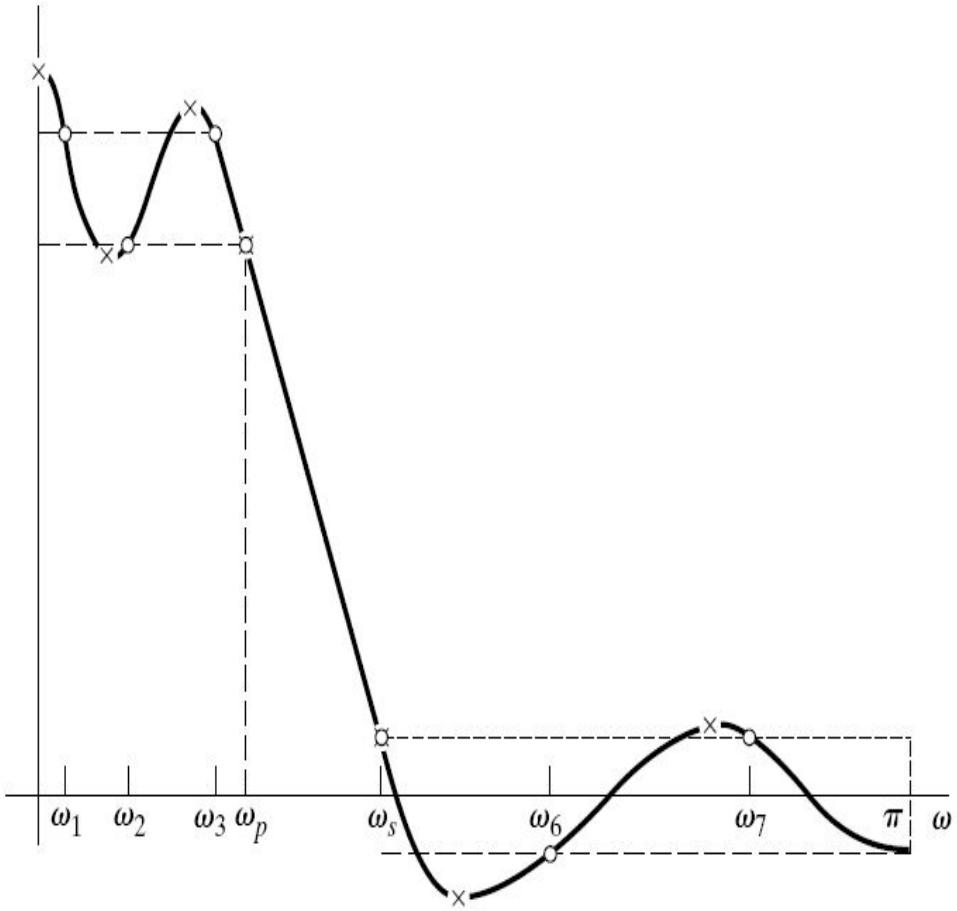

Figure 7.40 Illustration of the Parks–McClellan algorithm for equiripple approximation.

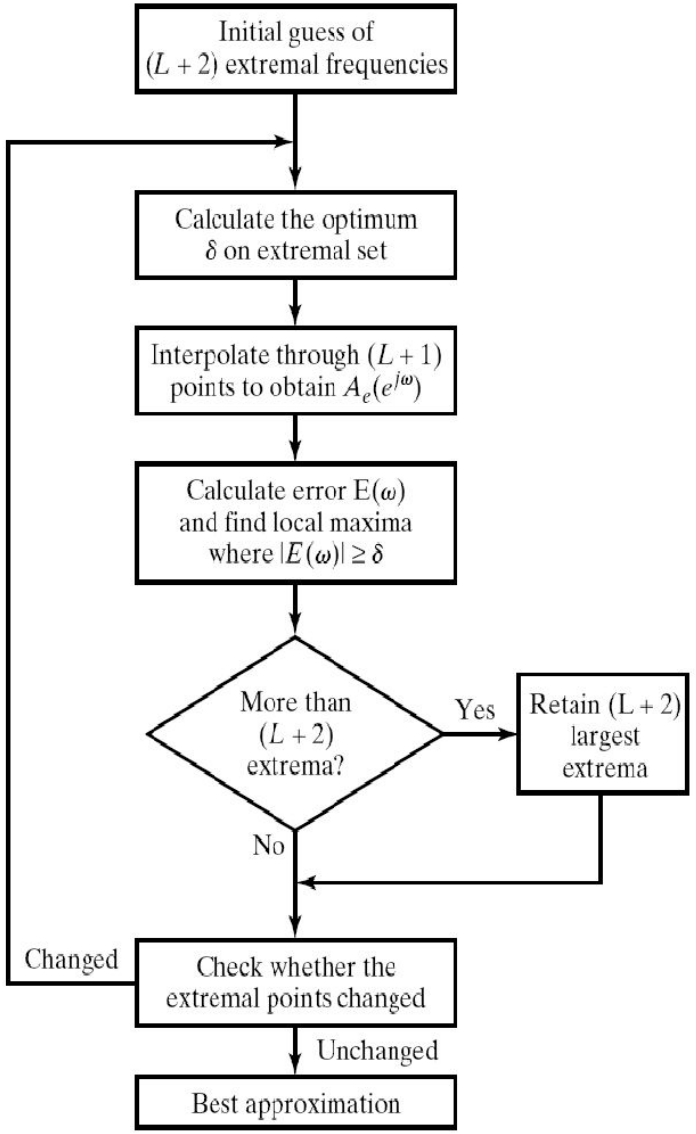

Figure 7.41 Flowchart of Parks–McClellan algorithm.

Постоянство осцилляций

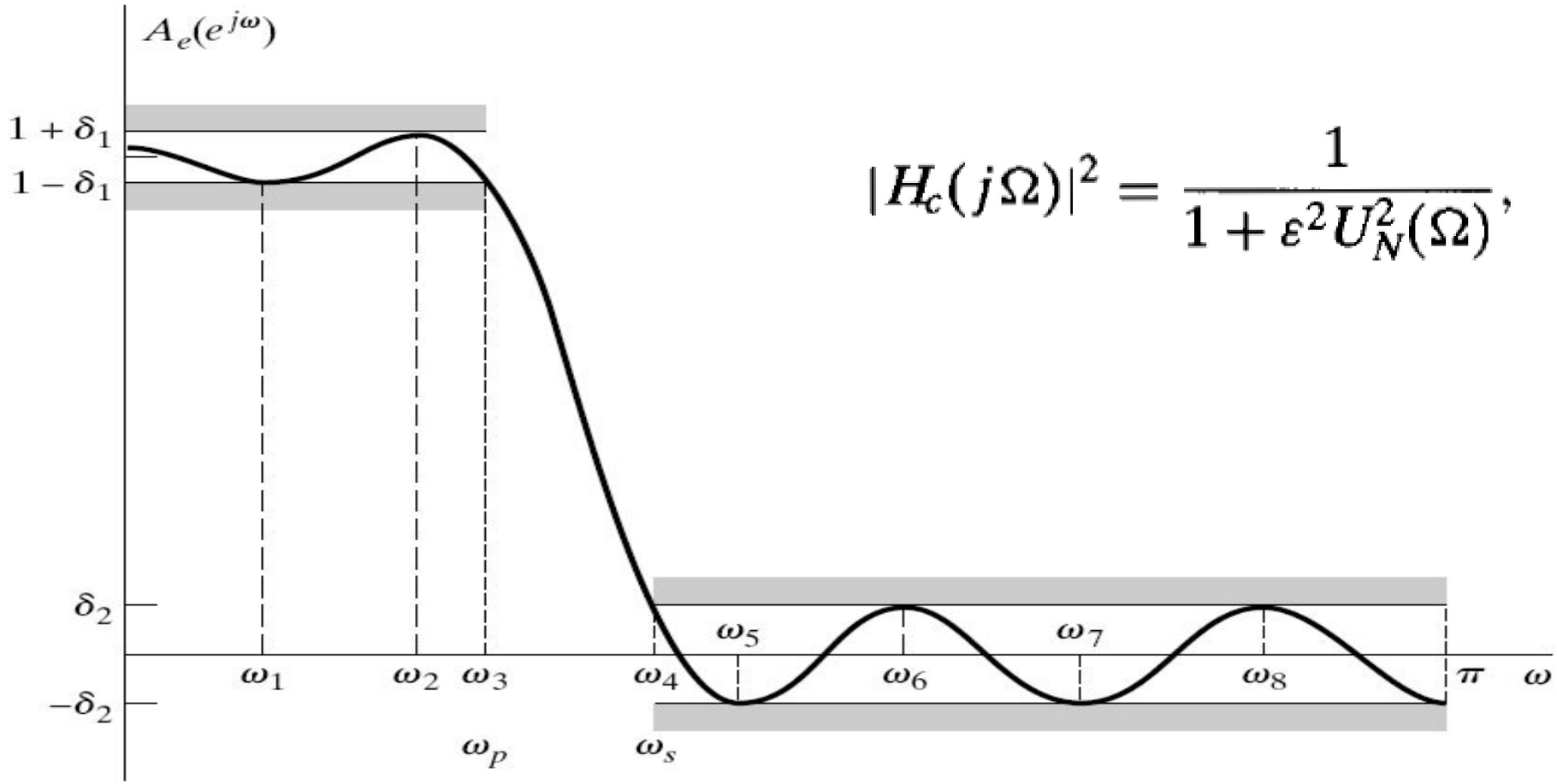

$$|H_c(j\Omega)|^2 = \frac{1}{1+\varepsilon^2 U_N^2(\Omega)},$$

Figure 7.35 Typical example of a lowpass filter approximation that is optimal according to the alternation theorem for $L = 7$.

Фильтр Баттерворта

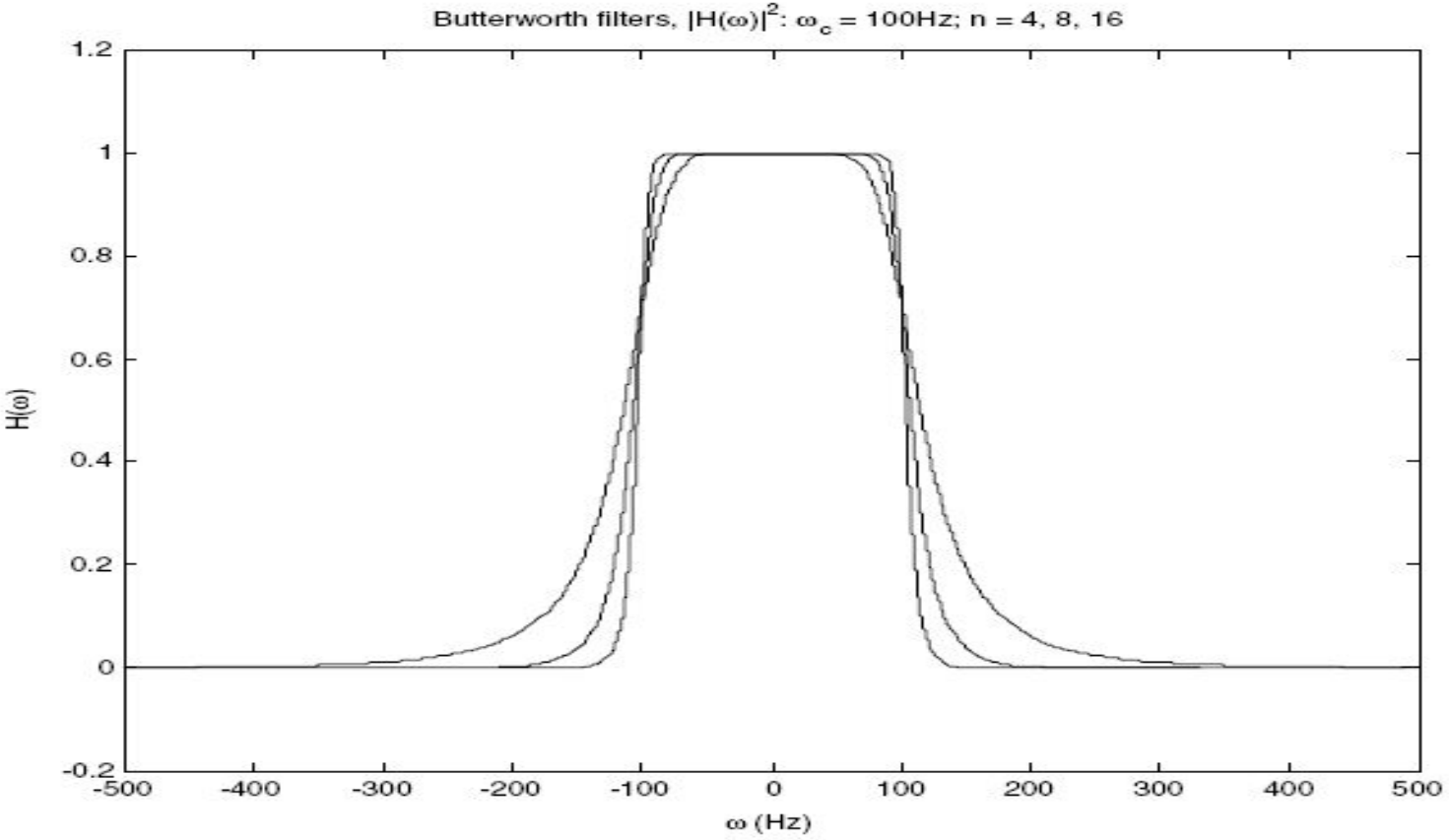

Fig. 9.30. Analog Butterworth filters for a few orders.

Butterworth filter by $(\Omega_c)^{-2n} = a_{2n}$. Thus, the *Butterworth filter* of order $N > 0$ is defined by its Fourier transform $H(\omega)$ (Figure 9.30):

$$H(\Omega) = \sqrt{\frac{1}{1 + \left(\frac{\Omega}{\Omega_c}\right)^{2N}}}; \qquad (9.84)$$

Баттерворт

$$H_c(s)\,H_c(-s) = \frac{1}{1 + (s/j\Omega_c)^{2N}}.$$

$$|H_c(j\Omega)|^2 = \frac{1}{1 + (j\Omega/j\Omega_c)^{2N}}.$$

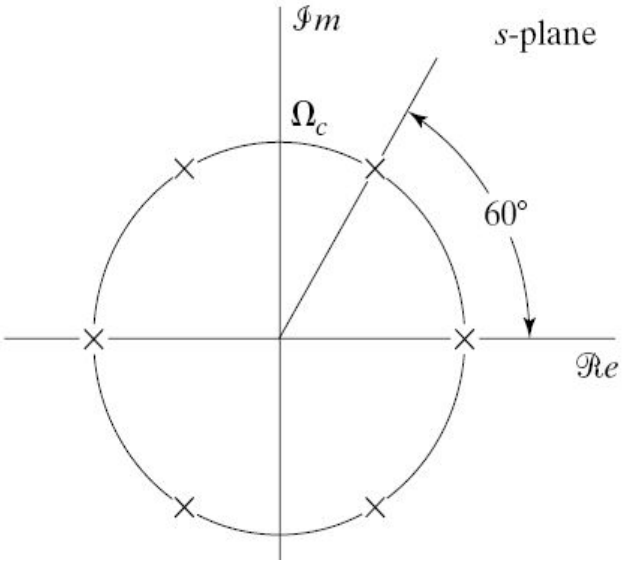

$$s_k = (-1)^{1/2N}(j\Omega_c) = \Omega_c e^{(j\pi/2N)(2k+N-1)},$$

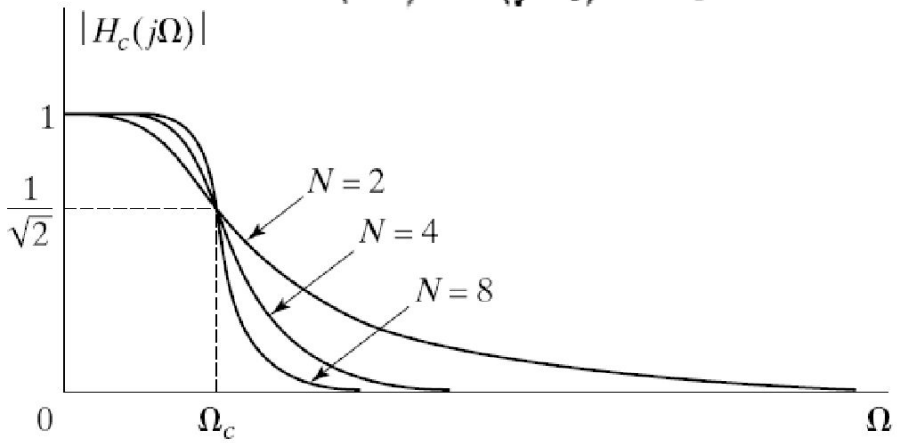

Figure B.2 Dependence of Butterworth magnitude characteristics on the order N.

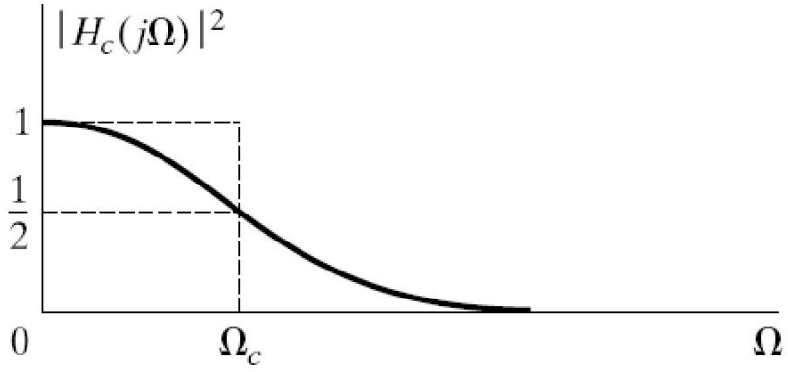

Figure B.1 Magnitude-squared function for continuous-time Butterworth filter.

Чебышев

$$|H_c(j\Omega)|^2 = \frac{1}{1+\varepsilon^2 V_N^2(\Omega/\Omega_c)},$$

$$|H_c(j\Omega)|^2 = \frac{1}{1+[\varepsilon^2 V_N^2(\Omega_c/\Omega)]^{-1}}.$$

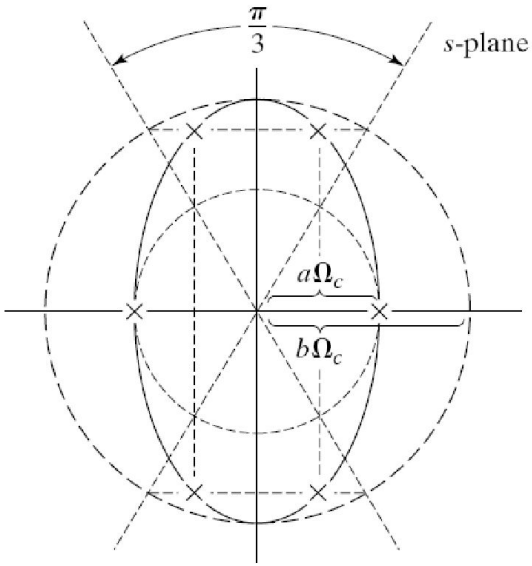

$$V_N(x) = \cos(N\cos^{-1}x).$$

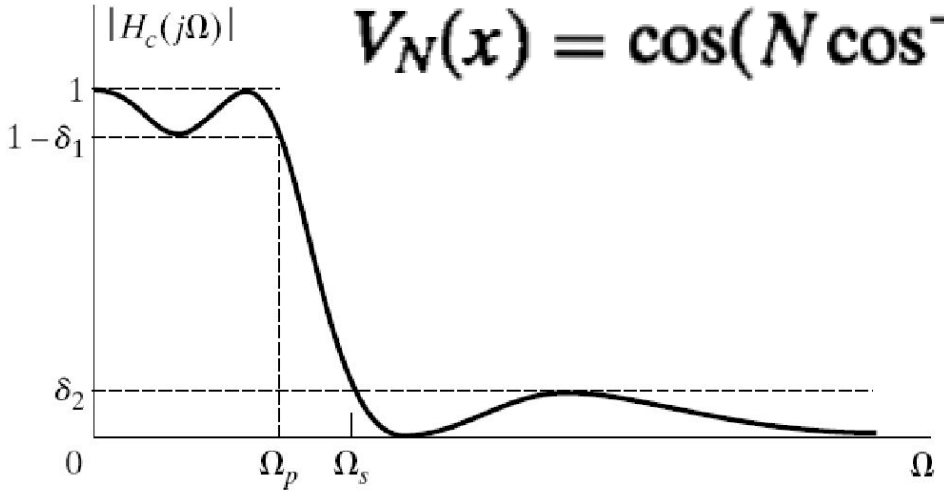

Figure B.6 Equiripple approximation in both passband and stopband.

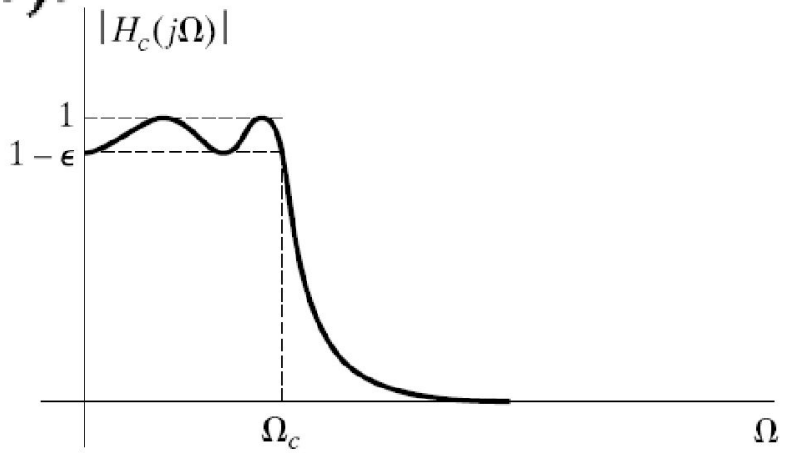

Figure B.4 Type I Chebyshev lowpass filter approximation.

Преобразование типа фильтра

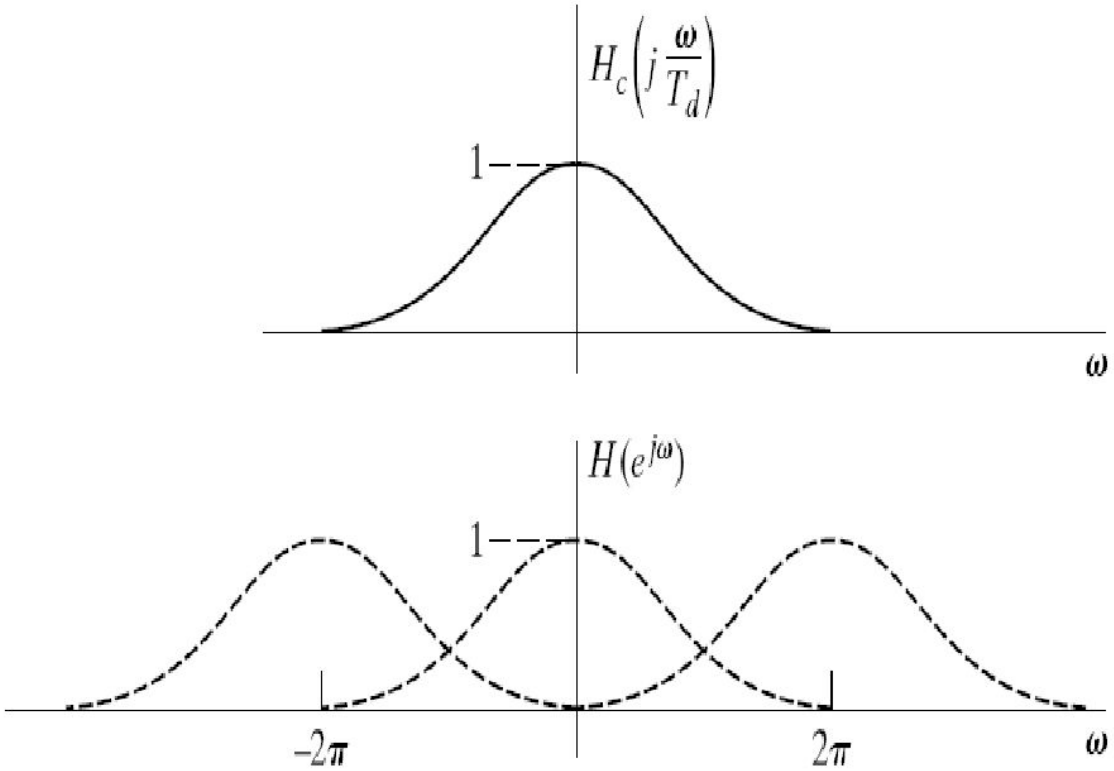

Figure 7.3 Illustration of aliasing in the impulse invariance design technique.

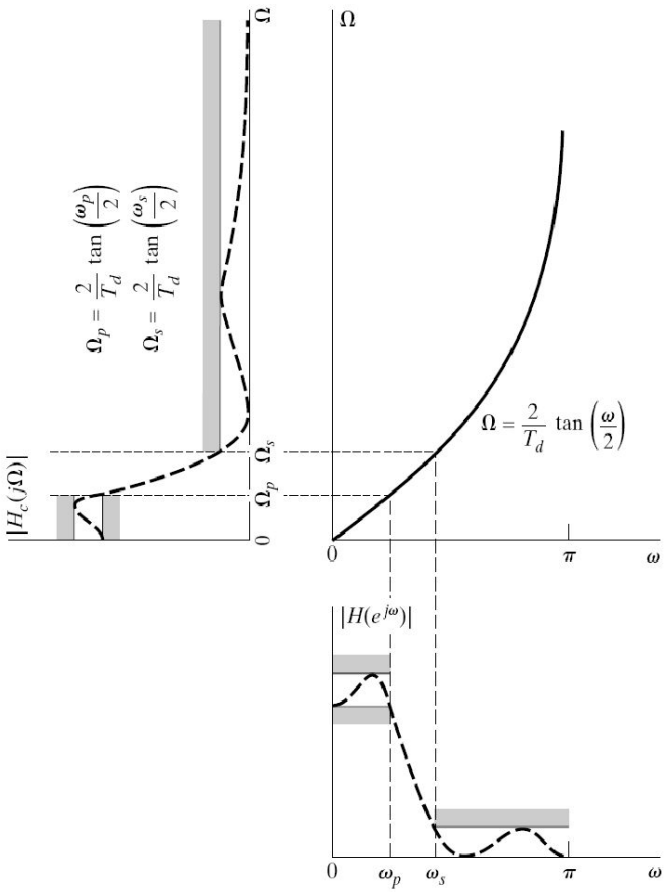

Figure 7.8 Frequency warping inherent in the bilinear transformation of a continuous-time lowpass filter into a discrete-time lowpass filter. To achieve the desired discrete-time cutoff frequencies, the continuous-time cutoff frequencies must be prewarped as indicated.

Повышение крутизны

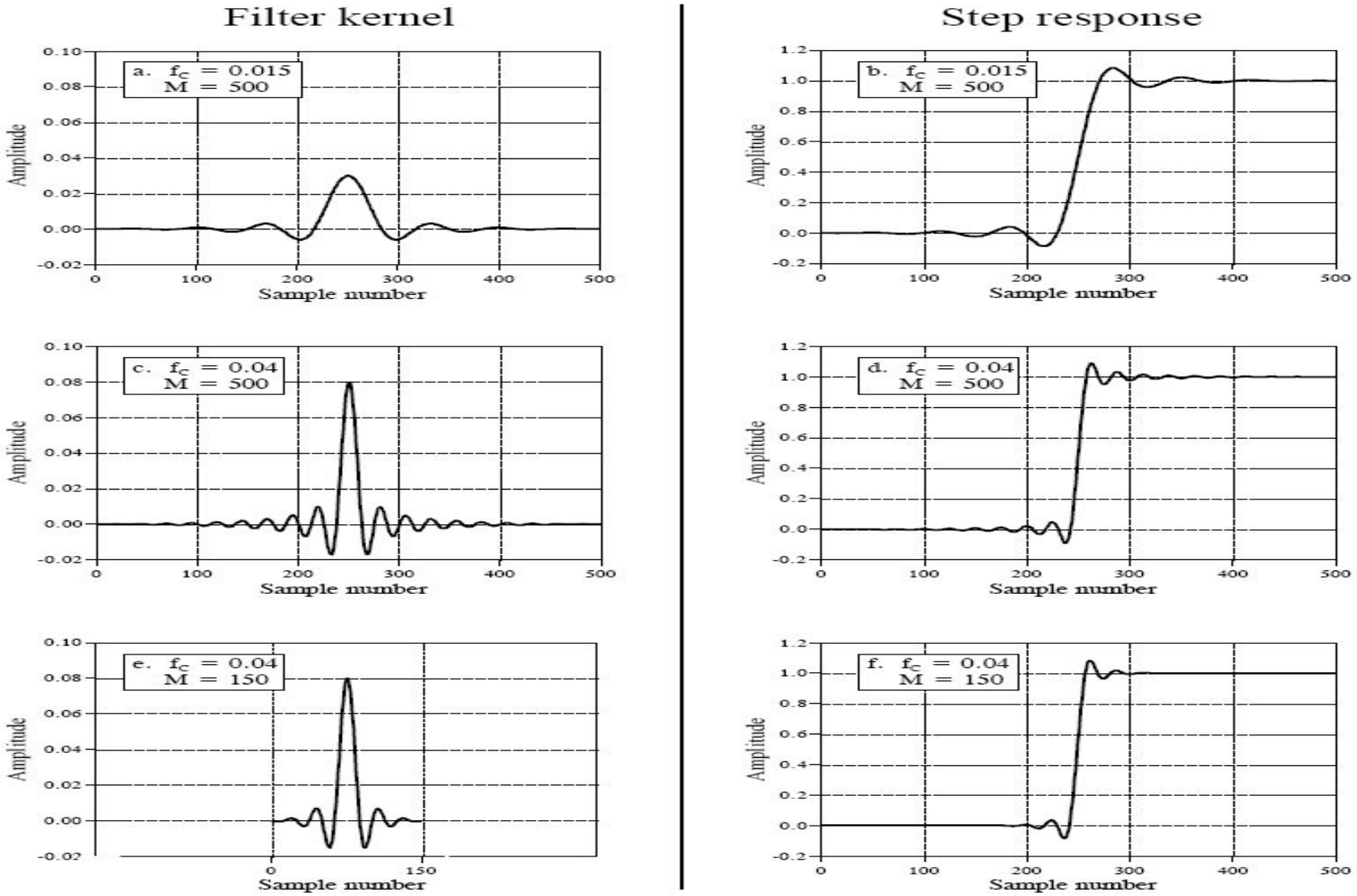

FIGURE 16-4
Example filter kernels and the corresponding step responses. The frequency of the sinusoidal oscillation is approximately equal to the cutoff frequency, f_C, while M determines the kernel length.

Линейная и логарифмическая АЧХ

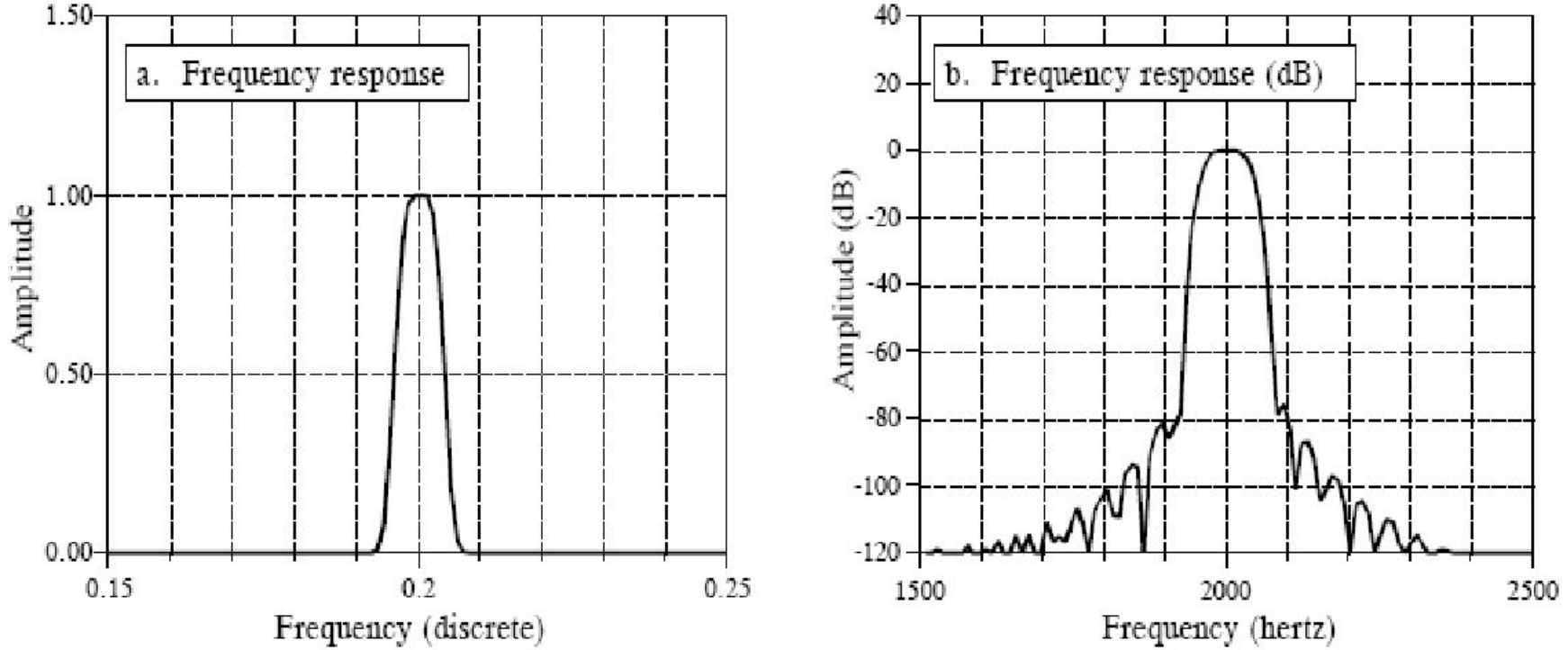

FIGURE 16-6

Example of a windowed-sinc band-pass filter. This filter was designed for a sampling rate of 10 kHz. When referenced to the analog signal, the center frequency of the passband is at 2 kHz, the passband is 80 hertz, and the transition bands are 50 hertz. The windowed-sinc uses 801 points in the filter kernel to achieve this roll-off, and a Blackman window for good stopband attenuation. Figure (a) shows the resulting frequency response on a linear scale, while (b) shows it in decibels. The frequency axis in (a) is expressed as a fraction of the sampling frequency, while (b) is expressed in terms of the analog signal before digitization.

Практически прямоугольная АЧХ

FIGURE 21-4
Maximum performance of FIR and IIR filters. The frequency response of the windowed-sinc can be virtually any shape needed, while the Chebyshev recursive filter is very limited. This graph compares the frequency response of a six pole Chebyshev recursive filter with a 1001 point windowed-sinc filter.

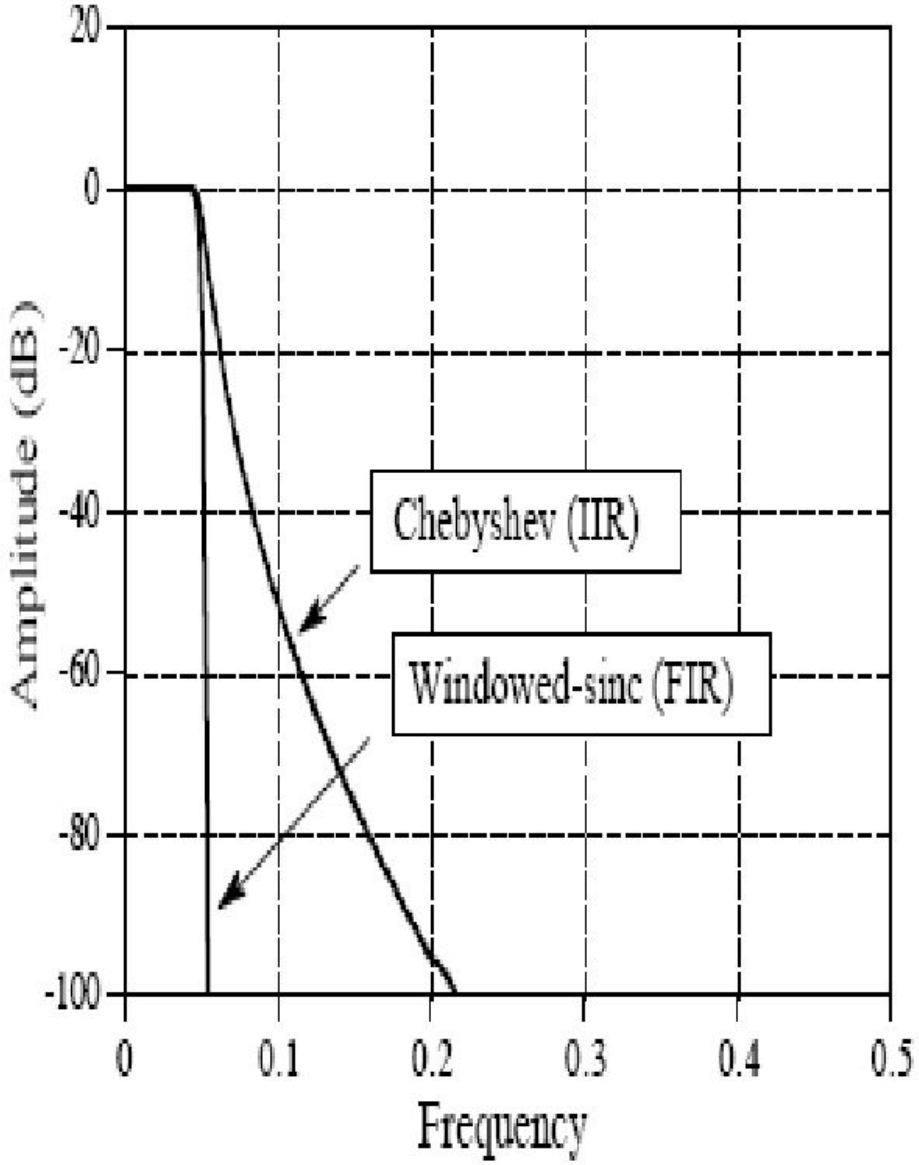

Трудоемкость фильтрации

FIGURE 21-5
Comparing FIR and IIR execution speeds. These curves shows the relative execution times for a windowed-sinc filter compared with an equivalent six pole Chebyshev recursive filter. Curves are shown for implementing the FIR filter by both the standard and the FFT convolution algorithms. The windowed-sinc execution time rises at low and high frequencies because the filter kernel must be made longer to keep up with the greater performance of the recursive filter at these frequencies. In general, IIR filters are an order of magnitude faster than FIR filters of comparable performance.

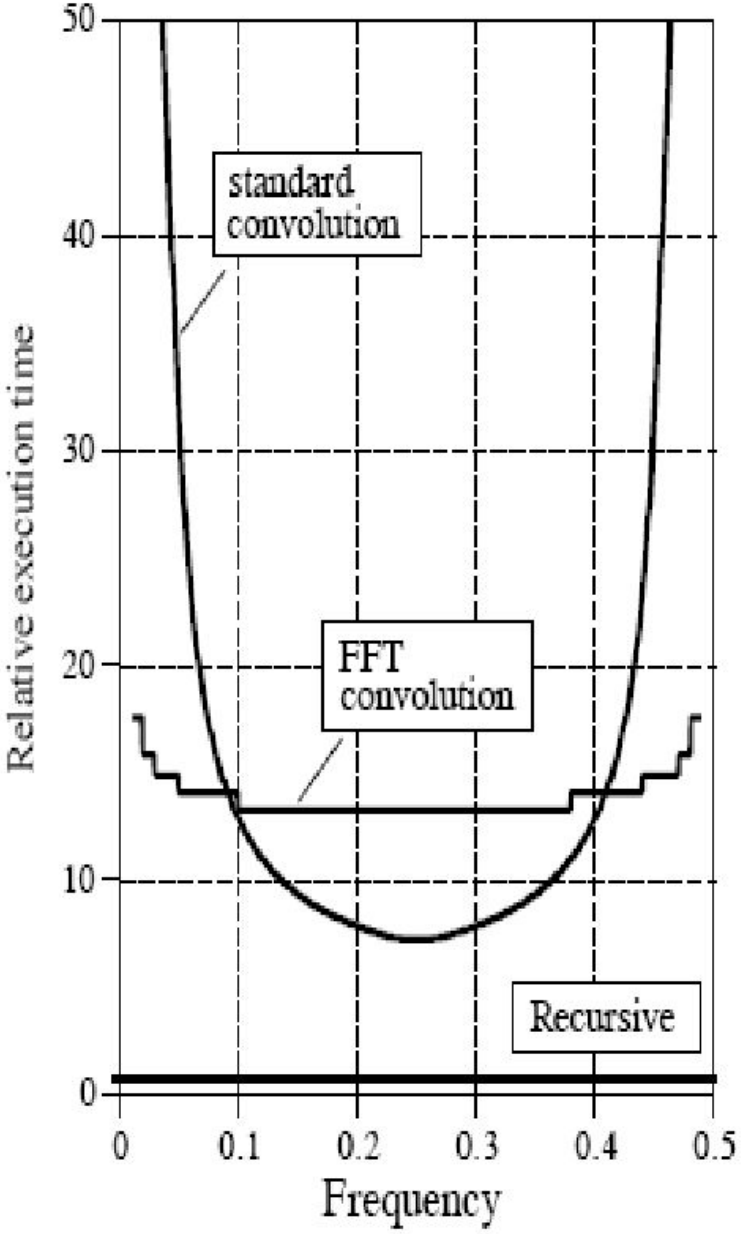

Осреднение и рекурсия

FIGURE 21-6
Moving average and single pole frequency responses. Both of these filters have a poor frequency response, as you should expect for time domain filters.

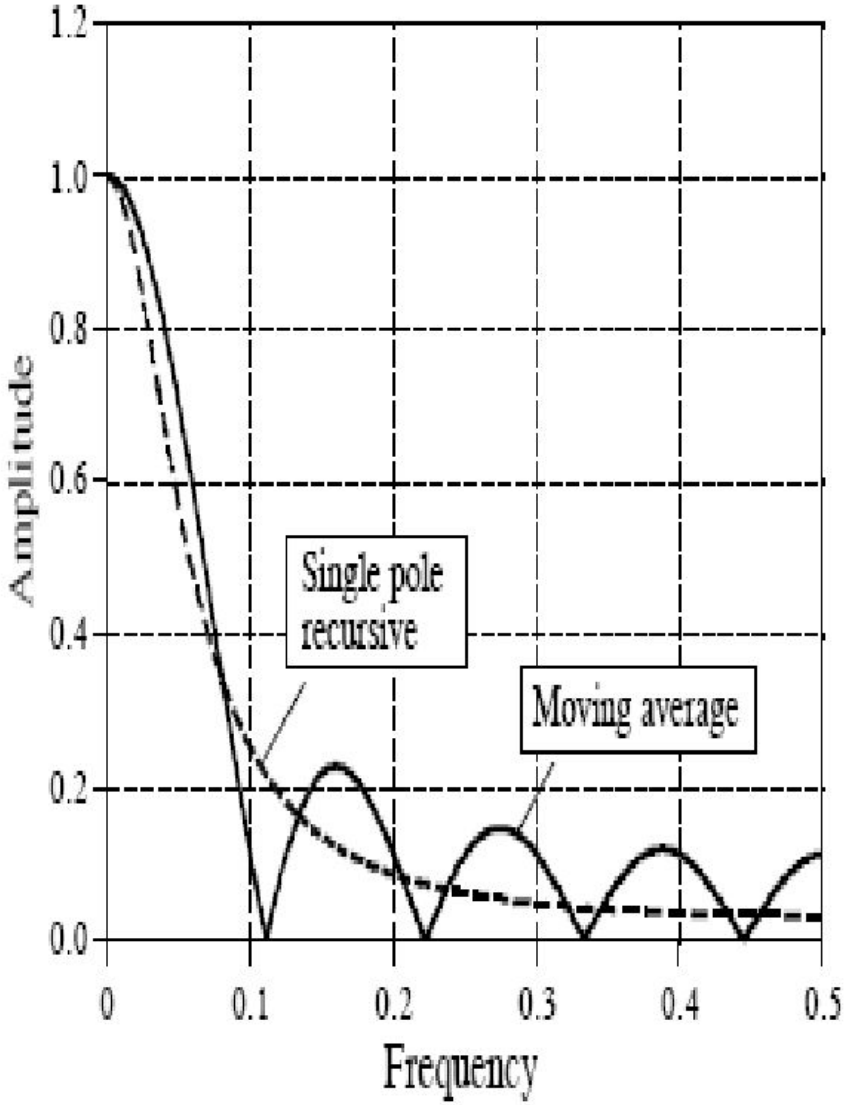

Осреднение и рекурсия

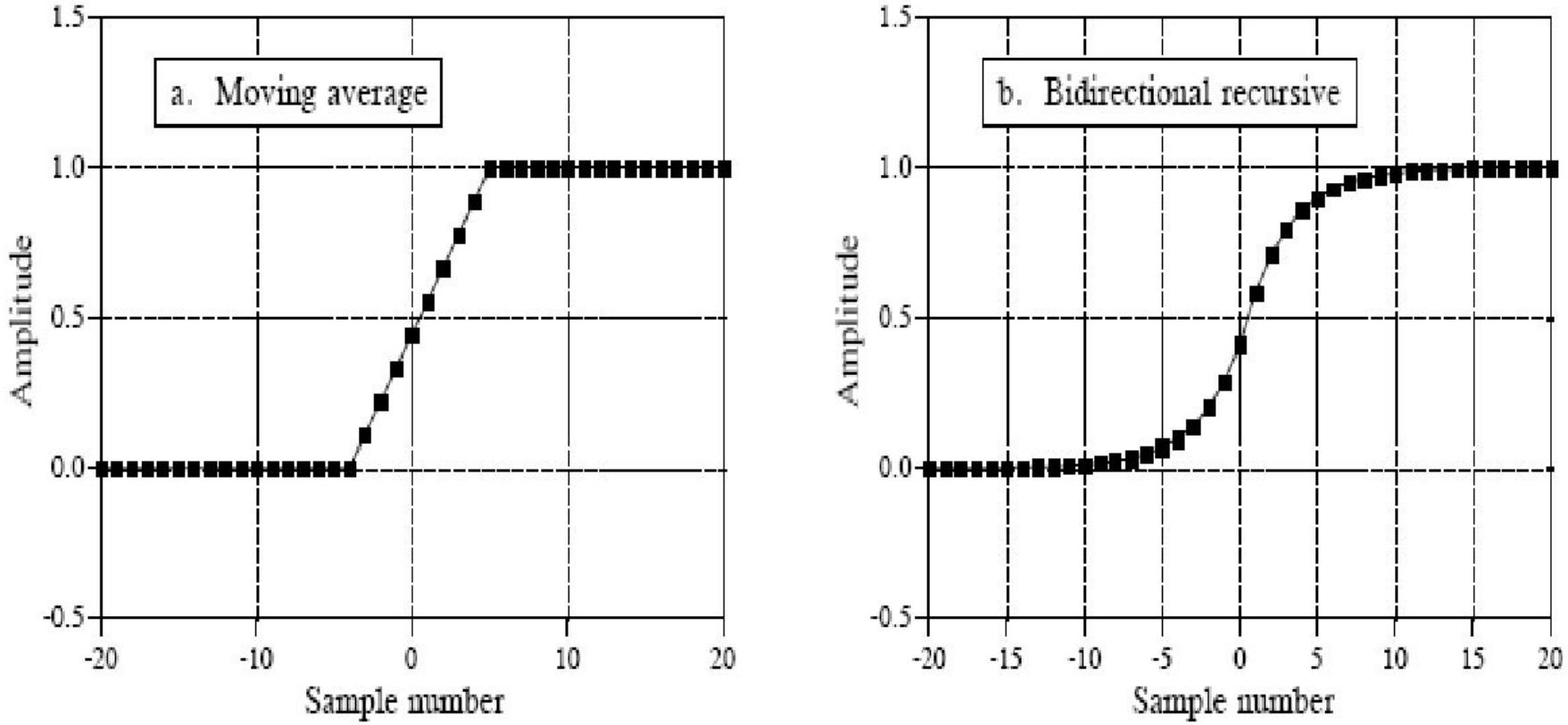

FIGURE 21-7
Step responses of the moving average and the bidirectional single pole filter. The moving average step response occurs over a smaller number of samples, while the single pole filter's step response is smoother.

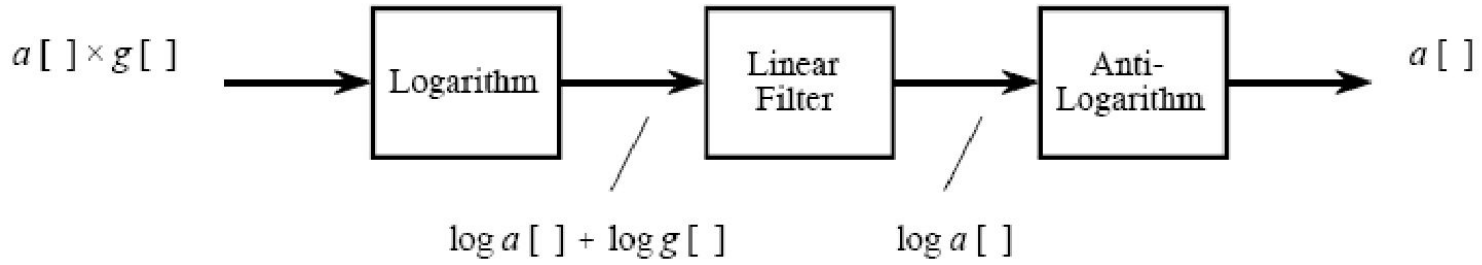

FIGURE 22-11
Homomorphic separation of multiplied signals. Taking the logarithm of the input signal transforms components that are *multiplied* into components that are *added*. These components can then be separated by linear filtering, and the effect of the logarithm undone.

Нелинейная фильтрация

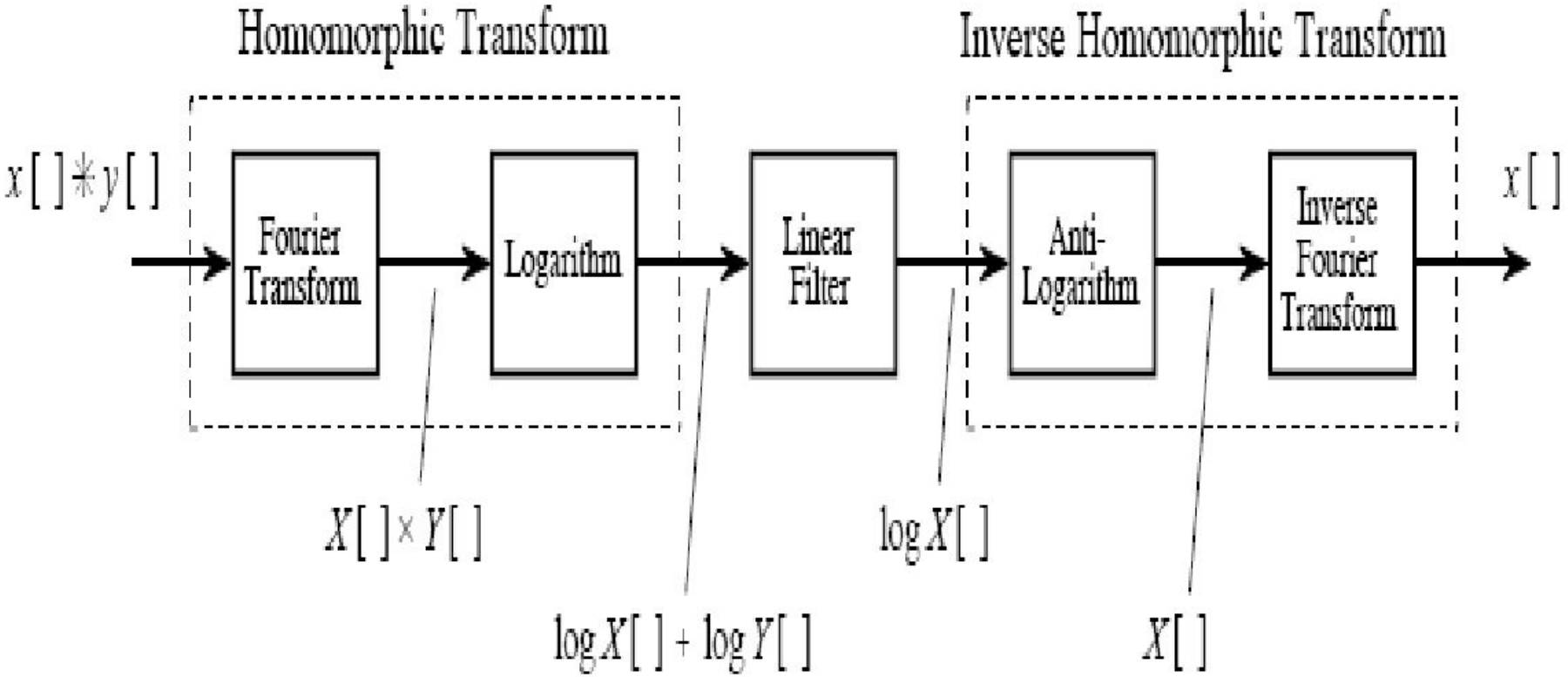

FIGURE 22-12

Homomorphic separation of convolved signals. Components that have been *convolved* are converted into components that are *added* by taking the Fourier transform followed by the logarithm. After linear filtering to separate the added components, the original steps are undone.

Окна и спектры

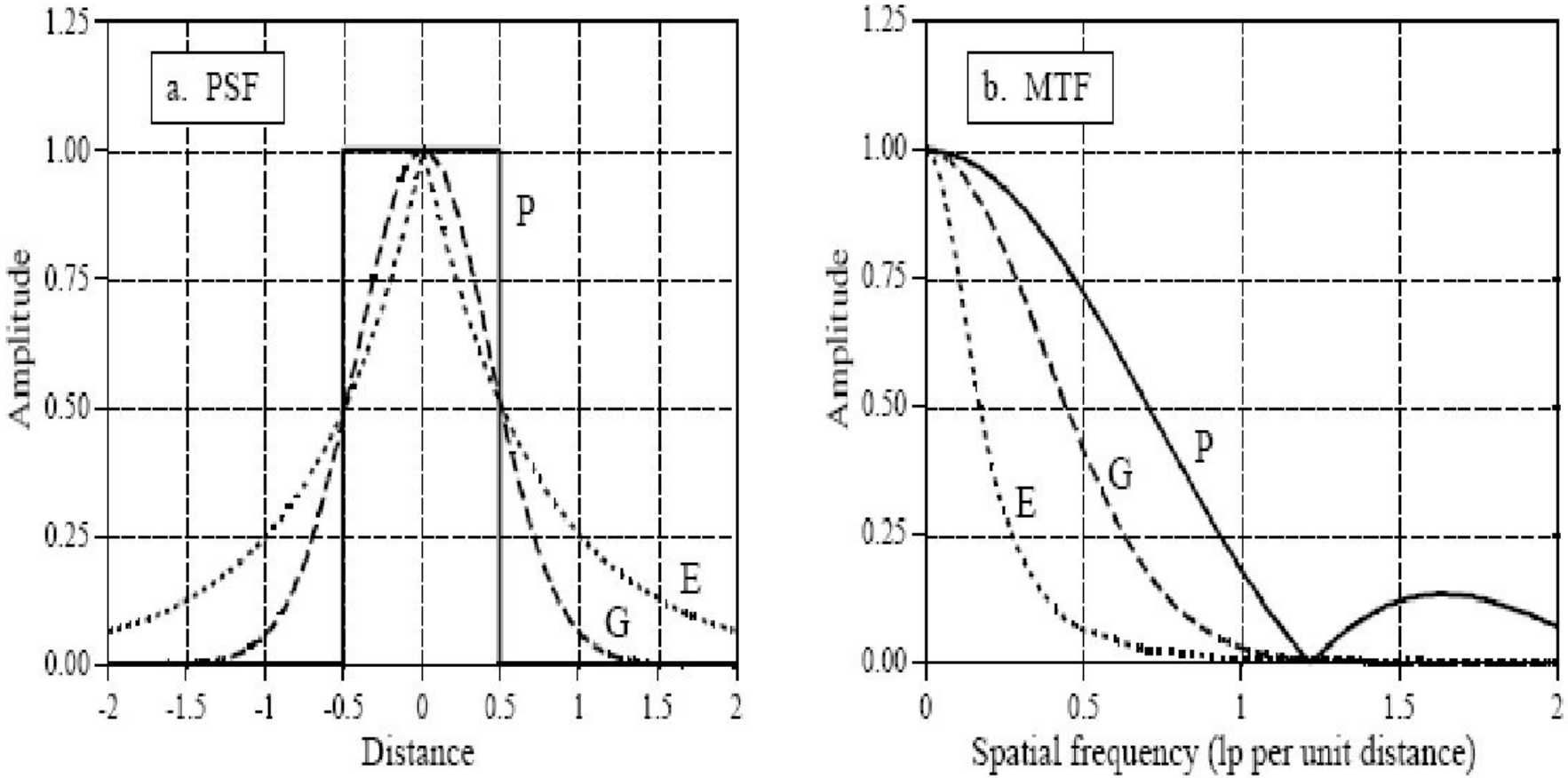

FIGURE 25-1
FWHM versus MTF. Figure (a) shows profiles of three PSFs commonly found in imaging systems: (P) pillbox, (G) Gaussian, and (E) exponential. Each of these has a FWHM of one unit. The corresponding MTFs are shown in (b). Unfortunately, similar values of FWHM do not correspond to similar MTF curves.

Похожи АЧХ, близки и реакции на ступеньку

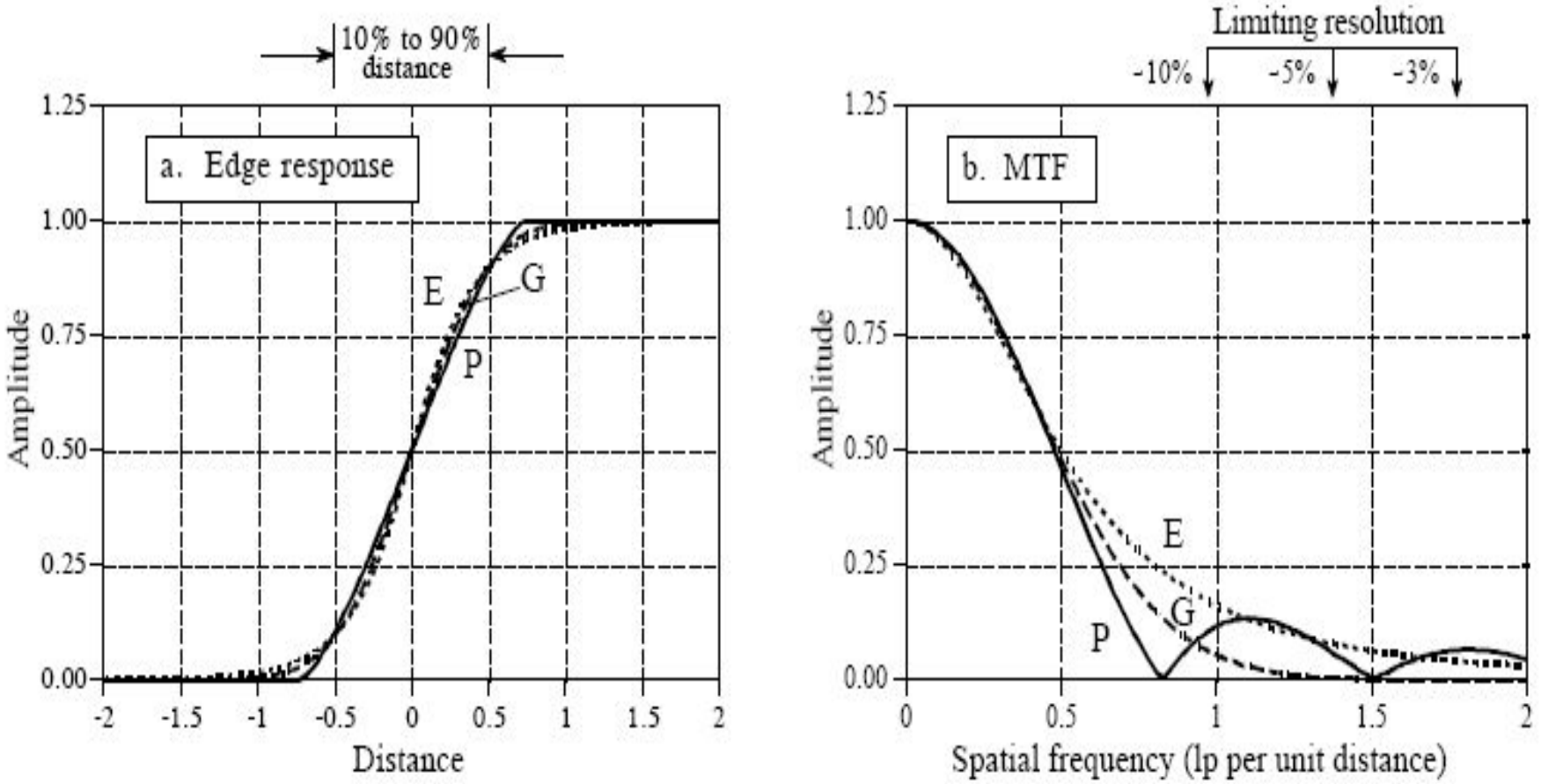

FIGURE 25-4

Edge response and MTF. Figure (a) shows the edge responses of three PSFs: (P) pillbox, (G) Gaussian, and (E) exponential. Each edge response has a 10% to 90% rise distance of 1 unit. Figure (b) shows the corresponding MTF curves, which are similar above the 10% level. *Limiting resolution* is a vague term indicating the frequency where the MTF has an amplitude of 3% to 10%.

АЧХ и импульсный отклик

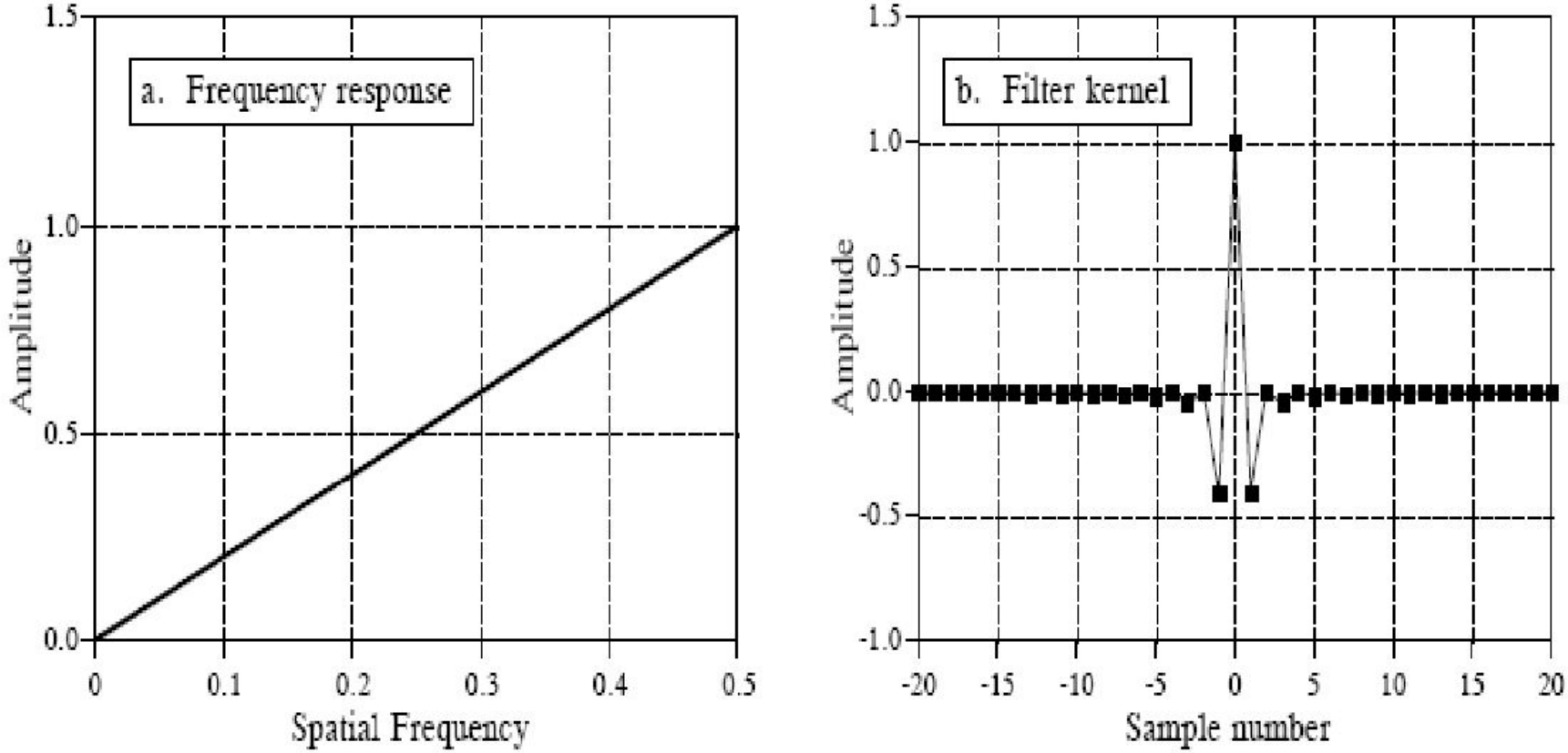

FIGURE 25-19
Backprojection filter. The frequency response of the backprojection filter is shown in (a), and the corresponding filter kernel is shown in (b). Equation 25-2 provides the values for the filter kernel.

Перерегулирование и неравномерность

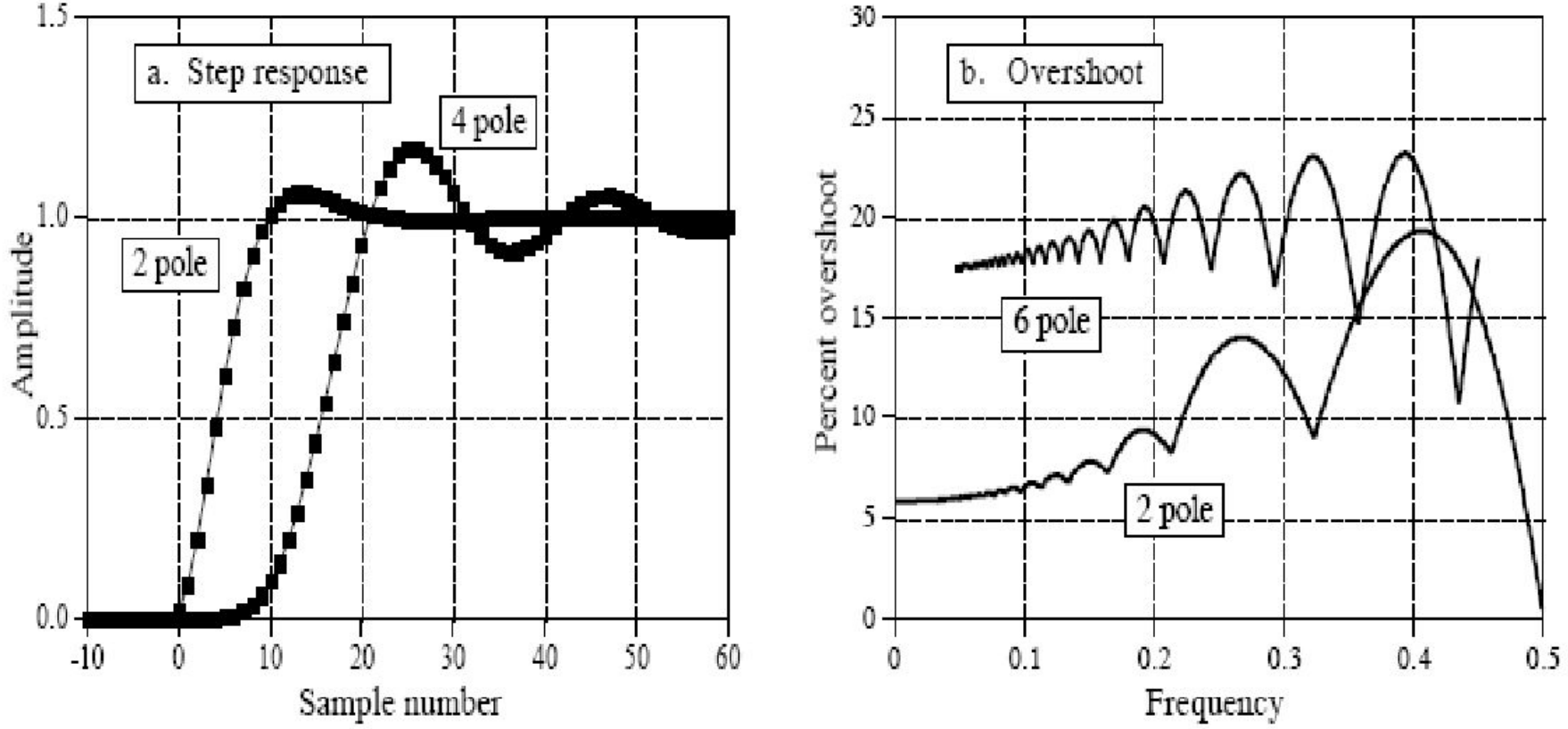

FIGURE 20-3
Chebyshev step response. The overshoot in the Chebyshev filter's step response is 5% to 30%, depending on the number of poles, as shown in (a), and the cutoff frequency, as shown in (b). Figure (a) is for a cutoff frequency of 0.05, and may be scaled to other cutoff frequencies.

Частота и крутизна среза

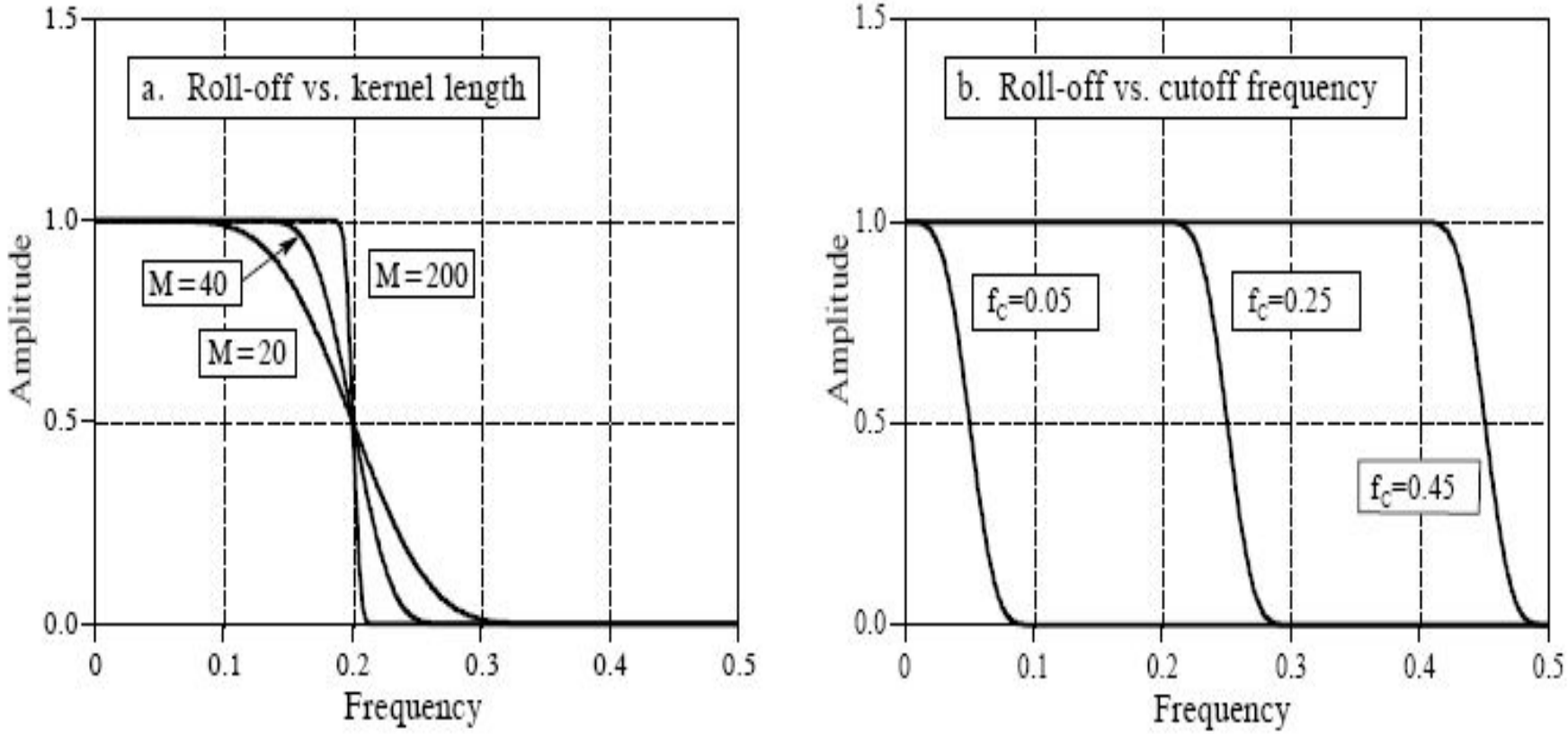

FIGURE 16-3
Filter length vs. roll-off of the windowed-sinc filter. As shown in (a), for $M = 20$, 40, and 200, the transition bandwidths are $BW = 0.2$, 0.1, and 0.02 of the sampling rate, respectively. As shown in (b), the shape of the frequency response does not change with different cutoff frequencies. In (b), $M = 60$.

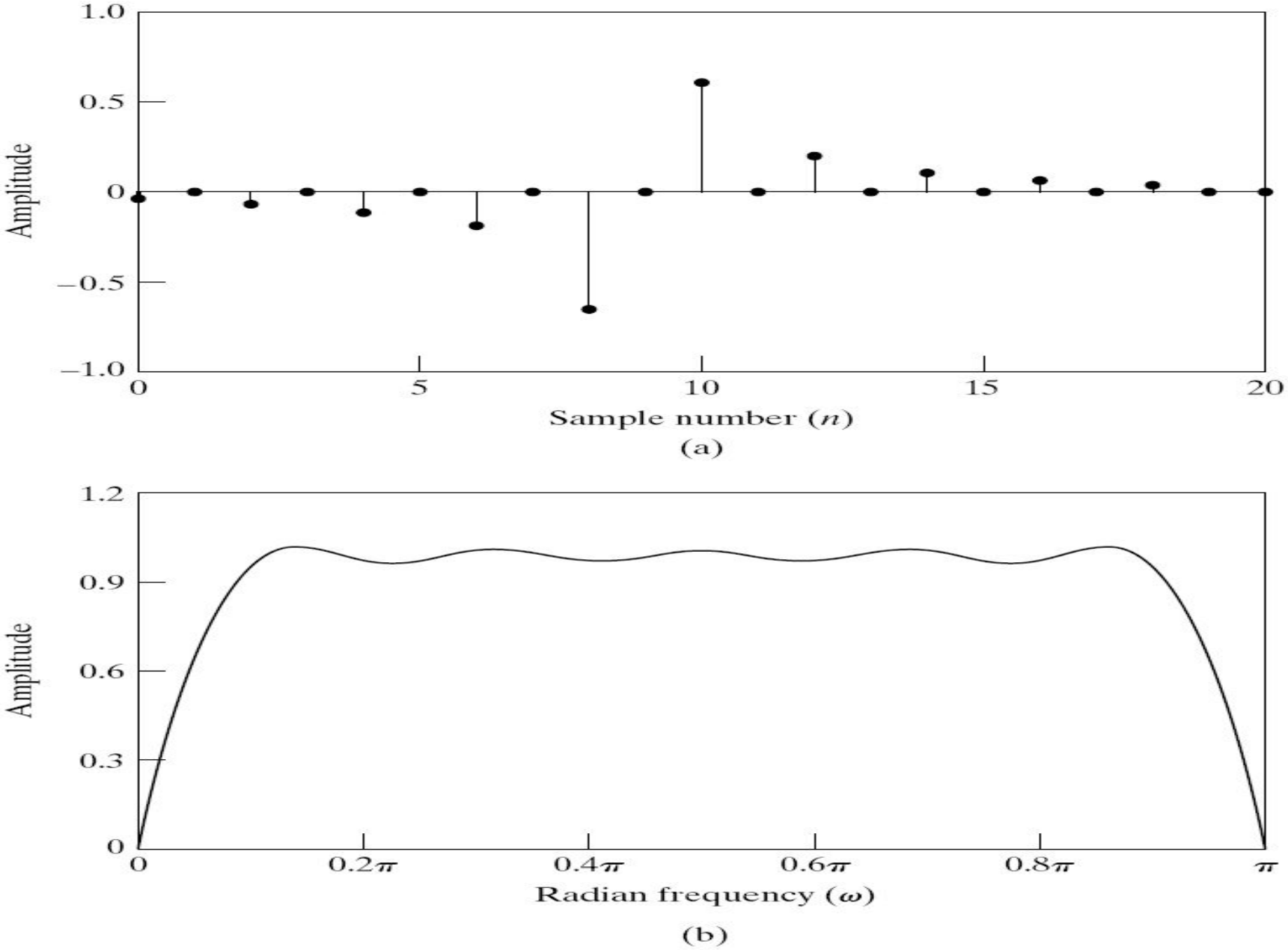

Figure 11.7 (a) Impulse response and (b) magnitude response of an FIR Hilbert transformer designed using the Kaiser window. ($M = 18$ and $\beta = 2.629$.)

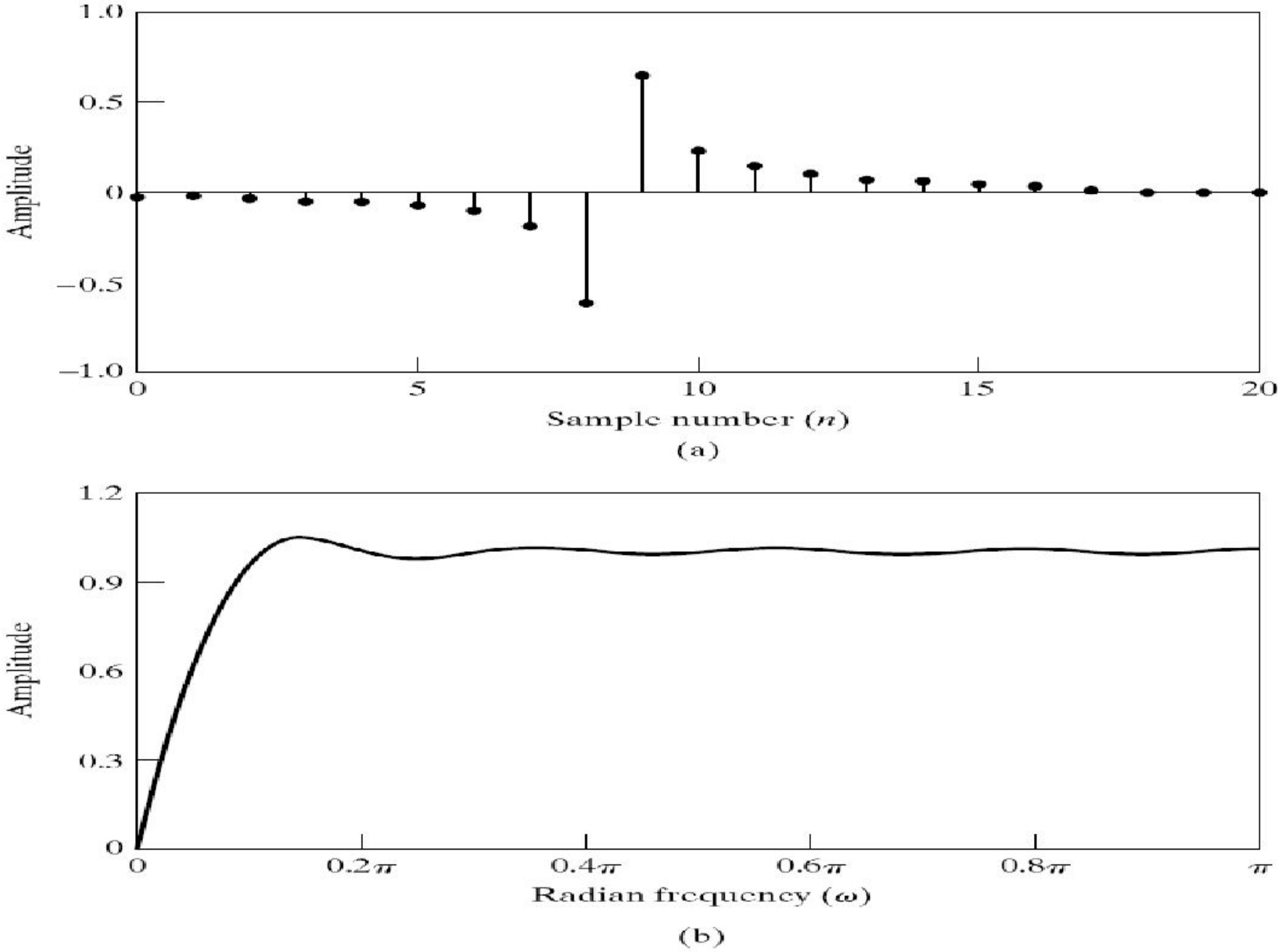

Figure 11.8 (a) Impulse response and (b) magnitude response of an FIR Hilbert transformer designed using the Kaiser window. ($M = 17$ and $\beta = 2.44$.)

Влияние разрядности

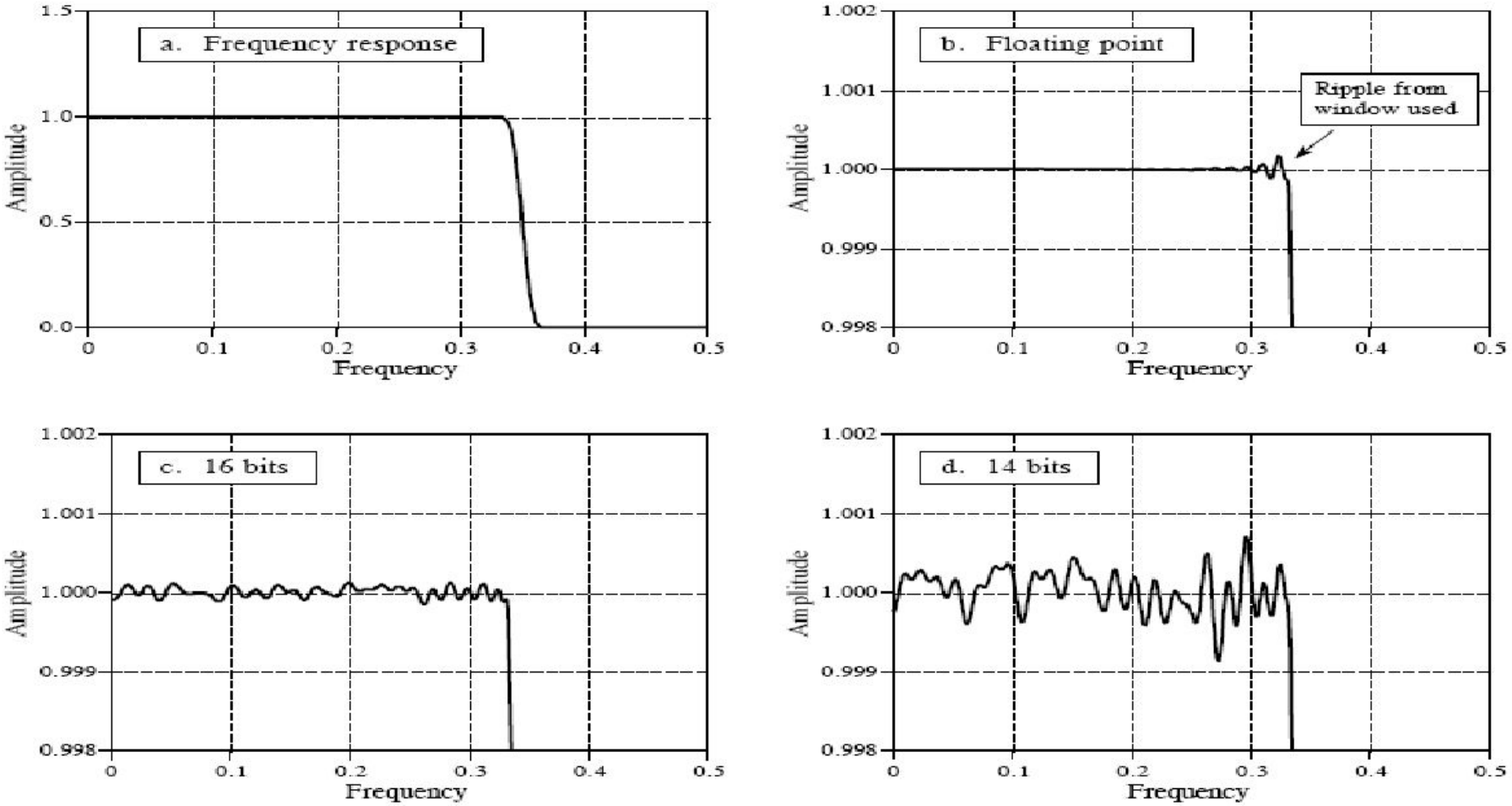

FIGURE 29-5
Round-off noise in the frequency response. Figure (a) shows the frequency response of a windowed-sinc low-pass filter, using a Blackman window and 150 points in the filter kernel. Figures (b), (c), and (d) show a more detailed view of this response by zooming in on the amplitude. When the filter kernel is represented in floating point, (b), the round-off noise is insignificant compared to the imperfections of the windowed-sinc design. As shown in (c) and (d), representing the filter kernel in fixed point makes round-off noise the dominate imperfection.

Электрические цепи и сигналы

FIGURE 30-6
RLC notch filter. This circuit removes a narrow band of frequencies from a signal. The use of complex substitution greatly simplifies the analysis of this and similar circuits.

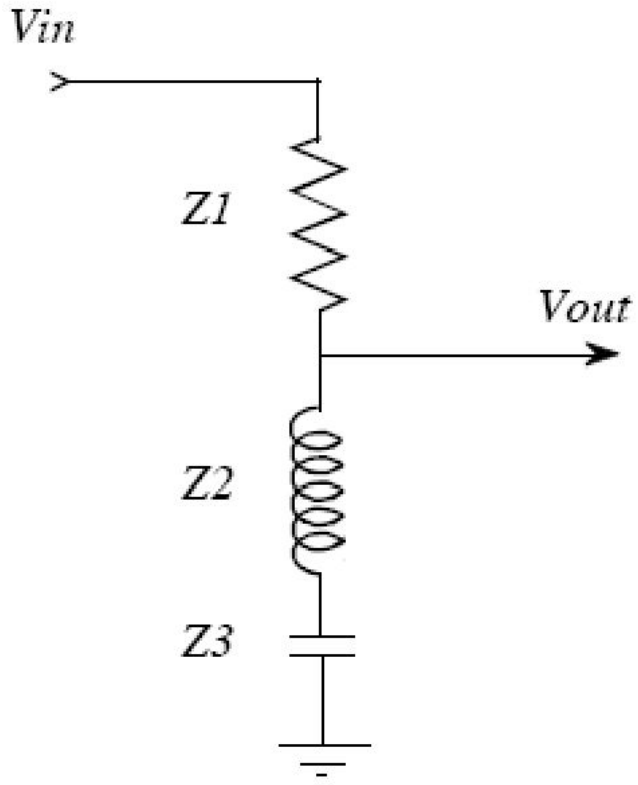

Электрические цепи и сигналы

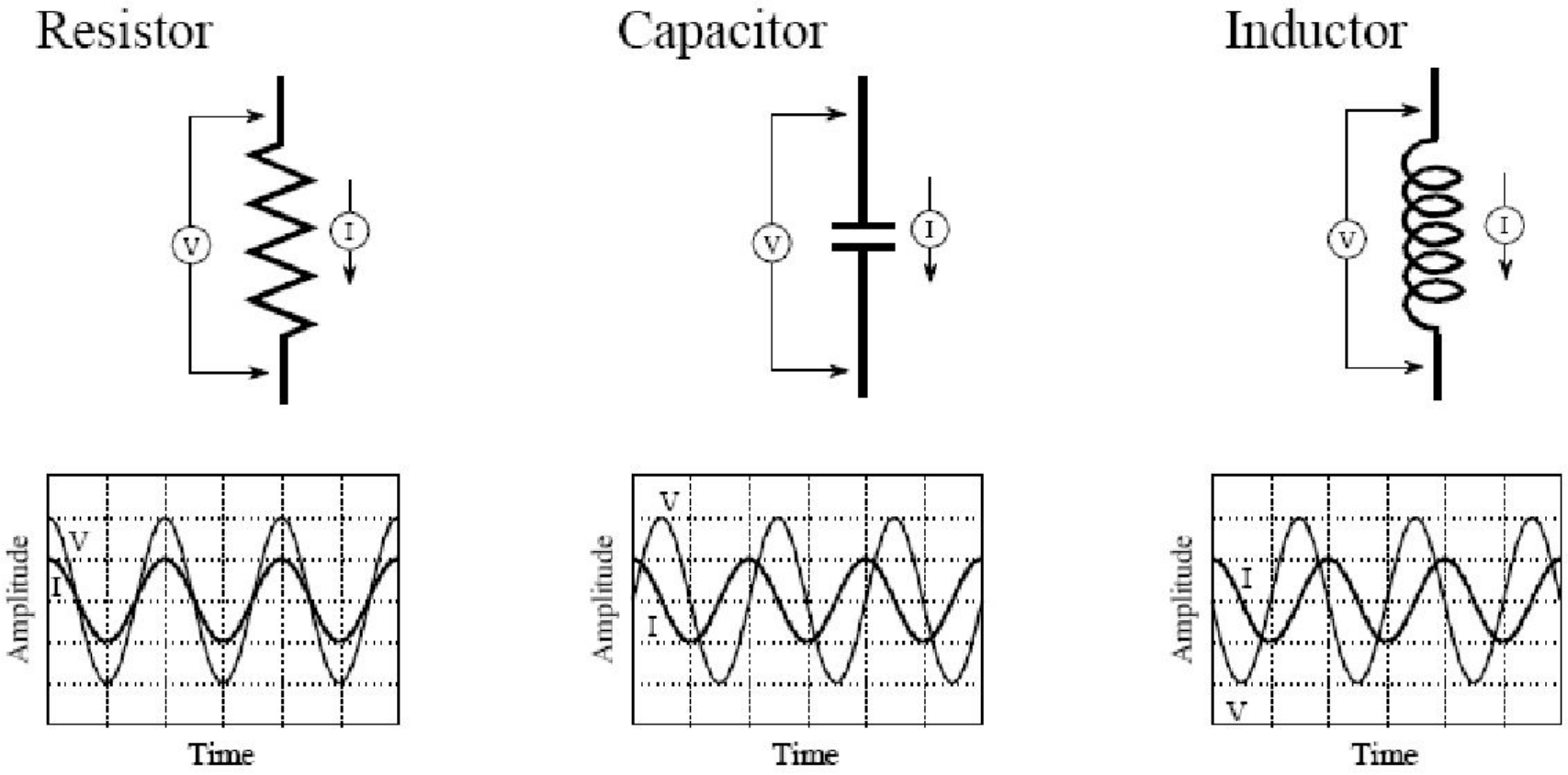

FIGURE 30-5
Definition of impedance. When sinusoidal voltages and currents are represented by complex numbers, the ratio between the two is called the *impedance*, and is denoted by the complex variable, Z. Resistors, capacitors and inductors have impedances of R, $-j/\omega C$, and $j\omega L$, respectively.

Переключаемые конденсаторы

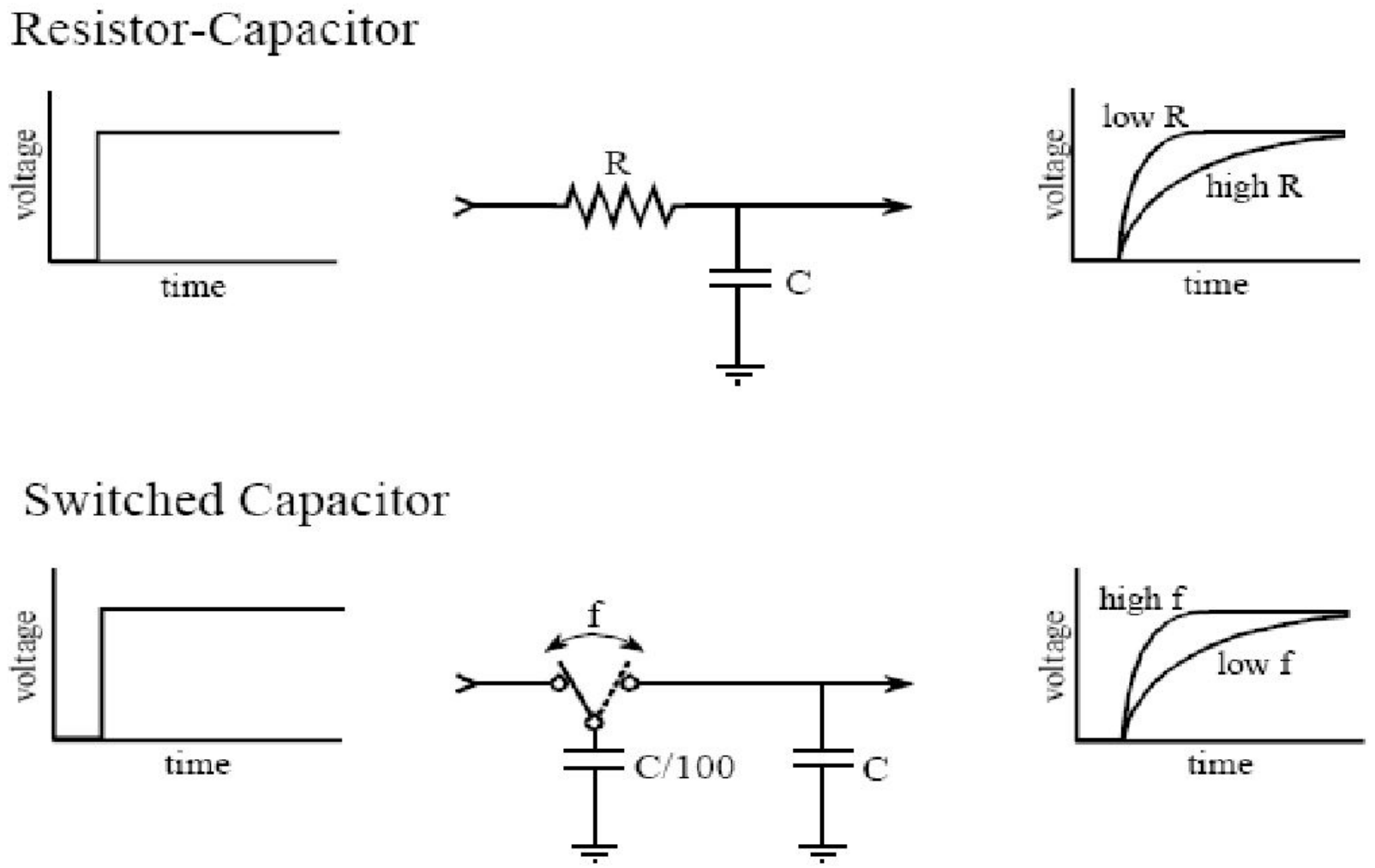

FIGURE 3-10
Switched capacitor filter operation. Switched capacitor filters use switches and capacitors to mimic resistors. As shown by the equivalent step responses, two capacitors and one switch can perform the same function as a resistor-capacitor network.

Аналоговый фильтр

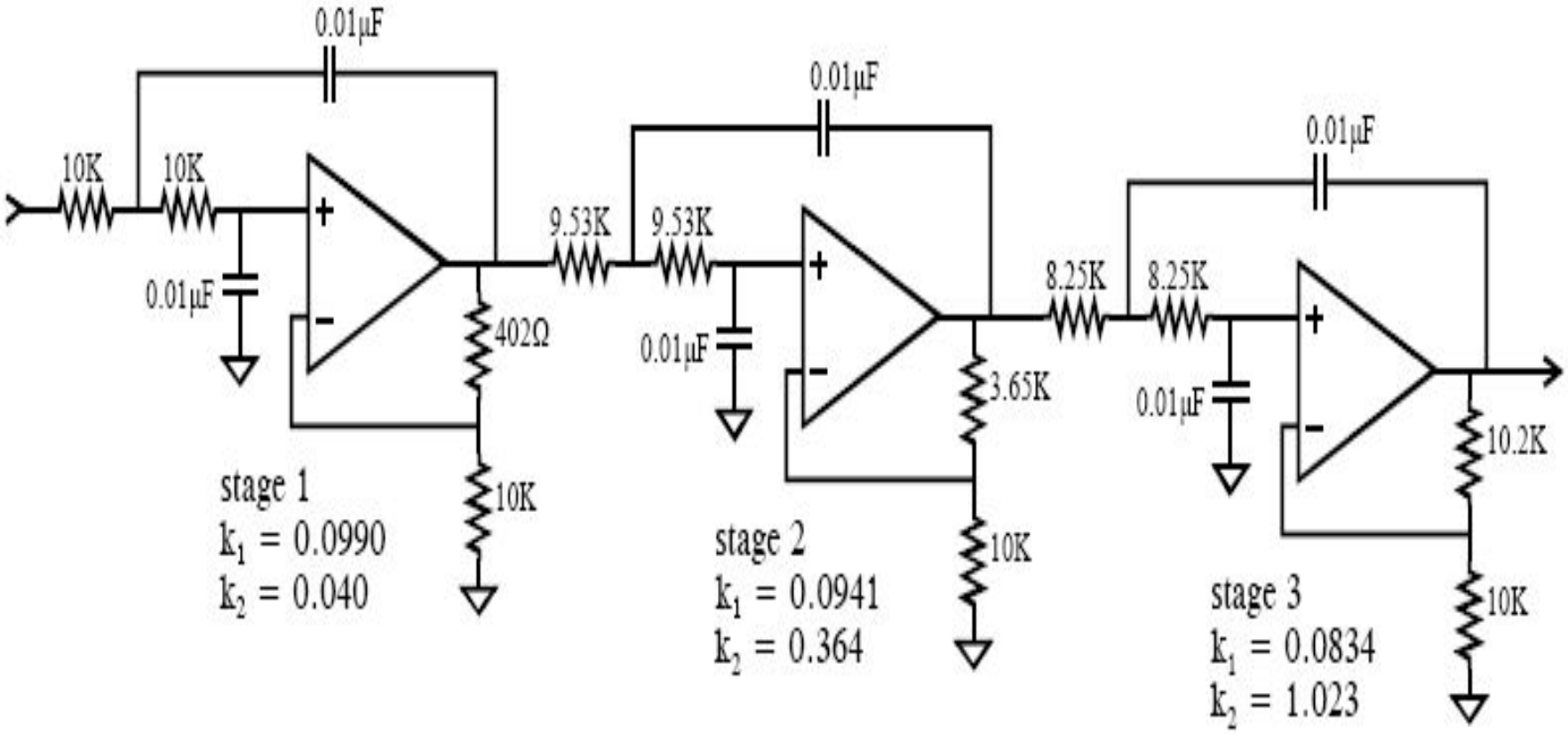

FIGURE 3-9

A six pole Bessel filter formed by cascading three Sallen-Key circuits. This is a low-pass filter with a cutoff frequency of 1 kHz.

Фильтр низких частот

FIGURE 3-8
The modified Sallen-Key circuit, a building block for active filter design. The circuit shown implements a 2 pole low-pass filter. Higher order filters (more poles) can be formed by cascading stages. Find k_1 and k_2 from Table 3-1, arbitrarily select R_1 and C (try 10K and 0.01μF), and then calculate R and R_f from the equations in the figure. The parameter, f_c, is the cutoff frequency of the filter, in hertz.

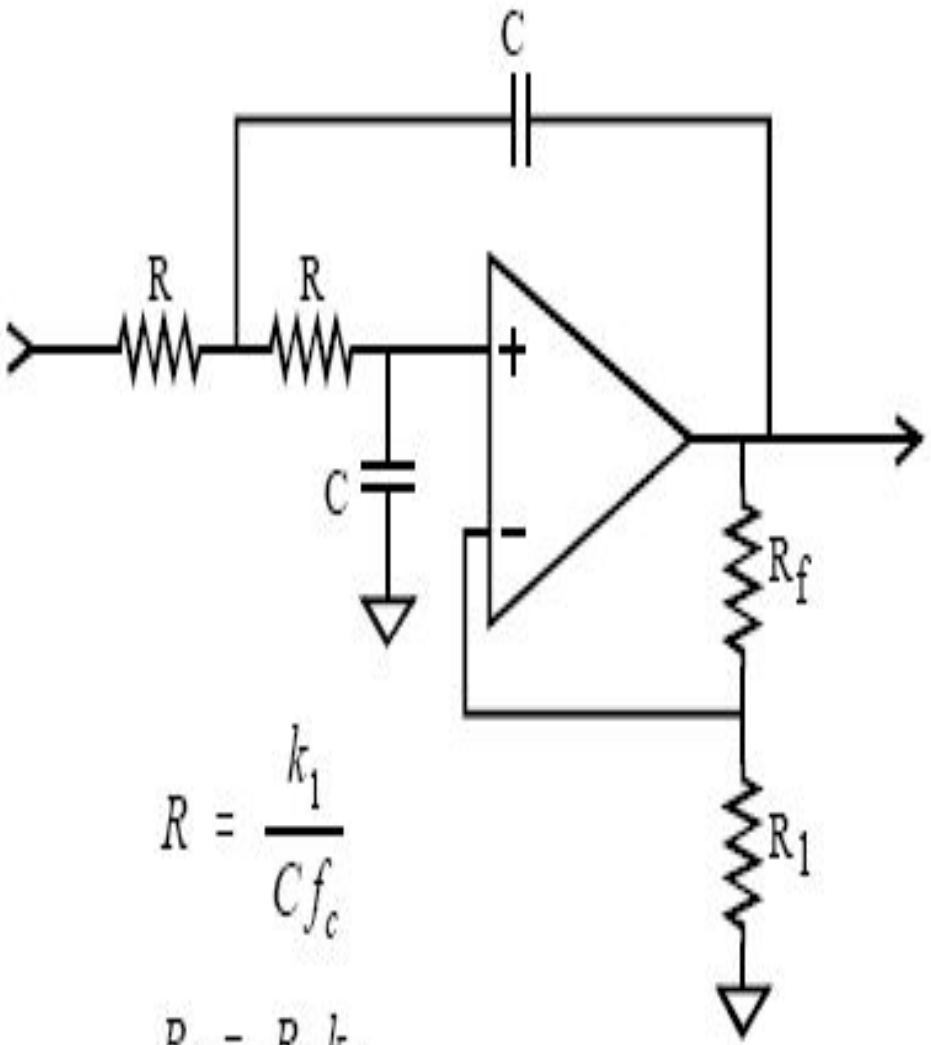

$$R = \frac{k_1}{C f_c}$$

$$R_f = R_1 k_2$$

REVIEW OF POPULAR ANALOG FILTERS

- Butterworth
  - All Pole, No Ripples in Passband or Stopband
  - Maximally Flat Response (Fastest Roll-off with No Ripple)
- Chebyshev (Type 1)
  - All Pole, Ripple in Passband, No Ripple in Stopband
  - Shorter Transition Region than Butterworth for Given Number of Poles
  - Type 2 has Ripple in Stopband, No Ripple in Passband
- Elliptical (Cauer)
  - Has Poles and Zeros, Ripple in Both Passband and Stopband
  - Shorter Transition Region than Chebyshev for Given Number of Poles
  - Degraded Phase Response
- Bessel (Thompson)
  - All Pole, No Ripples in Passband or Stopband
  - Optimized for Linear Phase and Pulse Response
  - Longest Transition Region of All for Given Number of Poles

IIR FILTER DESIGN TECHNIQUES

- Impulse Invarient Transformation Method
  - Start with H(s) for Analog Filter
  - Take Inverse Laplace Transform to get Impulse Response
  - Obtain z-Transform H(z) from Sampled Impulse Response
  - z-Transform Yields Filter Coefficients
  - Aliasing Effects Must be Considered
- Bilinear Transformation Method
  - Another Method for Transforming H(s) into H(z)
  - Performance Determined by the Analog System's Differential Equation
  - Aliasing Effects do not Occur
- Matched z-Transform Method
  - Maps H(s) into H(z) for filters with both poles and zeros
- CAD Methods
  - Fletcher-Powell Algorithm
  - Implements Cascaded Biquad Sections

COMPARISON BETWEEN FIR AND IIR FILTERS

IIR FILTERS	FIR FILTERS
More Efficient	Less Efficient
Analog Equivalent	No Analog Equivalent
May Be Unstable	Always Stable
Non-Linear Phase Response	Linear Phase Response
More Ringing on Glitches	Less Ringing on Glitches
CAD Design Packages Available	CAD Design Packages Available
No Efficiency Gained by Decimation	Decimation Increases Efficiency

DECIMATION OF A SAMPLED SIGNAL BY A FACTOR OF M

A: ORIGINAL OVERSAMPLED SIGNAL

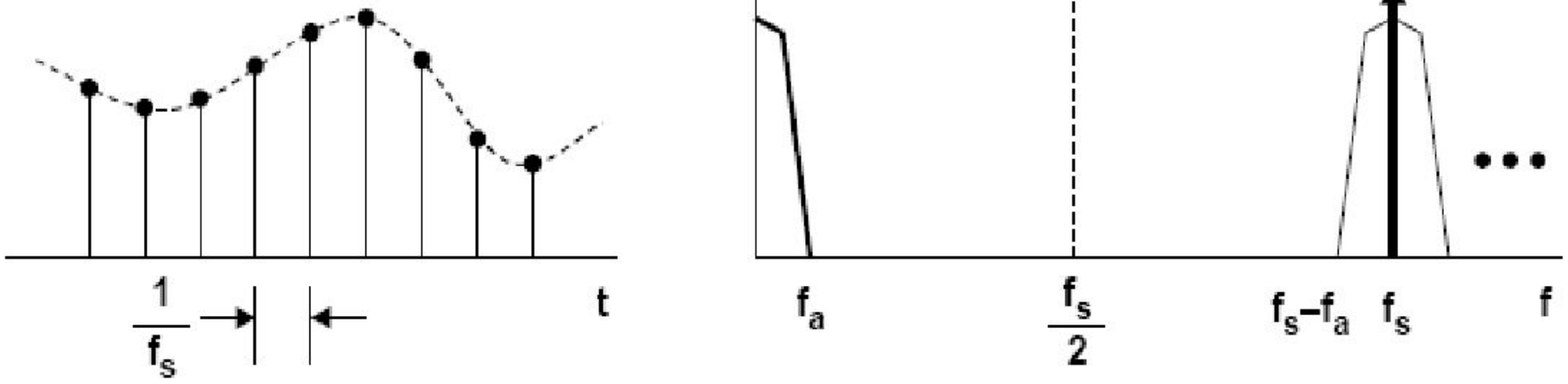

B: SIGNAL DECIMATED BY M

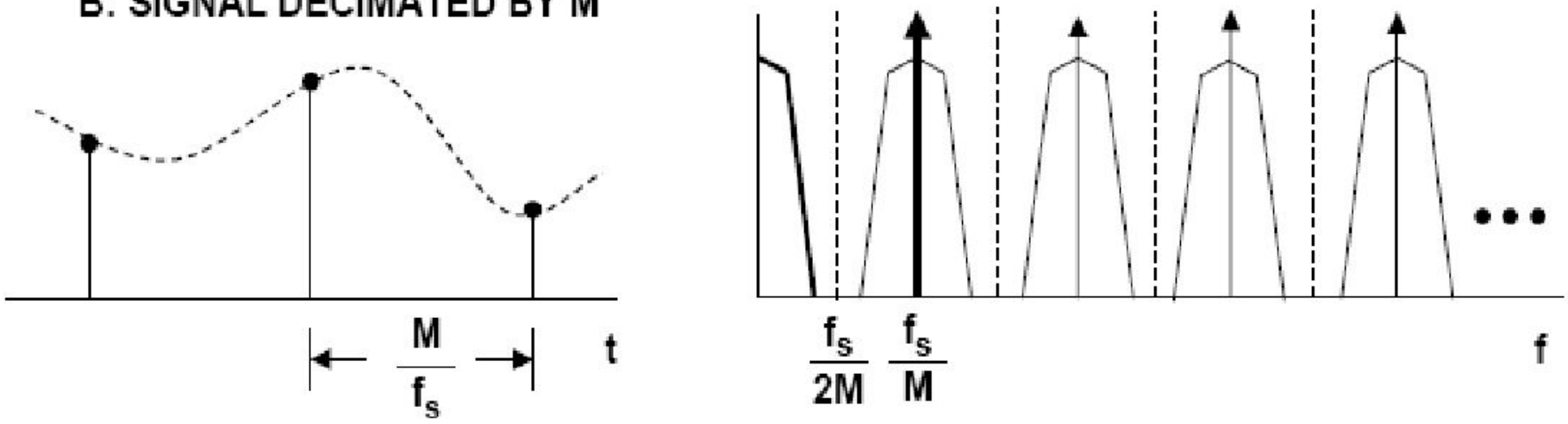

DECIMATION COMBINED WITH FIR FILTERING

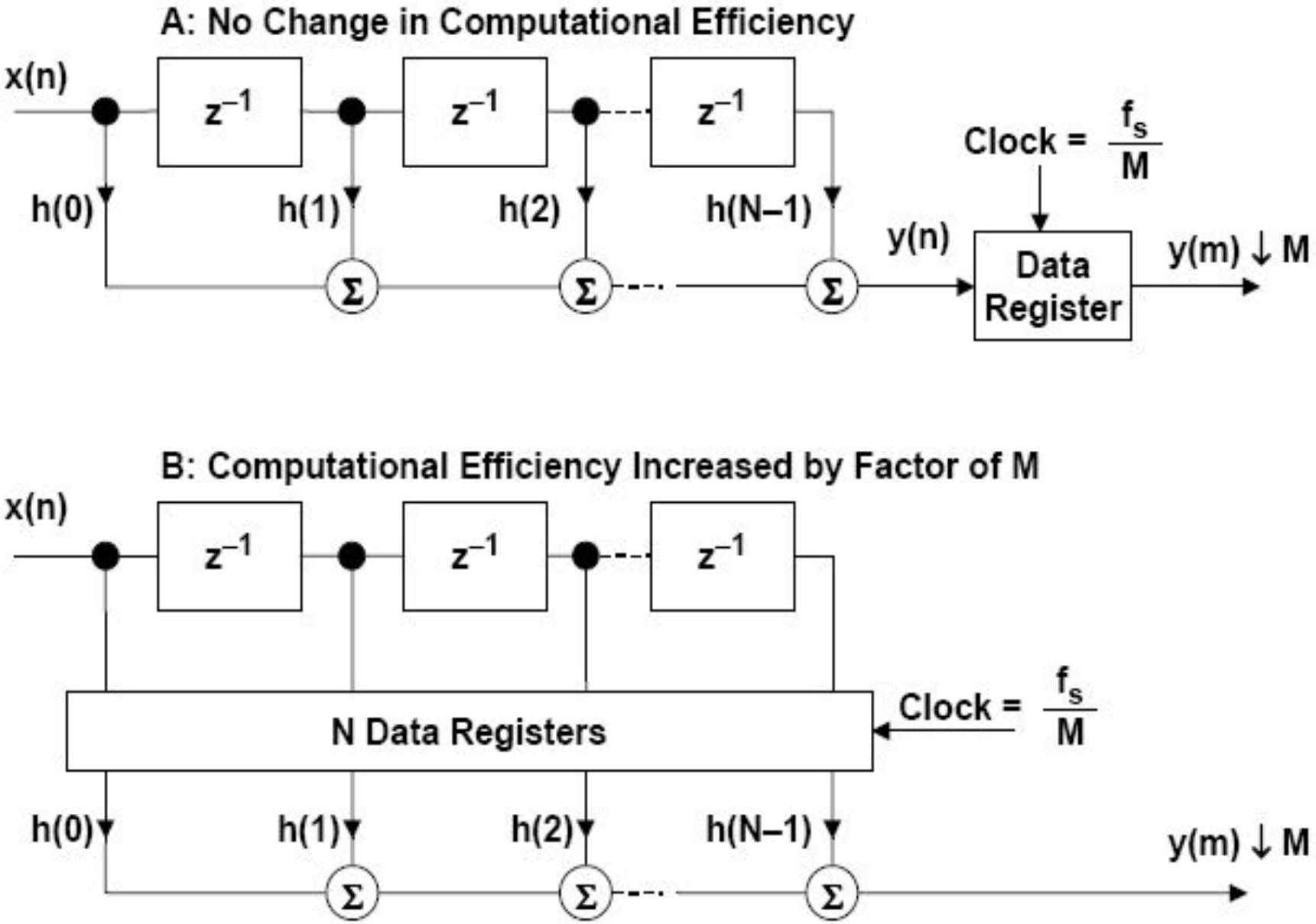

INTERPOLATION BY A FACTOR OF L

A: ORIGINAL SAMPLED SIGNAL

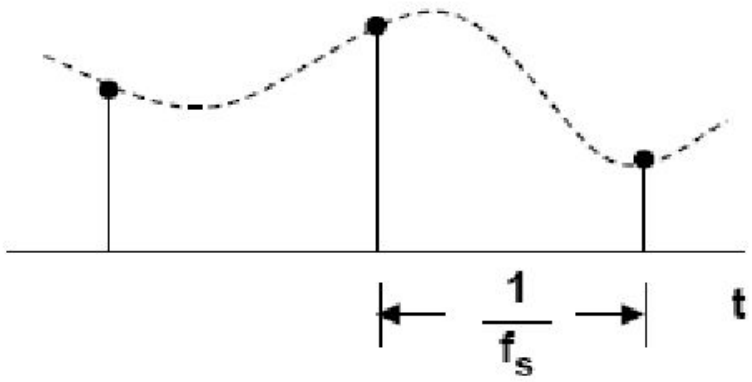

SAMPLING RATE = f_s

B: SIGNAL WITH ADDED ZEROS

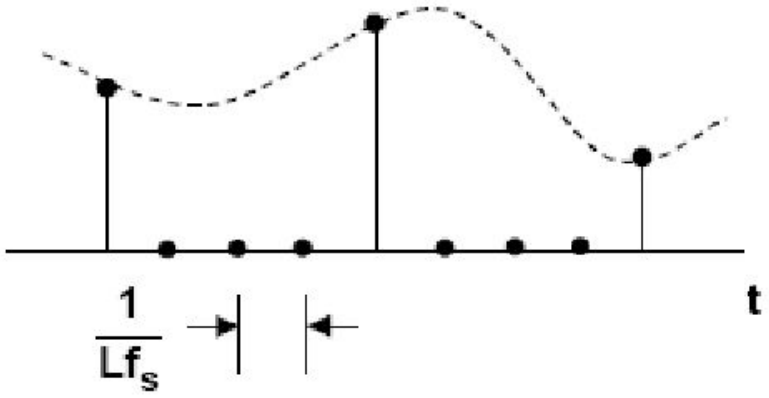

C: SIGNAL AFTER INTERPOLATING FILTER

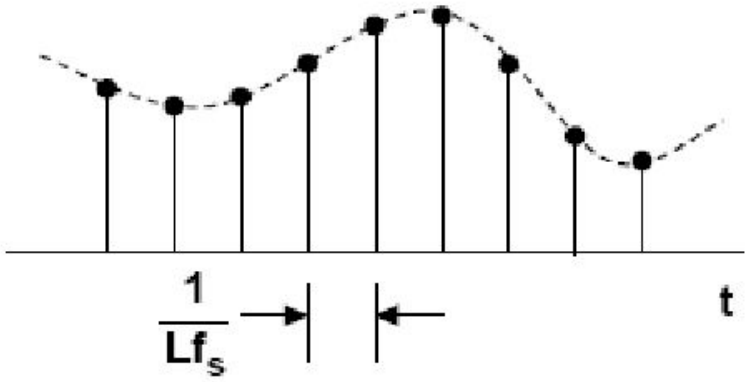

SAMPLING RATE = Lf_s

EFFECTS OF INTERPOLATION ON FREQUENCY SPECTRUM

ORIGINAL SIGNAL

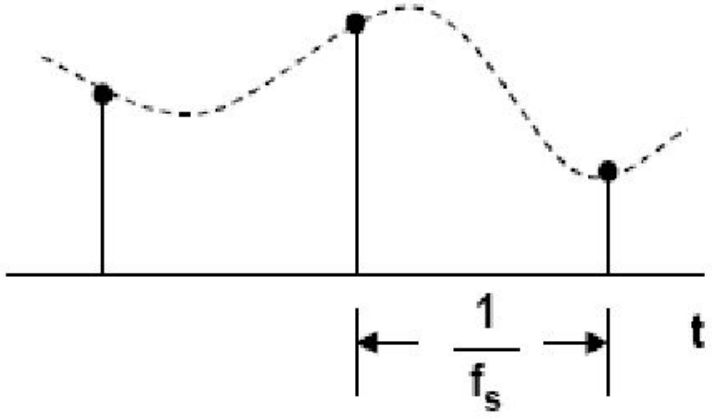

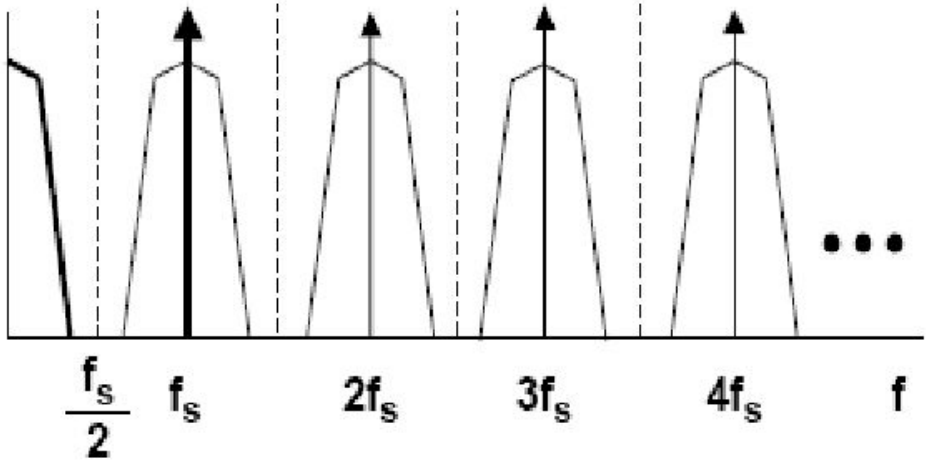

SIGNAL INTERPOLATED BY L

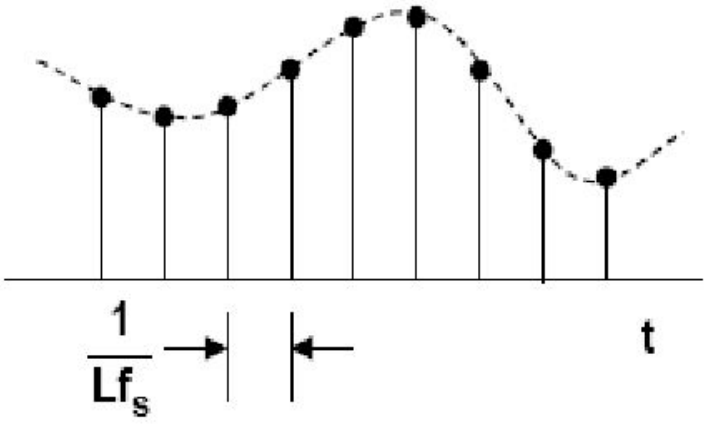

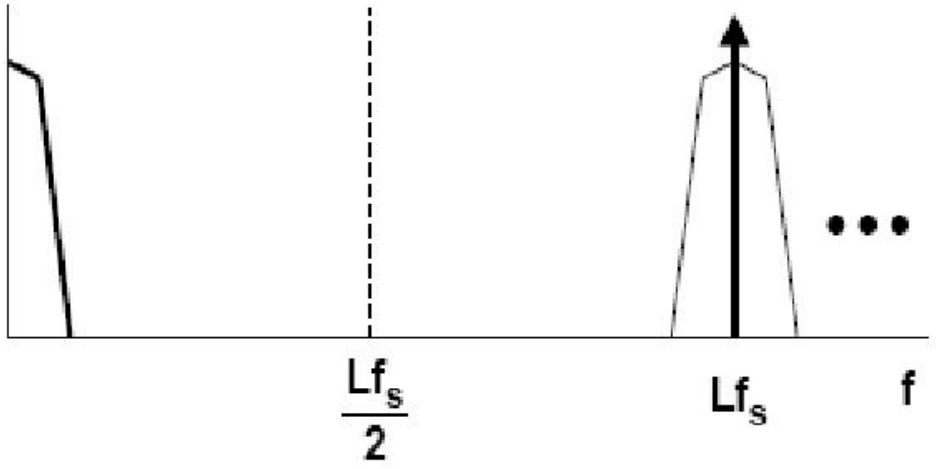

TYPICAL INTERPOLATION IMPLEMENTATION

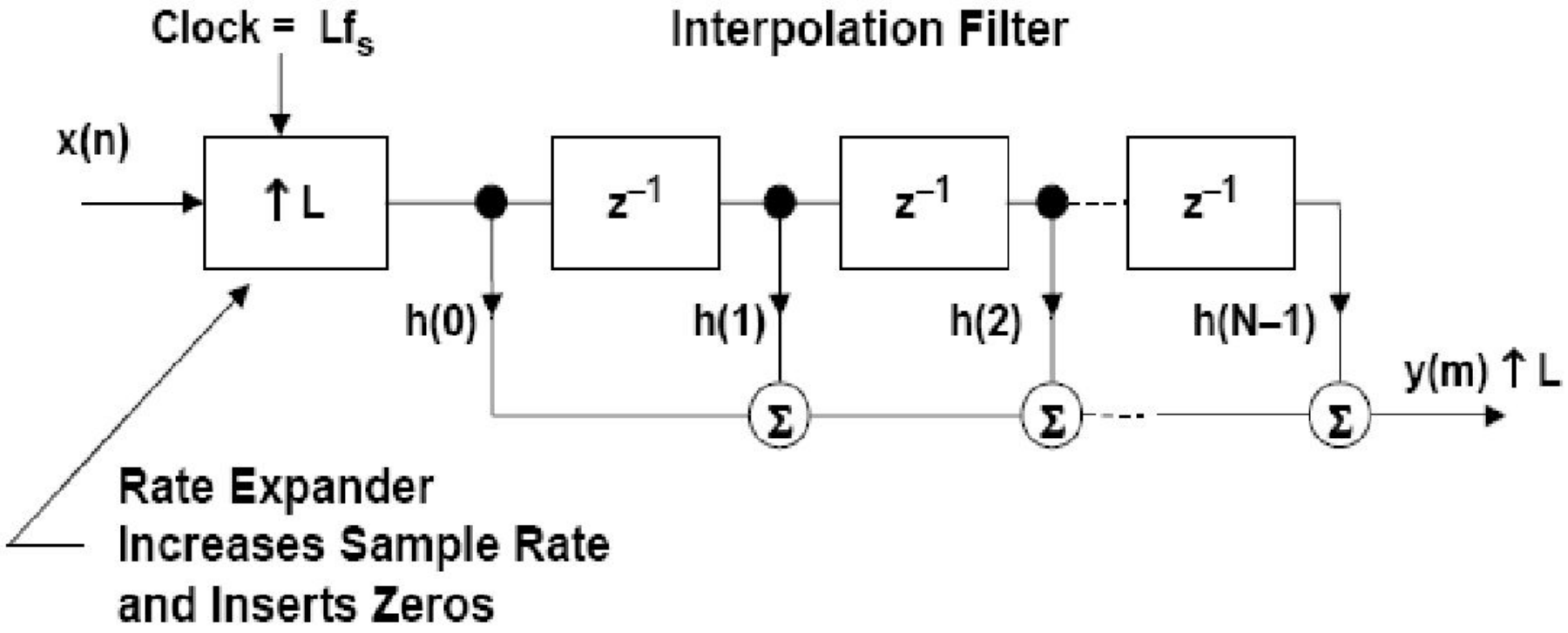

Efficient DSP algorithms take advantage of:

- Multiplications by zero
- Circular Buffers
- Zero-Overhead Looping

SAMPLE RATE CONVERTERS

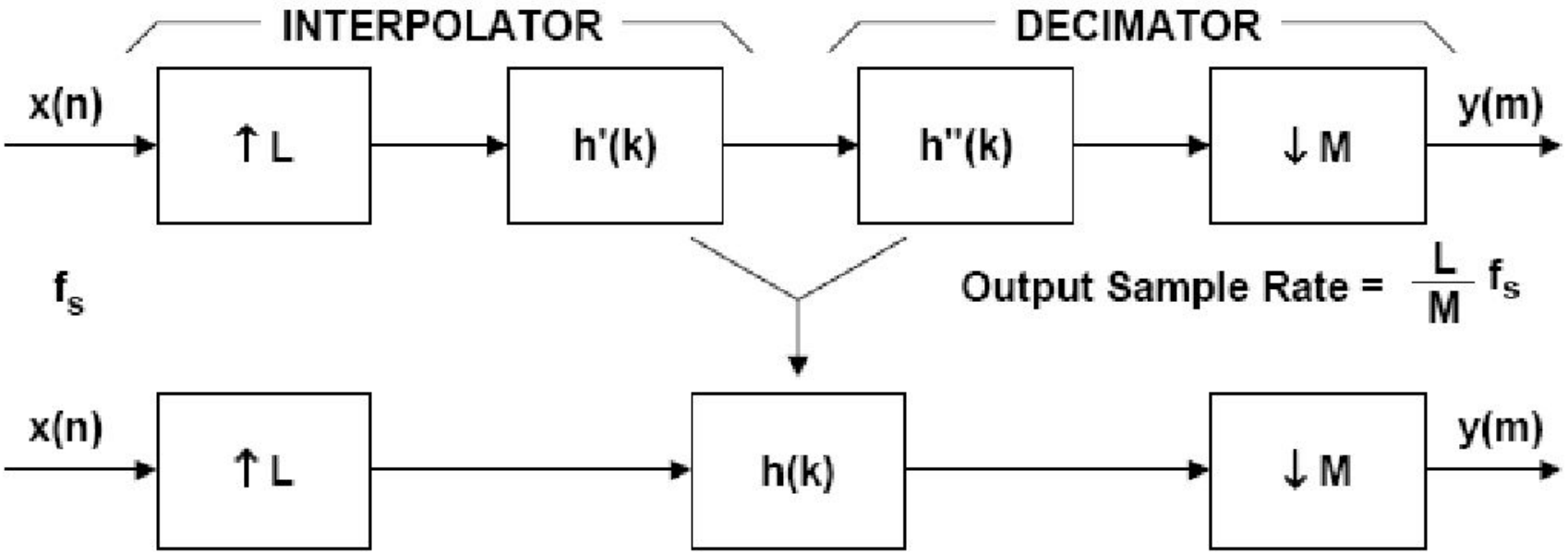

- Example: Convert CD Sampling Rate = 44.1kHz to DAT Sampling Rate = 48.0kHz
- Use L = 160, M = 147
- $f_{out} = \frac{L}{M} f_s = \frac{160}{147} \times 44.1\text{kHz} = 48.0\text{kHz}$

ADAPTIVE FILTER

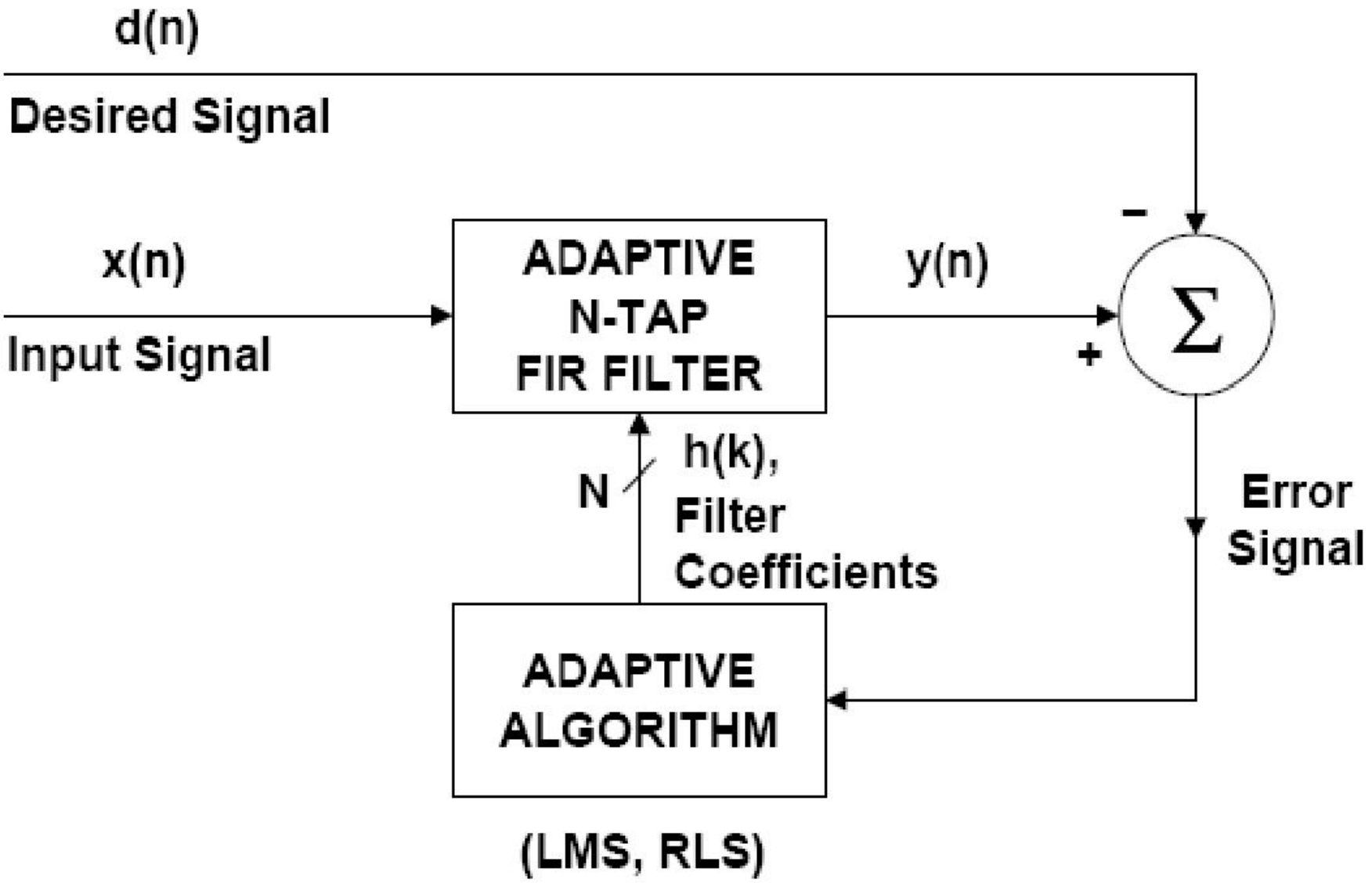

DIGITAL TRANSMISSION USING ADAPTIVE EQUALIZATION

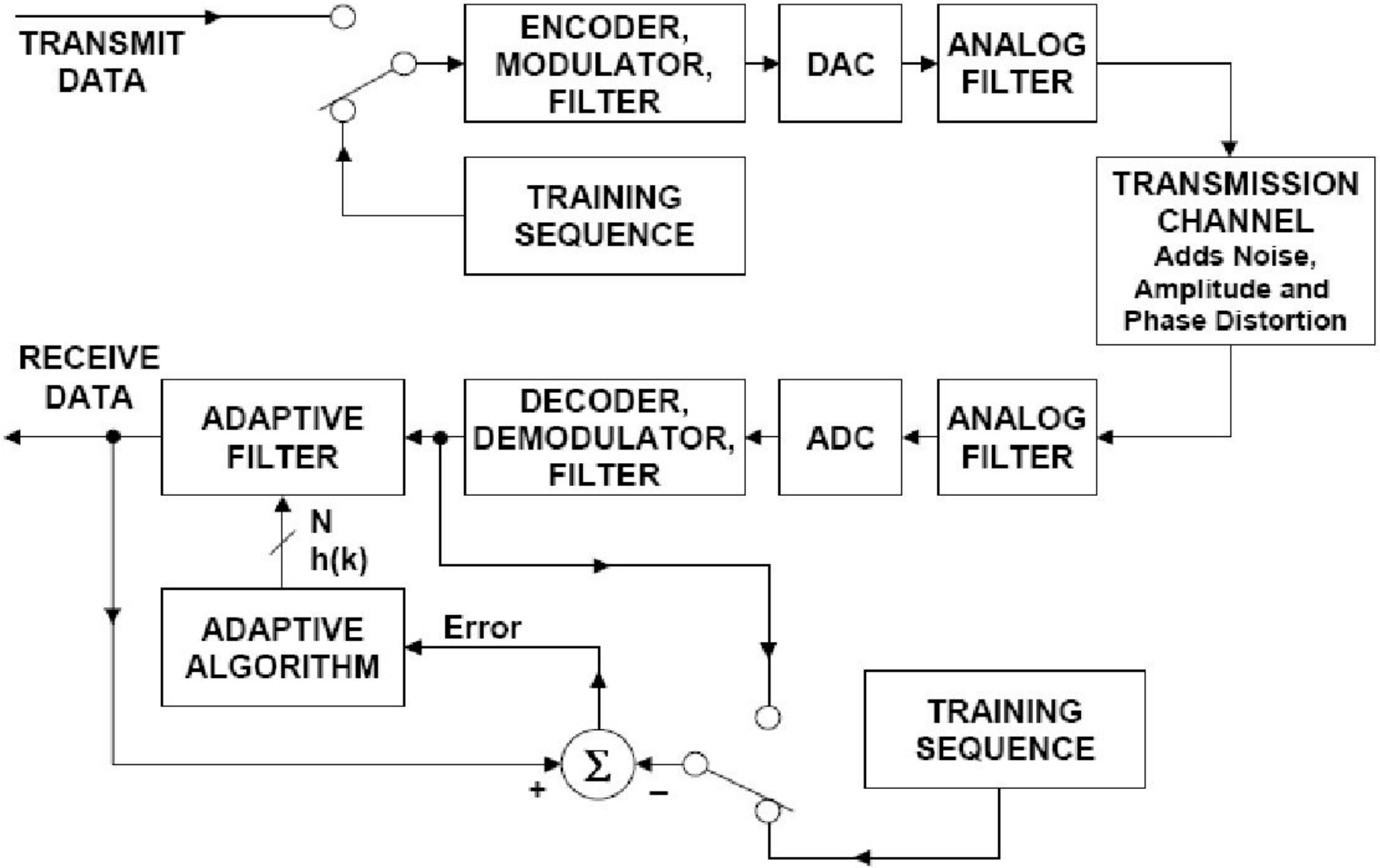

LINEAR PREDICTIVE CODING (LPC) MODEL OF SPEECH PRODUCTION

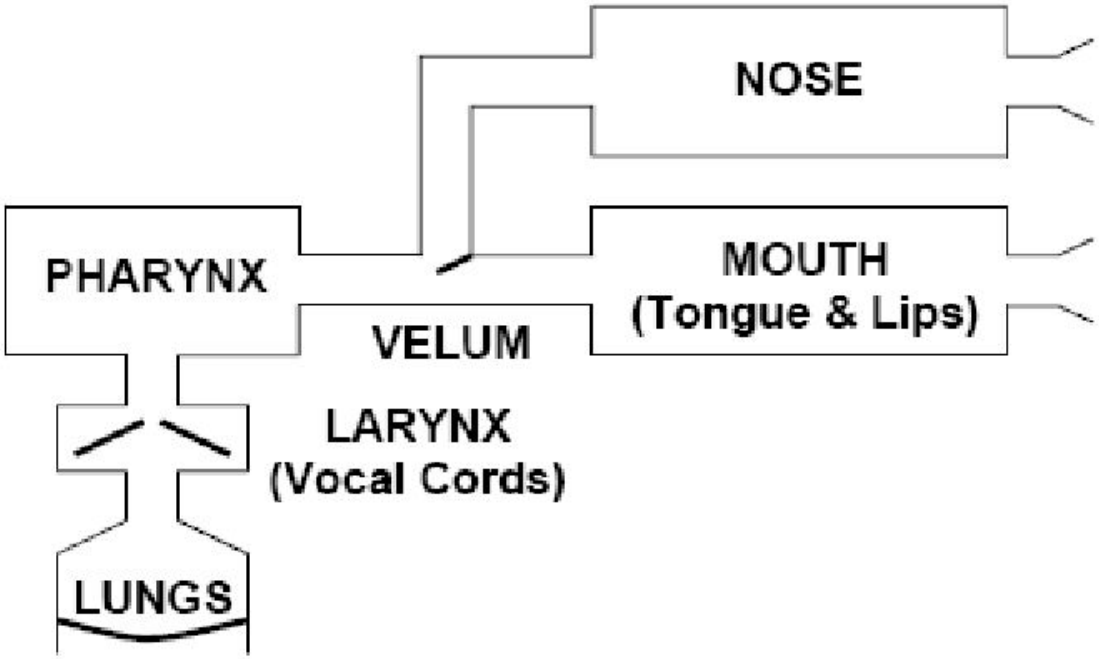

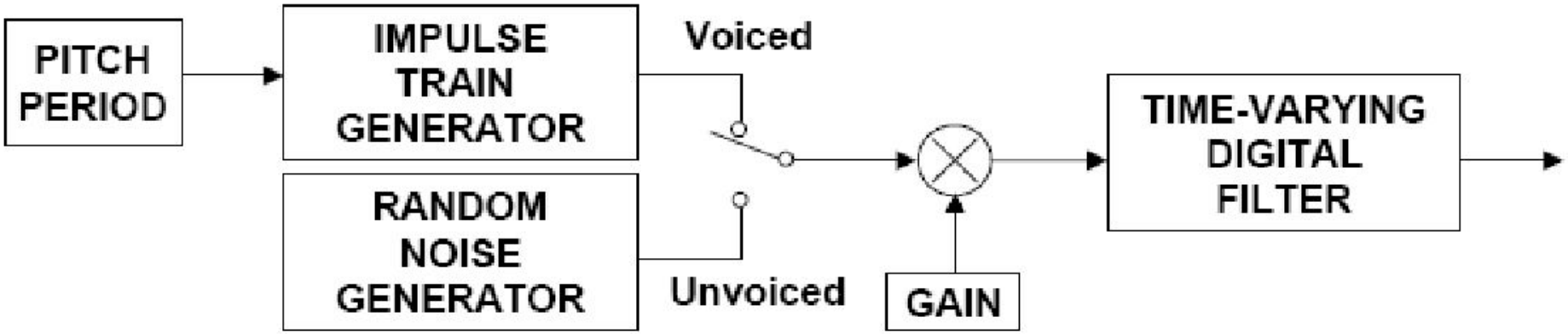

LPC SPEECH COMPANDING SYSTEM

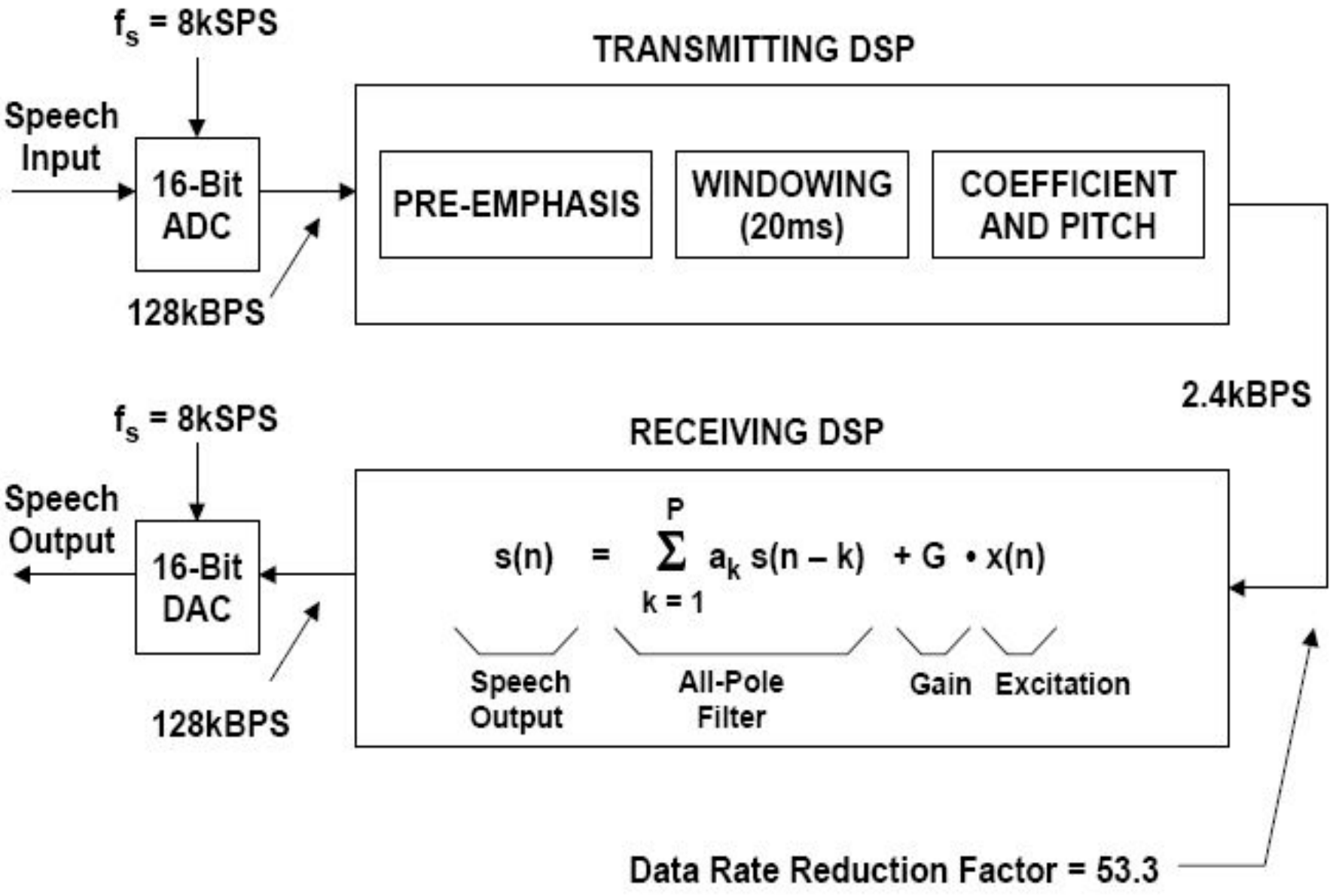

ALL POLE LATTICE FILTER

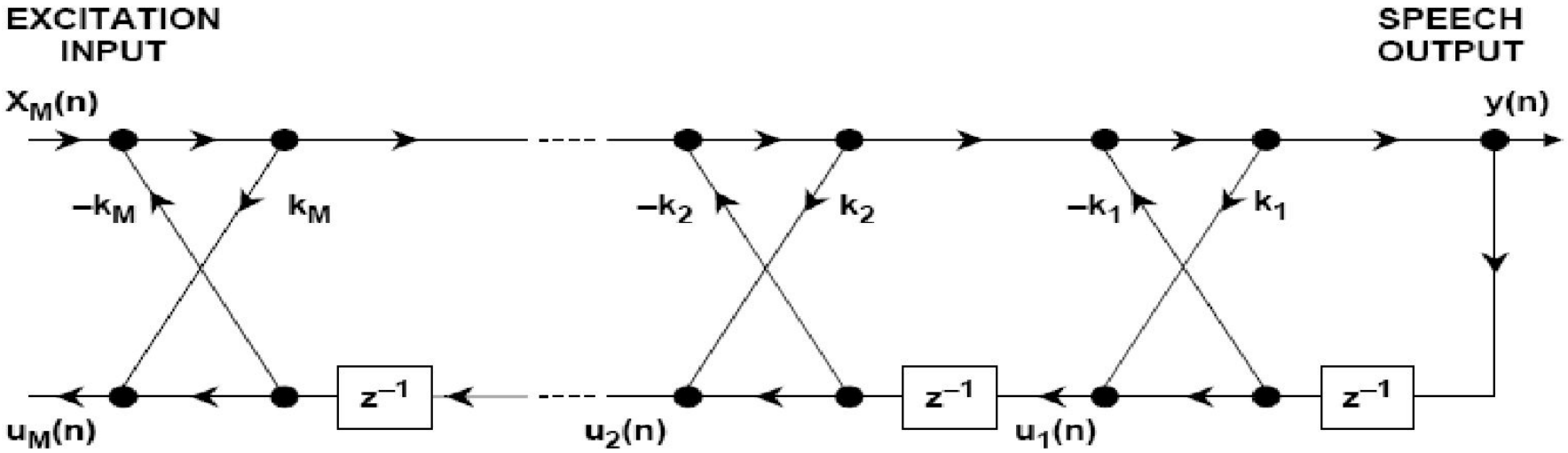

ESTIMATION OF LATTICE FILTER COEFFICIENTS IN TRANSMITTING DSP

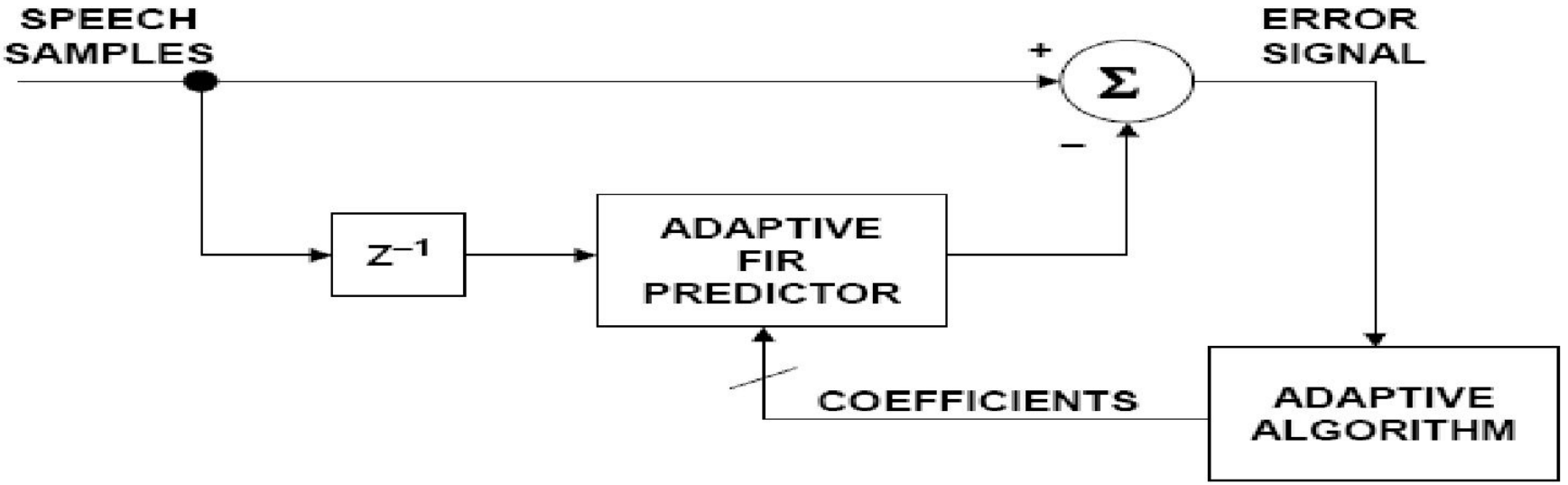

Идеология цифровой фильтрации

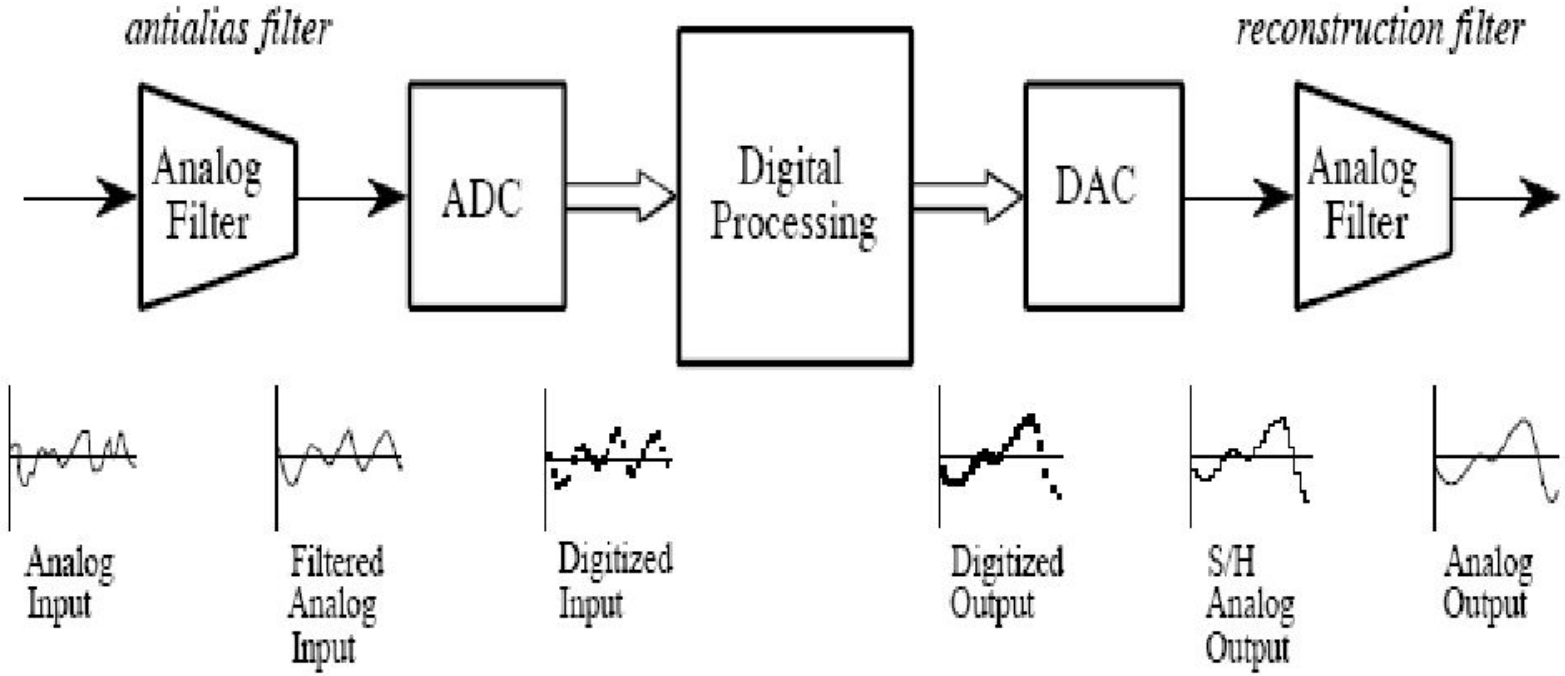

FIGURE 3-7
Analog electronic filters used to comply with the sampling theorem. The electronic filter placed before an ADC is called an *antialias filter*. It is used to remove frequency components above one-half of the sampling rate that would alias during the sampling. The electronic filter placed after a DAC is called a *reconstruction filter*. It also eliminates frequencies above the Nyquist rate, and may include a correction for the zeroth-order hold.

Временные окна

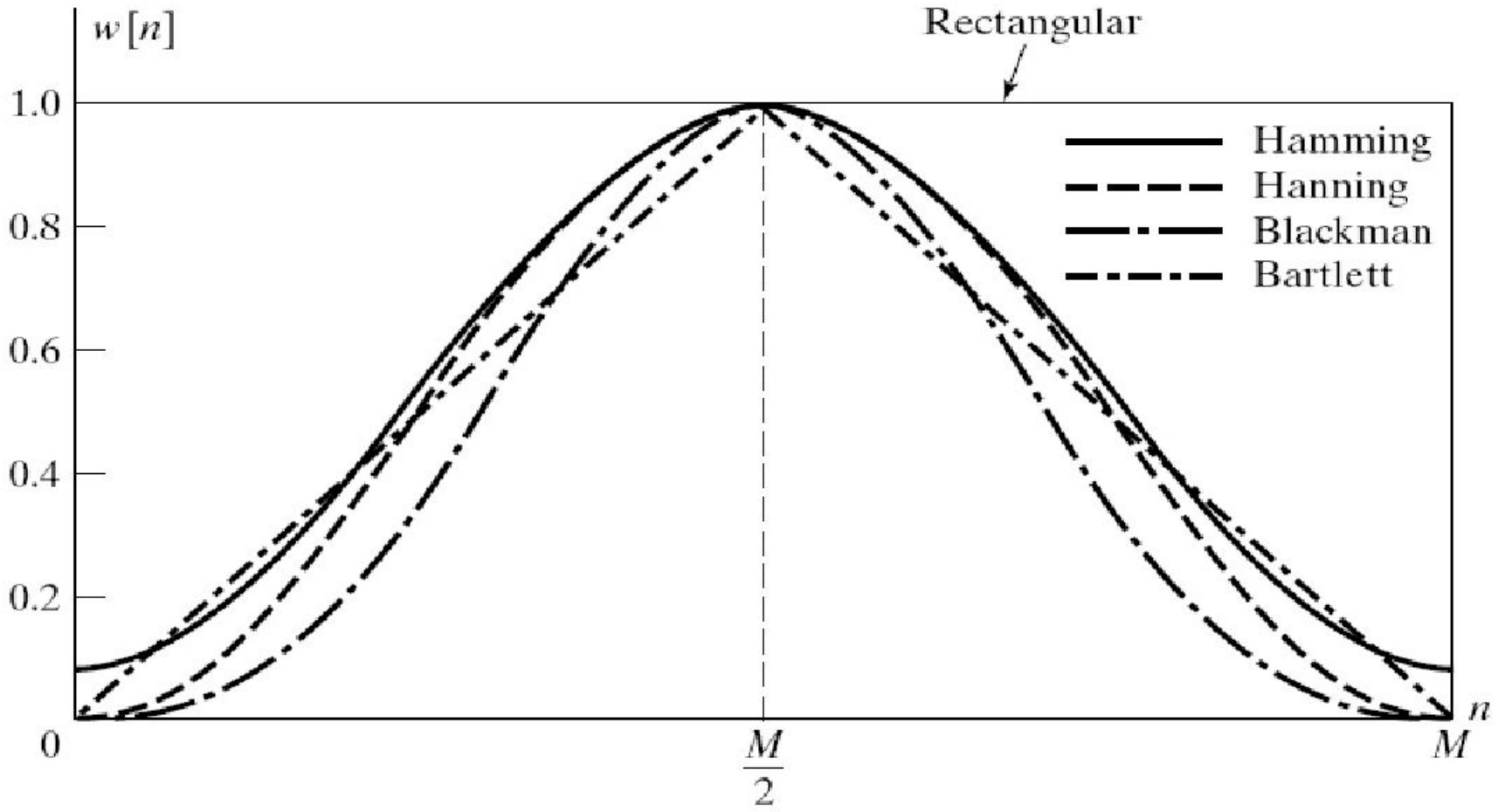

Figure 7.21 Commonly used windows.

Временные окна

Figure 7.22 Fourier transforms (log magnitude) of windows of Figure 7.21. with $M = 50$. (a) Rectangular. (b) Bartlett. (c) Hanning. (d) Hamming. (e) Blackman.

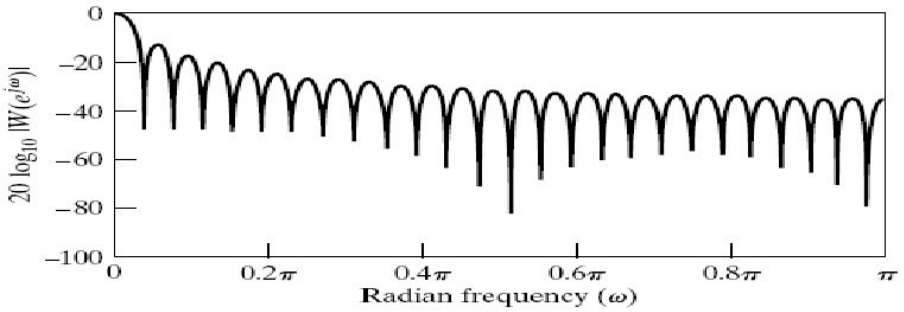

(a)

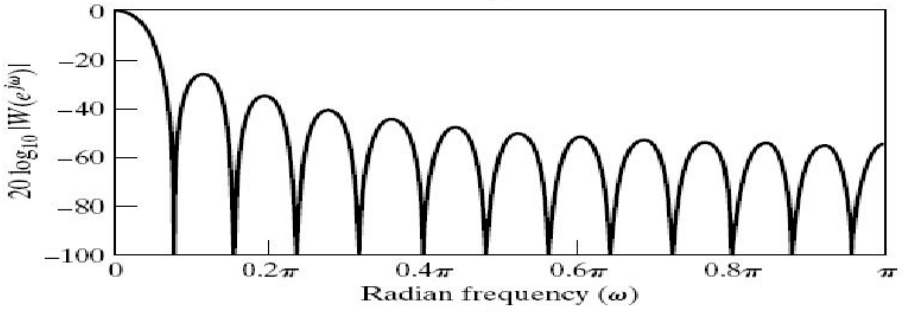

(b)

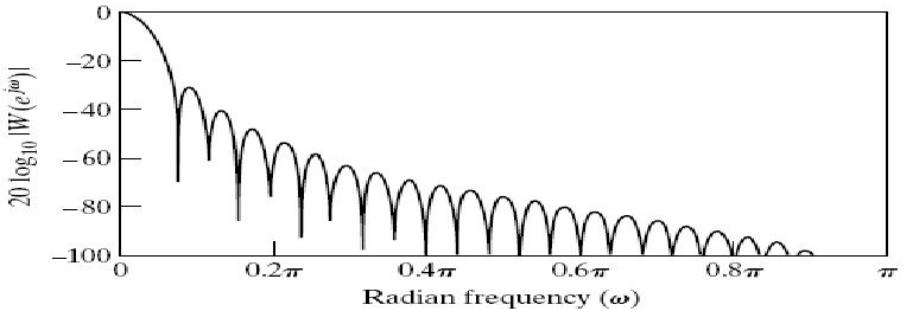

(c)

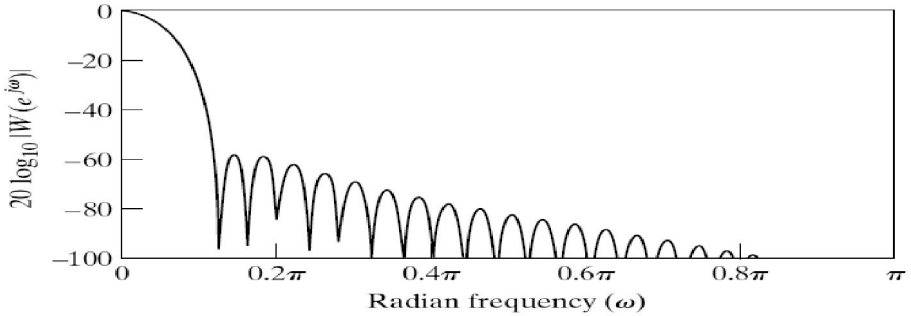

(e)

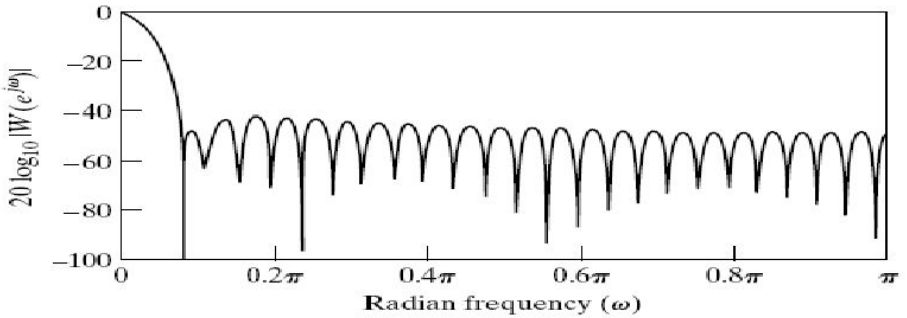

(d)

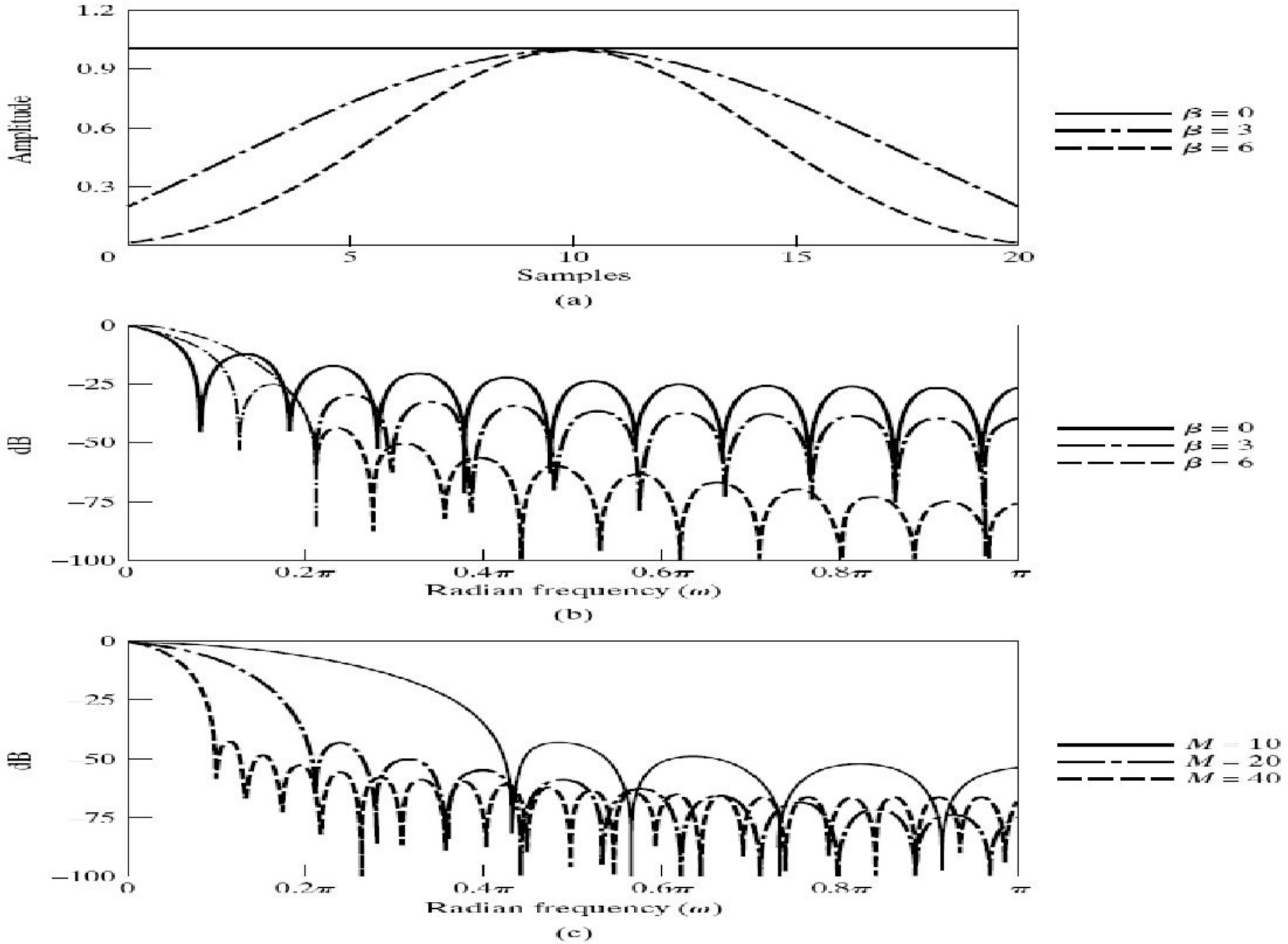

Figure 7.24 (a) Kaiser windows for $\beta = 0$, 3, and 6 and $M = 20$. (b) Fourier transforms corresponding to windows in (a). (c) Fourier transforms of Kaiser windows with $\beta = 6$ and $M = 10$, 20, and 40.

TABLE 9.2. Window Functions for $N > 0$ Samples[a]

Name	Definition
Rectangular	$w(n) = \begin{cases} 1 & \text{if } \lvert n\rvert \le \frac{N-1}{2} \\ 0 & \text{otherwise} \end{cases}$
Bartlett (triangular)	$w(n) = 1 - \frac{2\lvert n\rvert}{N-1} \quad \text{if } \lvert n\rvert \le \frac{N-1}{2}$
Hann	$w(n) = \frac{1}{2}\left[1 - \cos\frac{2\pi n}{N-1}\right] \quad \text{if } \lvert n\rvert \le \frac{N-1}{2}$
Hamming	$w(n) = 0.54 - 0.46\cos\frac{2\pi n}{N-1} \quad \text{if } \lvert n\rvert \le \frac{N-1}{2}$
Blackman	$w(n) = 0.42 + 0.5\cos\frac{2\pi n}{N-1} + 0.08\cos\frac{4\pi n}{N-1} \quad \text{if } \lvert n\rvert \le \frac{N-1}{2}$
Kaiser	$w(n) = \frac{I_0\left(\alpha\sqrt{1-\left(\frac{2n}{N-1}\right)^2}\right)}{I_0(\alpha)} \quad \text{if } \lvert n\rvert \le \frac{N-1}{2}$

Временные окна

TABLE 7.1 COMPARISON OF COMMONLY USED WINDOWS

Type of Window	Peak Side-Lobe Amplitude (Relative)	Approximate Width of Main Lobe	Peak Approximation Error, $20\log_{10}\delta$ (dB)	Equivalent Kaiser Window, β	Transition Width of Equivalent Kaiser Window
Rectangular	−13	$4\pi/(M+1)$	−21	0	$1.81\pi/M$
Bartlett	−25	$8\pi/M$	−25	1.33	$2.37\pi/M$
Hanning	−31	$8\pi/M$	−44	3.86	$5.01\pi/M$
Hamming	−41	$8\pi/M$	−53	4.86	$6.27\pi/M$
Blackman	−57	$12\pi/M$	−74	7.04	$9.19\pi/M$

Вариации топологии

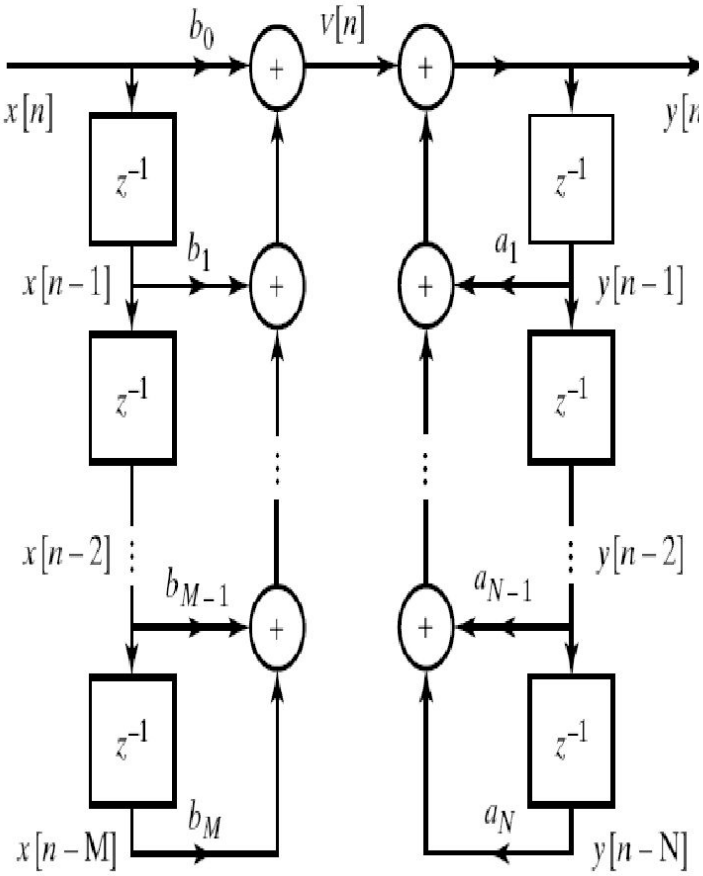

Figure 6.3 Block diagram representation for a general Nth-order difference equation.

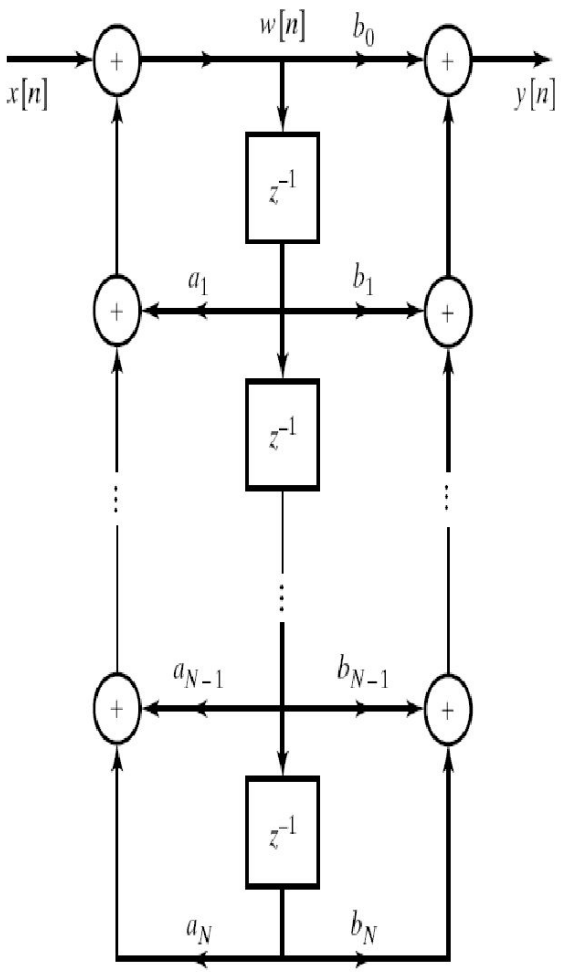

Figure 6.5 Combination of delays in Figure 6.4.

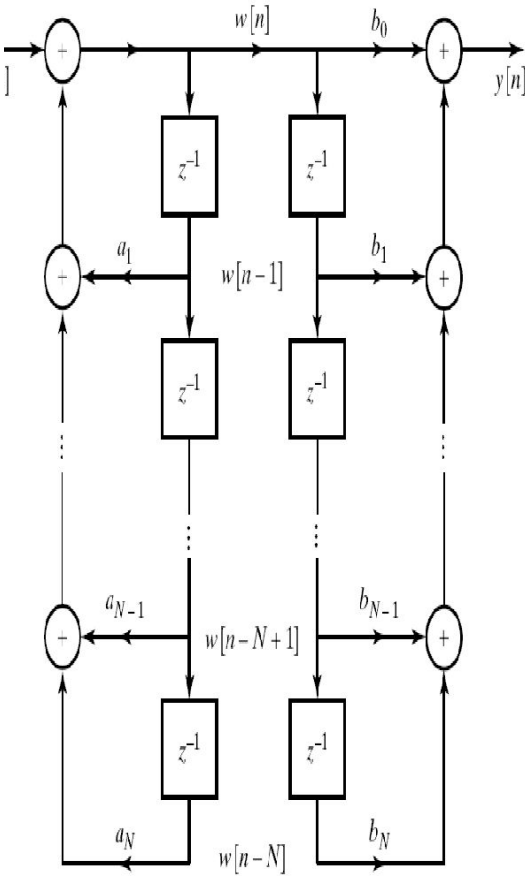

Figure 6.4 Rearrangement of block diagram of Figure 6.3. We assume for convenience that $N = M$. If $N \neq M$, some of the coefficients will be zero.

Примеры фильтров

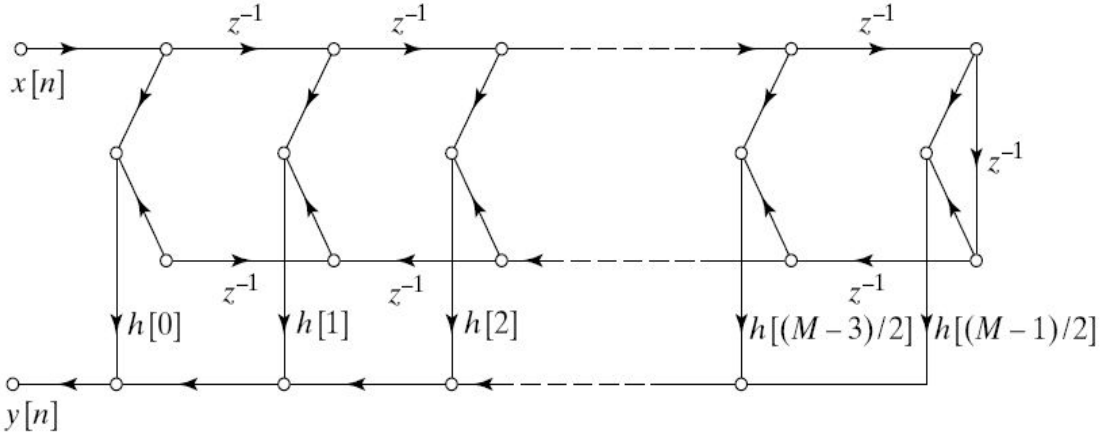

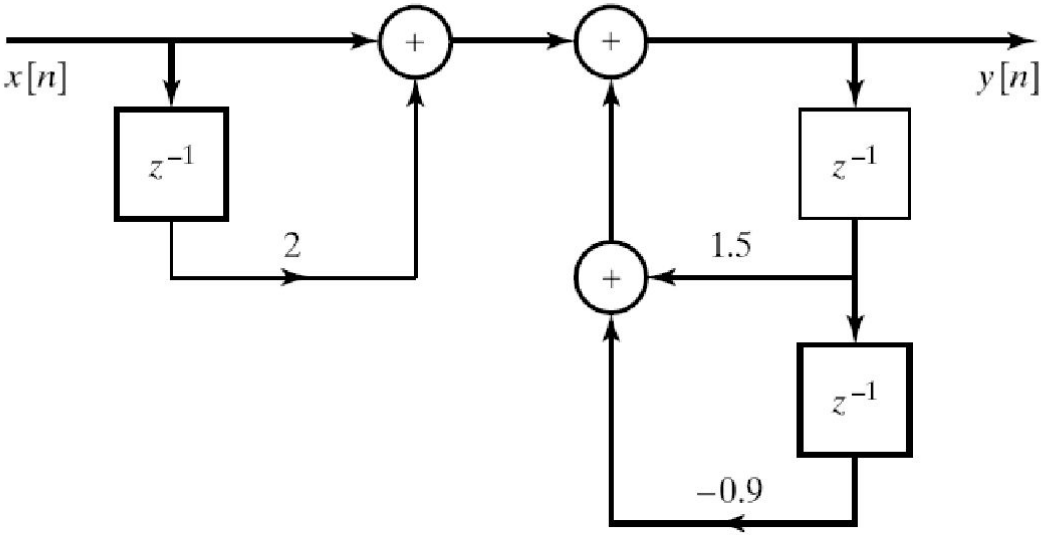

Figure 6.6 Direct form I implementation of Eq. (6.16).

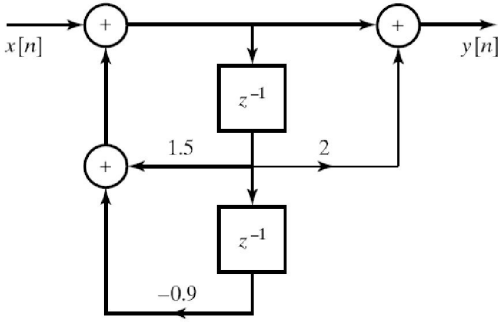

Figure 6.7 Direct form II implementation of Eq. (6.16).

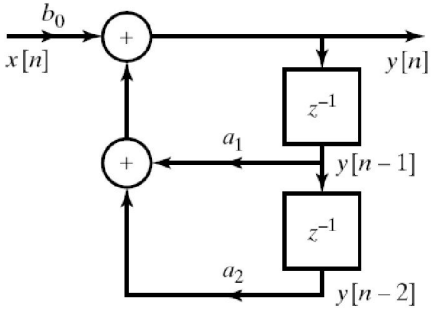

e 6.2 Example of a block diagram representation of a difference equation.

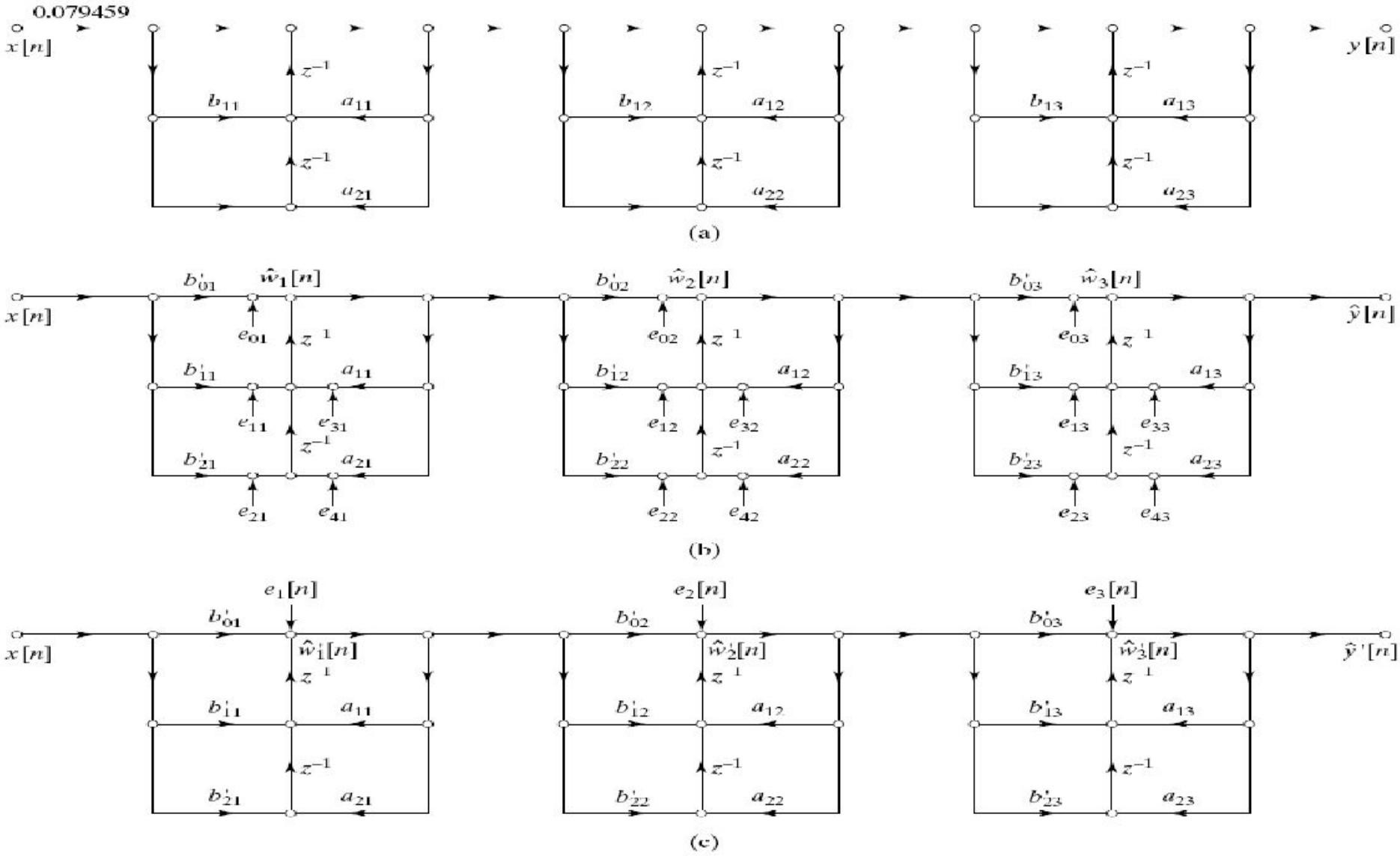

Figure 6.56 Models for sixth-order cascade system with transposed direct form II subsystems. (a) Infinite-precision model. (b) Linear-noise model for scaled system, showing quantization of individual multiplications. (c) Linear-noise model with noise sources combined.

Примеры фильтров

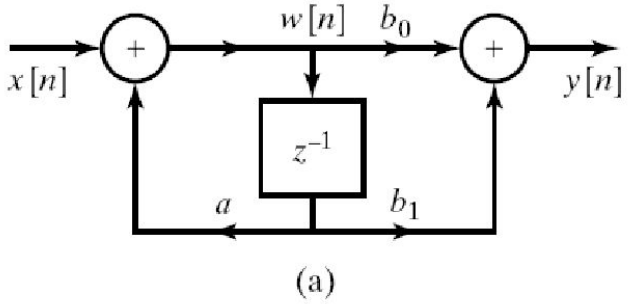

(a)

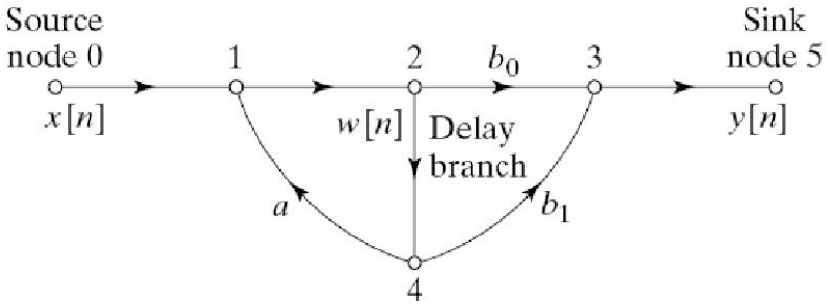

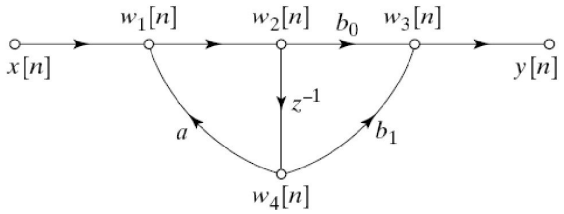

Figure 6.11 Signal flow graph of Figure 6.10(b) with the delay branch indicated by z^{-1}.

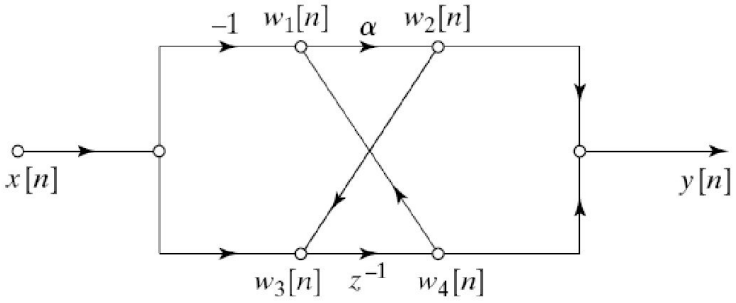

Figure 6.12 Flow graph not in standard direct form.

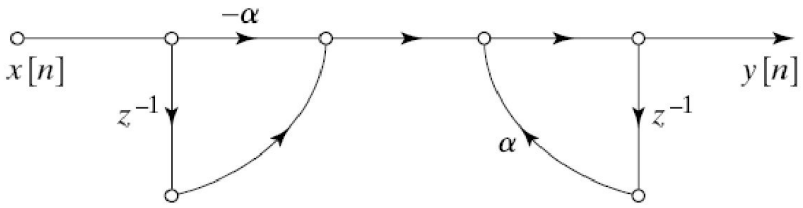

Figure 6.13 Direct form I equivalent of Figure 6.12.

TABLE 6.3 UNQUANTIZED AND QUANTIZED COEFFICIENTS FOR AN OPTIMUM FIR LOWPASS FILTER ($M = 27$)

Coefficient	Unquantized	16 bits	14 bits	13 bits	8 bits
$h[0] = h[27]$	1.359657×10^{-3}	45×2^{-15}	11×2^{-13}	6×2^{-12}	0×2^{-7}
$h[1] = h[26]$	-1.616993×10^{-3}	-53×2^{-15}	-13×2^{-13}	-7×2^{-12}	0×2^{-7}
$h[2] = h[25]$	-7.738032×10^{-3}	-254×2^{-15}	-63×2^{-13}	-32×2^{-12}	-1×2^{-7}
$h[3] = h[24]$	-2.686841×10^{-3}	-88×2^{-15}	-22×2^{-13}	-11×2^{-12}	0×2^{-7}
$h[4] = h[23]$	1.255246×10^{-2}	411×2^{-15}	103×2^{-13}	51×2^{-12}	2×2^{-7}
$h[5] = h[22]$	6.591530×10^{-3}	216×2^{-15}	54×2^{-13}	27×2^{-12}	1×2^{-7}
$h[6] = h[21]$	-2.217952×10^{-2}	-727×2^{-15}	-182×2^{-13}	-91×2^{-12}	-3×2^{-7}
$h[7] = h[20]$	-1.524663×10^{-2}	-500×2^{-15}	-125×2^{-13}	-62×2^{-12}	-2×2^{-7}
$h[8] = h[19]$	3.720668×10^{-2}	1219×2^{-15}	305×2^{-13}	152×2^{-12}	5×2^{-7}
$h[9] = h[18]$	3.233332×10^{-2}	1059×2^{-15}	265×2^{-13}	132×2^{-12}	4×2^{-7}
$h[10] = h[17]$	-6.537057×10^{-2}	-2142×2^{-15}	-536×2^{-13}	-268×2^{-12}	-8×2^{-7}
$h[11] = h[16]$	-7.528754×10^{-2}	-2467×2^{-15}	-617×2^{-13}	-308×2^{-12}	-10×2^{-7}
$h[12] = h[15]$	1.560970×10^{-1}	5115×2^{-15}	1279×2^{-13}	639×2^{-12}	20×2^{-7}
$h[13] = h[14]$	4.394094×10^{-1}	14399×2^{-15}	3600×2^{-13}	1800×2^{-12}	56×2^{-7}